University of Natural Resources and Life Sciences

Department for Agrobiotechnology, IFA-Tulln

Institute for Environmental Biotechnology

Master Thesis

Enzyme-responsive paper-based biosensing systems for diagnostics

Author:

Lukas Skopek, BSc

Master Programme Biotechnology

Supervisor:

Univ.Prof. Dipl.-Ing. Dr.techn. Georg M. Gübitz

Institute for Environmental Biotechnology

Co-Supervisor:

Dr.nat.techn. Claudia Tallian-Langer, MSc

Institute for Environmental Biotechnology

Tulln an der Donau, Mai 2020

Statutory declaration

I declare that I have authored this thesis independently, that I have not used other than the declared sources/resources, and that I have explicitly marked all material, which has been quoted either literally or by content from the used source.

Ich erkläre eidesstattlich, dass ich die Arbeit selbständig angefertigt habe. Es wurden keine anderen als die angegebenen Hilfsmittel benutzt. Die aus fremden Quellen direkt oder indirekt übernommenen Formulierungen und Gedanken sind als solche kenntlich gemacht. Diese schriftliche Arbeit wurde noch an keiner Stelle vorgelegt.

_____

Date, Signature

Preamble

This work is the result of a follow up project emerging from the EU “In-Fact” project at the Institute of Environmental Biotechnology at the University of Natural Resources and Life Sciences Vienna.

I want to thank Univ.Prof. Dipl.-Ing. Dr.techn. Georg M. Gübitz for the opportunity to work in this project and supervise this thesis. Also, I want to thank Dr.nat.techn. Claudia Tallian, Msc. for the outstanding help and support in this project.

Furthermore, I want to address my special thanks to my family and friends who always supported me during my studies and this work. In addition, I would like to thank all my colleagues at the IFA-Tulln for their help and the good working atmosphere that led to the formation of great friendships.

Abstract

This work should contribute to the development of a safe and fast point of care test in wound infection detection. Until now, the established method, to assess the wound status is a visual check-up of the affected area. This method is highly subjective and accompanied by a risk of misinterpretation. Also it is only possible to detect an infection, when it is already in an acute stage. Here, a simple point of care technique could bring an improvement in the safety of patients and clinical personnel.

The correlation between elevated enzyme levels and wound infections was used for the development of an assay, to monitor the wound status. Thereby, lysozyme was used as biomarker. Lysozyme catalyzes the hydrolysis of ß-(1.4)-glycosidic bonds found in chitosan. Thus, Chitosan was selected as lysozyme responsive material for the development of nanocapsules, equipped with a color-reactant, namely 5-bromo-4-chloro-3-indolyl phosphate-disodium salt (BCIP). This color reagent can be reduced by the enzyme Alkaline Phosphatase, resulting in a blue colored indigo product.

The developed and optimized nanocapsules carried 7.5 mg BCIP, had a hydrodynamic radius of 710.8 nm and showed a zeta potential of 21.64 mV. In different incubation experiments, the nanocapsules responded to the presence of lysozyme, with an enzyme activity, equivalent to the elevated enzyme activities in infected wounds, of 5000 U/ml in 60 min. Thus, it can be concluded, that the nanocapsules, developed in this work, could indicate the presence of the wound infection biomarker lysozyme within 60 min.

In a second step, a dipstick like assay was developed. Alkaline Phosphatase was bound onto the paper via chemical coupling and covered with a chitosan layer. In this approach lysozyme could break the chitosan barrier and the color reaction could take place, resulting in the blue colored product. With this dipstick, the presence of the biomarker could be detected after 45 min.

Keywords

Biopolymers, Dipstick assay, Indigo, Lysozyme, Wound Infection, Nanocapsules, 5-Bromo-4-chloro-3-indolyl phosphate-disodium, Ultrasound

Kurzfassung

Diese Arbeit beschäftigt sich mit der Entwicklung eines Schnelltests für die Feststellung von Wundinfektionen. Es gibt verschiedene Indikatoren für Wundinfektionen, die durch visuelle Kontrollen von klinischem Personal beurteilt werden. Die Erkennung von Wundinfektionen ist also sehr subjektiv. Da auch erhöhte Enzymaktivitäten zum Krankheitsbild gehören, könnten Tests, basierend auf der Anwesenheit von Wundenzymen, entwickelt werden. Ein vielversprechender Biomarker ist Lysozym. Dieses Enzym spielt bei infizierten Wunden eine große Rolle und kann β-1,4-glycosidischen Bindungen hydrolysieren. Da Chitosan aus teilweise acetylierten über β-1,4-Bindungen verbundenen Glucosamin-einheiten besteht, ist es Ausgangstoff für den hier vorgestellten Schnelltest.

In einem ersten Ansatz wurden Nanokapseln aus Chitosan hergestellt. Diese enthielten die Farbreagenz 5-Brom-4-chlor-3-indoxylphosphat (BCIP). Dieses Reagenz kann vom Enzym Alkalische Phosphatase umgesetzt werden, wobei der Farbstoff zu einem Indigokomplex reagiert. Das resultierende Produkt ist blau gefärbt und der entstehende Farbumschlag würde die Anwesenheit von Lysozym für den Anwender sichtbar machen.

Die entwickelten Nanokapseln zeichneten sich durch einen hydrodynamischen Radius von 710,8 nm und einem Zeta Potential von 21,64 mV aus. Die optimierten Nanokapseln wurden mit 7,5 mg BCIP geladen und reagierten auf die Anwesenheit von Lysozym, mit einer Enzymaktivität von 5000 U/ml nach nur 60 min. Die Enzymaktivität im Test, wurde so gewählt, dass sie der Aktivität in infizierten Wunden entspricht.

In einem zweiten Ansatz sollte ein dipstick assay entwickelt werden. Dazu wurde Alkalische Phosphatase auf den Papierstreifen gekoppelt und dieser anschließend mit Chitosan überschichtet. In einem typischen Versuchsaufbau wurden die Papierstreifen mit einer Lösung, die 5000 U/ml Lysozym und dem Farbstoff enthielt, inkubiert. Diese Inkubation führte zu einem Nachweis des Wundenzyms nach 45min.

Schlagworte

Biopolymere, Teststreifenanalyse, Indigo, Lysozym, Wundinfektion, Nanokapseln, 5-Brom-4-chlor-3-indoxylphosphat, Ultraschall

Table of Contents

List of Abbreviations

AP	Alkaline phosphatase
ATR	Attenuated-total-reflecion
BCIP	5-Bromo-4-chloro-3-indolyl phosphate
BSA	Bovine serum albumin
DA	Degree of acetylation
DLS	Dynamic light scattering
D_2O	Deuterium oxide
DSS	4,4-dimethyl-4-silapentane-1-sulfonic acid
EDC	1-Ethyl-3-[3-dimethylaminopropyl]carbodiimide hydrochloride
EDL	Electric double layer
HMC	Heppe Medical Chitosan (Crab Chitosan obtained from Heppe Medical)
iP	Isoelectric Point
KPO_4	Potassium phosphate
Na Alg	Sodium alginate
NHS	N-hydroxysuccinimide
UP-H_2O	Ultrapure Water
PNPP	p-Nitrophenyl phosphate
R_h	Hydrodynamic radius

1. Introduction

1.1 Scientific Background

Even to date, wound infections are a serious problem in modern medicine. Infections pose a high risk to become chronical and can lead to severe issues in the healing process of patients. Despite the sorrow of patients, infections lead to higher costs for the medical system. Thus, a tool to improve the monitoring of a wound status in real time, is from high importance for clinical personal. This could help in the reduction of stress for patients and reduce costs.

Until now, the wound status is examined by looking for the established signs of an infected wound, by visual examination. When a wound is showing the indicating signs of rubor (redness), dolor(pain), calor (heat emission) and tumor(swelling), clinical personal usually must decide on measures for further treatment, based on the estimation of these signs (Hasmann *et al.*, 2011). Thus, the current state of the art method is considered as highly subjective which could be improved by an efficient tool for monitoring the wound status in real time.

It is expected, that the annual costs for the health care system, resulting from chronic wound inflammations in Europe, is in the range of more than five billion Euro (Quadlbauer, 2018). Mostly undetected inflammations or wound infections which were detected too late, result in chronic wounds. This sorrow of patients as well, as the annual costs could be eliminated by the establishment of an effective point of care detection kit (Tegl *et al.* 2016).

1.1.1 Infection Detection

As stated before, a lot of personnel effort is connected to the monitoring of the wound status. Also, in infection detection, the evaluation of a wound status is accompanied with the high risk of misinterpretation. Therefore, a fast, real time diagnostic tool would be contributing to a better quality of clinical procedures. In addition, the established method relies on indicators, appearing, when the wound is already infected. Thus, many new approaches for a real time wound infection detection are done. Some new methods are based on molecular- or micro biological analysis are already published. (Tegl, 2015)

Here, biomarkers are expected to play a highly important role in the development of future infection detection assays. The high variety and diagnostic value of biomarkers is shown in Figure 1.

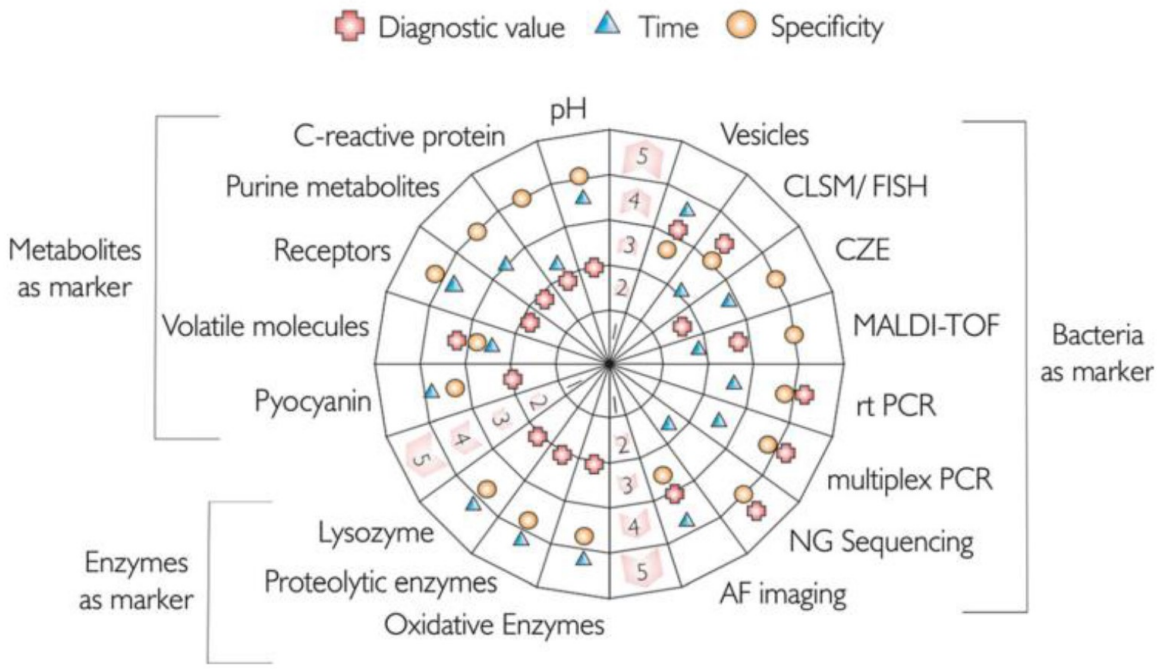

Figure 1: The role and importance of different biomarkers (graded from 1-5). Comprising strategies and the method for the detection (only for bacteria), enzymes as markers and metabolites as marker. The grading is based on the time, specificity and the diagnostic value. (Tegl, 2015)

In Figure 1 it is clearly visualized, that enzymes play an important role as biomarkers for monitoring the wound status. Despite enzymes as markers, the presence of bacteria can lead to a highly specific, diagnostic information. Still, the detection of bacteria is depending on highly sophisticated methods. In addition, these techniques are labor intense and take rather long, which is also visualized in Figure 1 by a rather bad grading for time. (Schiffer Doris et al., 2015; Tegl *et al*., 2015)

Metabolites as biomarkers on the other hand, are very specific, but the detection of metabolites is also labor intense, and a rather low diagnostic knowledge is gained from these biomarkers. Thus, enzymes can play a key role in the development of a real time diagnostic tool, as this biomarker is assigned with the best value for the factor of time. In addition, some enzymes are only produced by the immune system of an afflicted patient, rendering the biomarker highly specific and reliable. Thus, the development of a diagnostic tool to assess the wound status in real time should be based on detecting the presence of certain wound enzymes. (Schiffer Doris et al., 2015; Tegl *et al*., 2015)

1.1.2The wound healing process

The process of wound healing, comprises four major stages. Starting from hemostasis, leading to inflammation and proliferation and ending with the tissue remodelling phase (Figure 2) (Kawasumi *et al*. 2013).

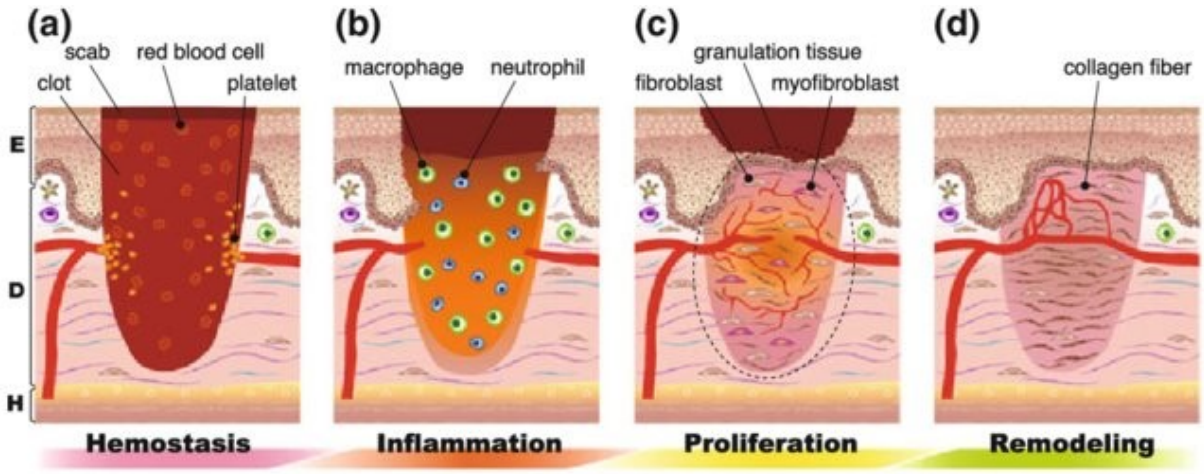

Figure 2: Model of the wound healing process including hemostasis (blood clotting to seal the injured area and stop further bleeding), inflammation (phagocytosic stage, where damaged cells and pathogens are disrupted by white blood cells), proliferation (ne tissue is growing in this phase) and remodeling (collagen is reshaped along the wound) (Kawasumi *et al.*, 2013)

The process of wound healing starts by the closure of the destructed tissue during hemostasis. Here red blood cells are clotting together with fibrin, closing the affected area. This should seal the wound to stop further bleeding. During inflammation, white blood cells are destructing pathogens like viruses and bacteria. In addition, damaged cells and debris are cleared out. Proliferation is the phase, in which new tissue is growing by collagen deposition and growth of fibroblasts. In addition, the wound is contracted by the action of the fibroblasts. In the last stage, the remodeling step, collagen is elongating along the destructed area, remodeling the structure of the original tissue. (Kawasumi *et al.* 2013)

Here, it should be mentioned, that the healing process is an ongoing process, with overlapping stages. Thus, the explained stages are not in a strictly defined row. Despite the overlapping of the stages, the steps also differ in their duration. Hemostasis is concluded in a timeframe of minutes to hours, while inflammation can take days to weeks, to be completed. Proliferation and remodeling can take weeks to months or even years, depending on the size and severity of the wound. (Häggström, 2014)

When the process of wound healing is interrupted, or one step of this cascade is not completed properly, a wound can become chronical, whereby the tissue is constantly under pressure of inflammations and infections (Tegl *et al.* 2016). The most popular issues in the healing process are disruptions of the signaling cascade and extreme infiltration. In the first case, due to the disruption of the complex cascade, the expression of growth factors is amplified. Although a high number of growth factors is produced, the process cannot be completed and is not leading to a functional outcome. (Schultz, Wysocki, 2009)

In the second case, infiltration of neutrophils, can lead to chronic inflammation. Due to the enzymes released into the wound, connective tissue is degraded (e.g. by collagenase). This leads to a constantly inflamed wound, which the body cannot cope with any longer. (Diegelmann, Evans, 2004)

1.1.3 Lysozyme

Due to the high informative value, enzymes have a high potential to serve in future diagnostic tools as efficient biomarkers. However, at a closer look, especially the enzyme lysozyme, seems to play an important role in the detection of wound infections. (Tallian, 2019).

Lysozyme, which is also known as muramidase, is catalyzing the hydrolysis reaction of β-1,4-linkages between N-acetylmuramic acid and N-acetyl-D-glucosamine in peptidoglycan layers. Since these molecules are contributing to the cell walls of gram-positive bacteria, lysozyme is an important antimicrobial enzyme, made by the immune system of different organisms. It can be found in many organisms like mammalians, birds and even among bacteria and other microorganisms. (Sigma-Aldrich Inc.,2016; Stokke *et al.* 1995)

The structure of lysozyme is displayed in Figure 3. This relatively small enzyme, made from 129 amino acids, has a molecular weight of 14.3 kDa. The conformation of the protein structure can be found in two states. Either in the open, active conformation, or the closed, inactive form.

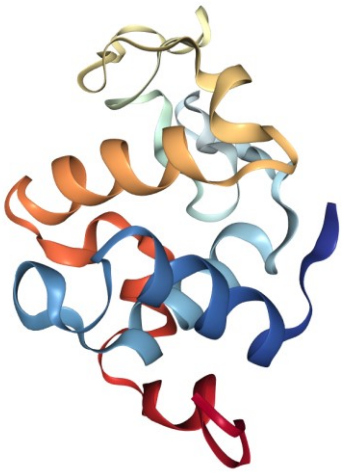

Figure 3: Protein structure of hen egg white lysozyme (Pechkova *et al.*, 2010)

The classification of lysozyme is connected to the origin and the catalyzed reactions. Despite the well-known c-type lysozyme, which is derived from chicken egg white, other types of lysozyme exist. For example, the g-type. This type is derived from goose and has a higher catalytic activity on the β-1,4- linkages of chitin. Although it is reported, that the g-type lysozyme is hydrolyzing chitosan more effectively, this work was focusing on the c-type lysozyme from

hen egg white, as this is more closely related to the human immune system. (Huang *et al.*, 2011; Irwin *et al.*, 2011)

Lysozyme has its highest activity at a pH between 6.0 to 9.0 (Sigma-Aldrich, 2008). The catalyzed hydrolysis of β-(1→4)-glycosidic bonds between N-acetyl-muraminic acid and N-acetyl-D-glucosamine in peptidoglycan layers, can also be used for the breakdown of chitin and chitosan. (Stokke *et al.*, 1995; Wu *et al.*, 2011)

1.1.4 Chitin and Chitosan

One of the most abundant biopolymers found on earth is chitin. (Weinhold *et al.,* 2009) The polysaccharide made from β-1,4 connected N-acetylglucosamine subunits is especially contributing to the structure of cell walls in fungi. It is also a major component of the exoskeleton of insects, or sea animals like shrimp. (Zargar *et al.*, 2015)

Due to the high availability and the fact, that chitin (Figure 4) is a by-product of many economies, like seafood production, the biomaterial chitin is of high interest in green economy. Despite the good availability and thus the cheap price, chitin has additional positive features, like biodegradability, biocompatibility and chemical features which allow many functionalization possibilities. (Dutta, Tripathi, 2003)

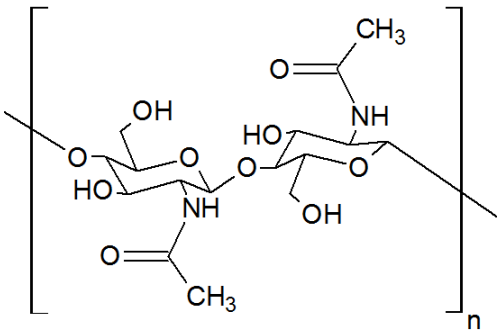

Figure 4: Chemical structure of chitin

Nowadays, chitin is already used as gelling agent, drug carrier or as healing agent in wound care (Pillai *et al.*, 2009). Still, there are some drawbacks connected to the biopolymer. Since chitin has a semi-crystalline structure, it is insoluble in most organic and diluted aqueous solvents, which might hinder the usage in some processes. (Zargar *et al.*, 2015)

Nevertheless, there are chemical procedures, to render chitin soluble in aqueous solutions. By deacetylation and depolymerization reactions, chitin can be converted to the more reactive chitosan (Figure 5). It is considered as heteropolymer and consists of β-1,4-2-amino glucose and β-1,4-2-acetamido glucose. (Harish PrashanthK. V., Tharanathan R. N, 2007)

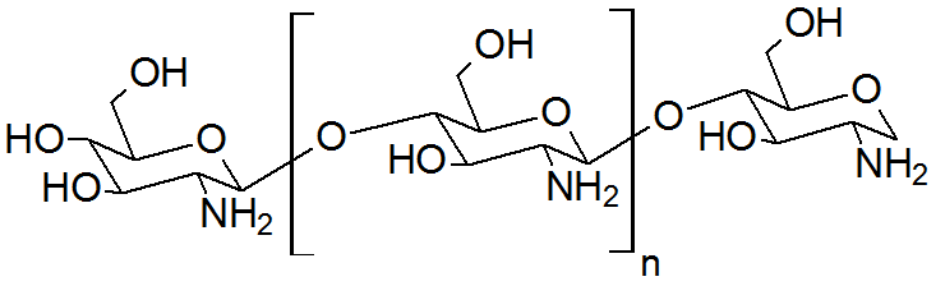

Figure 5: Chemical structure of chitosan

One important feature is the possible re-acetylation of chitosan. The re-acetylated chitosan (Figure 6) combines both features of chitosan and the before mentioned chitin (Gorgieva, Kokol, 2012). It is degradable, like chitin and, soluble like chitosan.

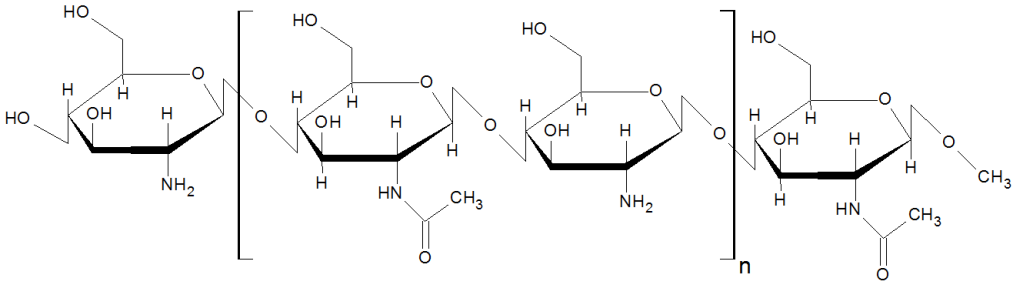

Figure 6: Chemical structure of N-acetylated chitosan

Especially in the medical industry, re-acetylated N-acetylated chitosan is a promising substance, due to the beforementioned benefits of chitin and the chitosan related, chemical features.

1.1.5 5-Bromo-4-chloro-3-indolyl phosphate and Indigo dyes

The chemical 5-Bromo-4-chloro-3-indolyl phosphate (BCIP) is a synthetic chromogenic reactant, used for different colorimetric detection reactions. Especially in the field of clinical analytics, BCIP is frequently used for the detection of alkaline phosphatase (AP), an enzyme, capable of oxidizing phosphate groups in different molecules (De Jong, Van Kessel-Van Vark and Raap, 1985). Here, the presence of AP in serum can be seen as biomarker for osteopenia (Abdallah *et al.*, 2016), or as indicator for liver diseases (Hilscher *et al.*, 2016).

In the case of BCIP, AP would oxidize the phosphate group and render the BCIP molecule rather reactive. In the colorimetric reaction cascade, two dephosphorized BCIP molecules can react under the formation of one Indigo molecule (Figure 7).

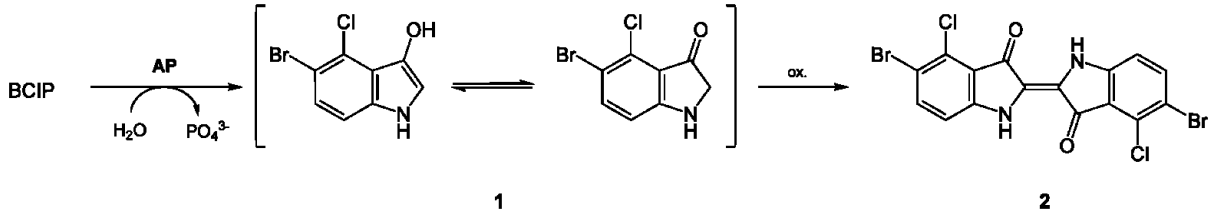

Figure 7: Reaction mechanism of the colorless BCIP to blue Indigo. When AP is introduced to a BCIP solution, it dephosphorizes the BCIP-molecule and changes it to a 5-Bromo-4-chloro-indolyl moleculeas seen in (1). When two molecules of 5-Bromo-4-chloro-indolyl are oxidized by contact to air, they react to one molecule of Indigo (2). (Yikrazuul, 2008)

The well-known Indigo complex (Figure 8) is of a naturally occurring dark blue color, originating from a variety of plants from the *Indigofera* genus. The name results from the discovery of these plants in India. Although many plants, like woad in Europe or anil in Central- and South-America can create the dye molecule, most of the plants from this genus are found in the tropical zones of the planet. (Schmidt, 1997)

Since the demand for the dark blue dye is high, and natural indigo was expensive, an effective process for the chemical synthesis of Indigo was established quite fast, rendering the availability of Indigo quite easy and cheap.

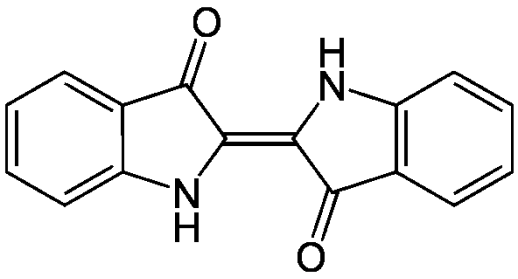

Figure 8: Chemical structure of the Indigo molecule

Considering the chemical structure of Indigo, the parallels to the beforementioned BCIP compound can be seen. As the dye molecule consists of two BCIP molecules, connected by a double bond between the two indoxyl groups.

1.1.6 Alkaline Phosphatase

The before mentioned enzyme alkaline phosphatase (Figure 9), can be found among different species like mammalians, prokaryotes and eukaryotes and belongs of the class of hydrolases acting on ester bonds. In the case of alkaline phosphatase, the catalyzed reaction is a hydrolyzation of phosphate monoesters. (Millán, 2006a)

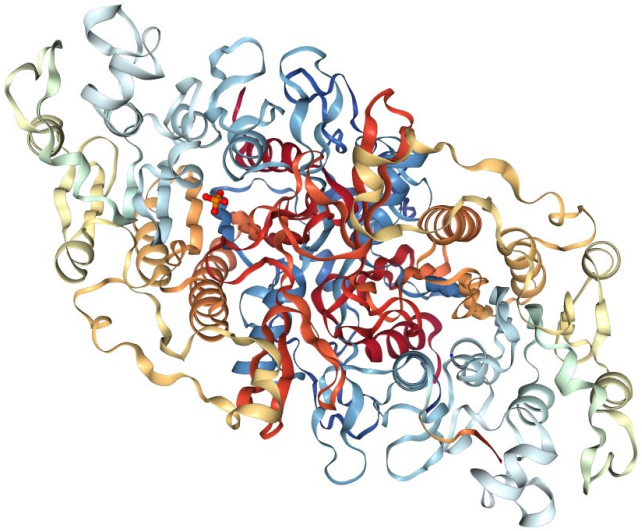

Figure 9: Protein structure of alkaline phosphatase (Wang *et al.*, 2009)

Looking at the structure of AP, it is visible, that the enzyme is composed of two subunits. In addition, the dimer containing zinc and magnesium ions, forming the active site of the enzyme. The average molecular weight of AP from *E. coli* is 86 kDa. Which is resulting from the two subunits made from 429 amino acids, linked by cysteine residues. (Coleman, 1992; Millán, 2006a)

However, looking at the reaction mechanism of the enzyme, the zinc seems to play a more important role, as the reaction is based on the geometrical coordination of the substrates between the zinc in the active site. Magnesium seems to be contributing to the electrostatic potential of the active site. (Millán, 2006b)

The general reaction mechanism synthesized by AP is stated in Equation 1.

$$Phosphate\ monoesters + H_2O \rightarrow Alcohol + p_i$$

Equation 1: Basic reaction mechanism of reactions catalyzed by alkaline phosphatase

This reaction is important for different biochemical processes in an organism. Thus, AP can be found in blood samples and can be related to issues of the liver or kidneys. Therefore, it is also already well investigated and established as biomarker in clinical practice. (Millán, 2006a).

1.1.7 Nanocapsules in medical applications

Nanomaterials like nanocapsules are mainly used as transport system for targeted drug delivery (Singh, Lillard, 2009). In contrast to nanoparticles, which are defined as solid particles with a uniform distribution of the drug in the matrix and a size of 10-1000 nm (Rao, Geckeler, 2011), nanocapsules are defined as vesicular systems enclosing a core of material in a different form (e.g. solutions carrying the drug). (Singh, Lillard, 2009)

Nanocapsules based on chitosan are already used in targeted drug delivery, as a specific stimulus like enzymes or pH changes can induce the degradation of the chitosan shell. (Singh, Lillard, 2009; Nagpal *et al.*, 2010)

The preparation of chitosan-based nanocapsules relies on the functional amino side groups of chitosan. Methods used are ionotropic gelation, crosslinking or self-assembling (Hudson, Margaritis, 2014). In addition, Rollett *et al.* (2012) developed a toxin free, sonochemical method for nanoparticle production, based on the self-assembly of proteins between aqueous and an organic phase. (Rollett *et al.*, 2012)

1.1.8 Dipstick assays

The beforementioned necessity for rapid point of care assays in clinical practice also goes hand in hand with user-friendliness. A classic and simple tool are dipstick assays. They are used for many different tests like drug tests, pregnancy tests or simple pH measurements.

In general, dipstick assays are made of the dipstick itself, and a responsive layer, that can show the presence of the analyte. A well-known example for dipstick assays are pregnancy- or drug tests. Here, the appearance of a distinct color is connected to the analyte, present in the testing solution.(Yetisen, Akram, Lowe, 2013)

1.2 Techniques

1.2.1 Enzyme Characterization

1.2.1.1 Bradford Assay

The protein concentration of enzymatic solutions was evaluated with the Bradford assay. This method is based on the reaction between proteins and the Coomassie Brilliant Blue G-250 dye. When Protein is bound to the dye, the absorption maximum is shifted from green (465 nm) to blue (595 nm). The increase in absorption at 595 nm is dependent on the amount of bound protein and can be related to the protein concentration.(Bradford, 1976)

By the preparation of an external calibration, with known concentrations of a Bovine Serum Albumin (BSA)- Standard, the protein concentration of the sample can be determined. Therefore, the absorption signal of the sample is converted into the protein concentration by using the linear function of the calibration curve.

1.2.1.2 Lysozyme activity assay

In order to quantify the enzyme activity of lysozyme, powder of *Micrococcus lysodeikticus* was dissolved in MQ-H_2O which resulted in a turbid solution. Since Lysozyme can destroy the cell walls of this gram-positive strain, it can be used to measure the activity of Lysozyme. When the turbid solution of freeze dried *Micrococcus lysodeikticus* cells is mixed with lysozyme, it becomes clear after a certain time, due to the degradation of the bacterial cells. The time for this process corresponds to the activity of the enzyme. By measuring the absorbance over time, a curve, that reflects the enzymes activity, can be made. (Sigma-Aldrich Inc., 1994b)

1.2.1.3 Activity Assay of Alkaline Phosphatase

The activity of AP was measured by a Method based on the chemical reaction seen in Equation 2.

$$pNitrophenylphosphate + H_2O \rightarrow pNitrophenol + p_i$$

Equation 2: Chemical reaction catalyzed by Alkaline Phosphatase

The colorless substrate, p-Nitrophenyl Phosphate (PNPP) is converted to the yellow colored product p-Nitrophenol. The increasing absorbance of the yellow appearing product at 405 nm, is recorded over a certain time period. The resulting slope of the created curve, can be related to the activity of the enzyme. (Sigma-Aldrich Inc., 1994a)

1.2.2 Sonification process

Ultrasonic waves in the range of 16 kHz to 1.5 MHz can be used to boost reactivity of certain chemicals. Especially the high power of low frequency ultrasound ranging from 20 to 100 kHz is influencing the media and reactivity of solutes. The energy input of sonic waves results in four phenomena, namely heat formation, acoustic cavitation, acoustic streaming, and Nebulization. Especially cavitation is contributing to the formation of nanocapsules, since the energy input of collapsing cavitation bubbles helps to overcome energy barriers and allows polymerization, cross-linkages, leading to the formation of a nanocapsule shell. (Tallian *et al.*, 2018)

Thus, the energy input of an ultrasound probe can be used to create nanocapsules out of the polymerizable chitosan solutions.

1.2.3 Zeta potential analysis

Like many other molecules, also nanocapsules in aqueous solutions are covered by charged ions. These ions are forming a double layer which is known as electric double layer (EDL). The EDL consists of two layers, the inner Stern layer and the outer diffuse layer. In the diffuse layer, the ions are of mixed charge and not uniform as in the Stern layer. When charges are applied to the particle solution, the particle layers are moving towards the opposite charge. In this model, a plane interfers between the diffuse layer and the solution. This so-called slipping plane, can be related to the zeta potential. It is used, to define the stability and repelling or agglomerating behavior of a particle solution. The electron layers and zeta potential curve are visualized in Figure 10. (Kirby, Hasselbrink, 2004; Bhattacharjee, 2016)

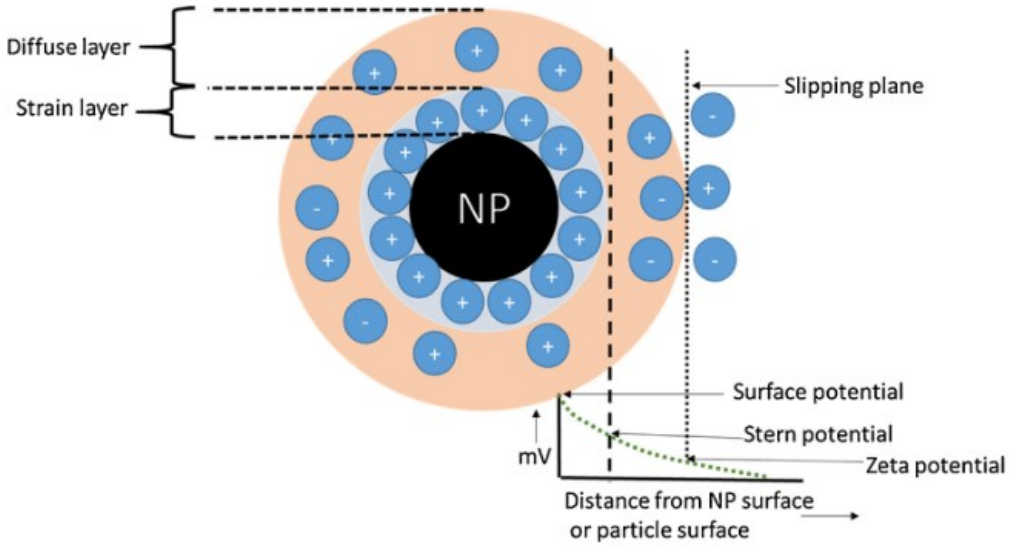

Figure 10: Graphical visualization of a nanoparticle (NP) with the EDL in solution, taken from Behera *et al.* (2017) The nanoparticle itself is displayed as black circle with the uniform positive loaded strain layer around it. The strain layer is surrounded by the diffuse layer and the slipping plane. The relation between charge [mV] and distance from the nanoparticle is displayed in the graph below the particle. The zeta potential and the connection of charge to the position of the slipping plane is also displayed in the figure. Illustration taken from (Behera *et al.*, 2017)

The zeta potential is measured by an indirect method that is scattering light on the moving particles. The frequency shift can then be measured and converted into the zeta potential. The calculation of the potential is based on Equation 3 and Equation 4

$$\Delta f = \frac{2v + sind(\theta 2)}{\lambda}$$

Equation 3: Mathematical equation to calculate the frequency shift

f …. Frequency
v …. Particle velocity
λ …. Laser wavelength
θ …. Scattering angle

$$\mu_e = \frac{v}{E} = \frac{\varepsilon r \varepsilon_0 \zeta}{\eta}$$

Equation 4: Helmholtz-Smoluchowski equation

μe …. Electrophoretic mobility
E …. Electric field strength
εr …. Relative permittivity/dielectric constant
ε0 …. Permittivity of vacuum
ζ …. Zeta potential
η …. Viscosity

A zeta potential can be negative or positive, depending on the nature of the particle, but in general a zeta potential close to zero can be related to an agglomerating behavior, while high zeta potentials indicate higher stability of the emulsions. (Kirby, Hasselbrink, 2004; Bhattacharjee, 2016)

1.2.4 Dynamic Light Scattering

Another technique for particle characterization is dynamic light scattering (DLS). When the spherical particles are moving through the solution and a monochromatic laser beam is hitting the particle, it will move in a certain direction and change the path of the incoming light. Because the hydrodynamic radius (R_h) can be related to the shift of the light, the particle size can be calculated using the Stokes-Einstein-Equation seen in Equation 5. (Khun, 1977)

$$Rh = \frac{kT}{6\pi\eta D}$$

Equation 5: Stokes-Einstein equation

Rh …. Hydrodynamic radius
k …. Boltzmann's constant
T …. Absolute temperature
η …. Solvent viscosity
D …. Translational diffusion coefficient

1.2.5 Fourier transform infrared spectroscopy

Infrared light in the range of 4000cm^{-1} to 400 cm^{-1} can be used to define functional groups of certain molecules in Fourier transform infrared spectroscopy (FTIR). To generate an infrared spectrum in this range, the wavelength of infrared-light is adjusted by two moving mirrors in the pathway of the light (Figure 11).

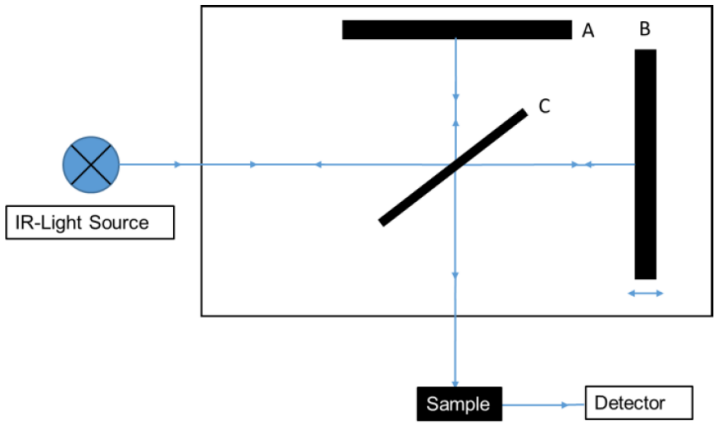

Figure 11: Lightpath of infrared (IR)-light in an FTIR-Device. The light beam is exiting the source and reflected from the first semi reflective mirror (C) onto a fixed mirror (A) where it is reflected back to the sample. When the light beam is not reflected towards the fixed mirror, it passes the semi reflective mirror onto a moveable mirror (B). Due to the overlaying and extinction of the light wave a spectrum of different wavenumbers is generated. Illustration taken from Cammann, 2001

Furthermore, Attenuated-Total-Reflection-crystals (ATR) can be used in combination with FTIR to allow non- destructive analytics. In ATR-mode, the attenuation of light between the infrared absorbing sample and the reflecting crystal is measured (Figure 12).

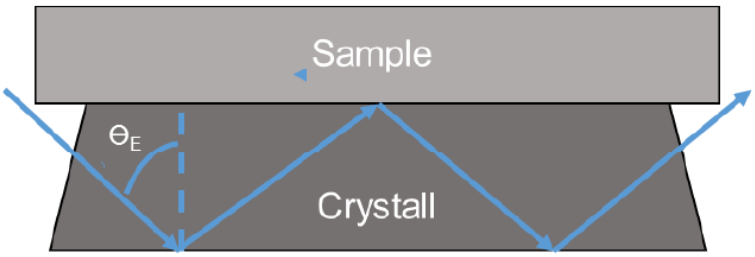

Figure 12: IR-light path in an ATR-crystal. Light is passing the crystal and becomes reflected on the edge. When a sample is pressed onto the surface, the light beam can interact with the sample, leading to reflection or absorption of certain wavenumbers. Figure adopted from Cammann, 2001

As stated above, the spectrum is recorded from 400 cm^{-1} to 4000 cm^{-1}. The so-called fingerprint area below 1500 cm^{-1} represents the whole molecule, whereas the characteristic peaks for certain bonds themselves are above this area. Especially the amide I bond at 1650 cm^{-1} that represents carbonyl stretching and the amide II at 1550 cm^{-1} which is a combination of the NH-bend and CH-stretch swinging. Because these peaks are very close to the water peak, it is very important that the samples are dry.(Hesse *et al.*, 1989; Kazarian, Chan, 2013)

1.2.6 Nuclear Magnetic Resonance Spectroscopy

Nuclear magnetic resonance (NMR) spectroscopy is a method to investigate atomic properties and the interactions with other atoms. Giving detailed information on the structure of molecules. By measuring the change of excitation of molecules taking up energy. By absorbing energy, as quanta, organic molecules change of their electrical or mechanical state. The necessary energy is depending on the molecule and yields characteristic information. The intensity and frequency of light reflected from the sample is detected and related to the nature of the molecule. When the sample takes up energy, the baseline changes. This can be transformed to a spectrogram that yields information about the structural environment of the nuclei of the certain elements. Mostly it is referred to hydrogen and carbon. (Radeglia, 1989; Vollhardt P., Schore N., 2015)

1.2.7 Ultraviolet/ Visible Spectroscopy

Because some molecules absorb light of certain frequencies, the resulting change of light intensity can be related to the specific concentration of the molecules.

In detail, absorbance is based on the phenomenon that some molecules take up the energy of light, which is transferred to shell electrons, leading to excitation of these electrons. The effect of this behavior, the change of absorption is described by the Lambert-Beer-Law (Equation 6).

$$\Delta A = c * \varepsilon * d * DF$$

Equation 6: Lambert Beer law

A …. Absorbance
c …. Concentration
ε ... Extinction coefficient
d …. Path length
DF .... Dilution factor

1.2.8 Chemical coupling

In order to create a user-friendly dipstick assay, the lysozyme responsive materials should be coupled to a cellulosic material like filter paper. One of the most popular method, is the binding with a zero length crosslinker, namely 1-Ethyl-3-[3-dimethylaminopropyl]carbodiimide hydrochloride (EDC). Together with N-hydroxysuccinimide esters (NHS). A two-step coupling reaction can be performed. Hence, EDC reacts with a carboxylic acid group while forming an amine reactive intermediate. This intermediate is stabilized by the NHS increasing the efficiency of EDC-mediated coupling. This principle should be graphically described in Figure 13.(Bart *et al.*, 2009; Thermo Fisher, 2012)

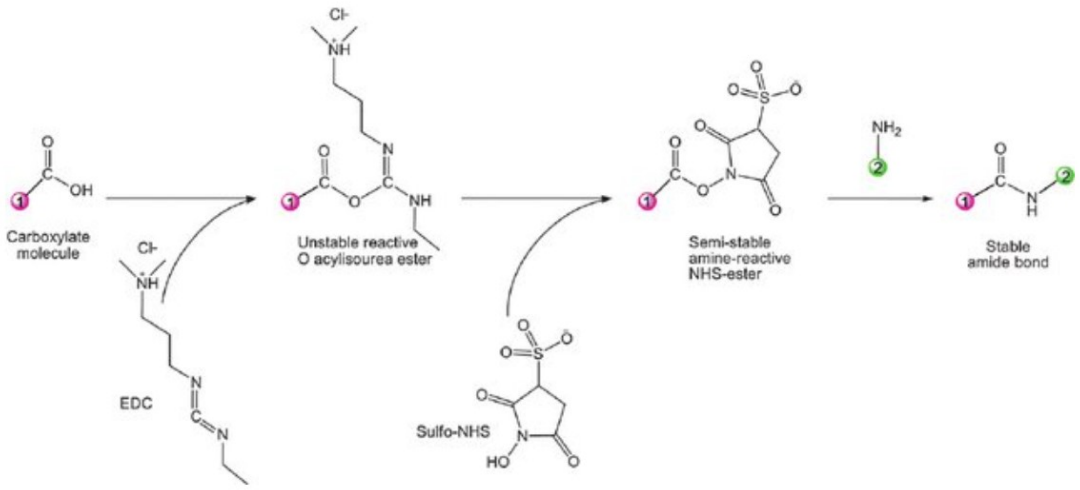

Figure 13: Basic mechanism of the EDC-NHS coupling method. When EDC reacts with a carboxylic acid group, the amine reactive intermediate is formed. By the addition of NHS, this intermediate is stabilized and a stable amide bond can be formed between the carboxylic acid (1) and the amine group (2). The figure was taken from Bart *et al.*, 2009.

Here, the work of (Cao *et al.*, 2015) should be mentioned, as this article describes the usage of the coupling mechanism, for the preparation of a BCIP responsive paper surface. The idea of coupling AP to a cellulose surface, via EDC/NHS-coupling, could help in developing a lysozyme responsive material. Because EDC/NHS-coupling is a powerful tool for zero length crosslinking, the protocol of Cao *et al.* should be used to couple AP and even final nanocapsules on filterpaper, to create paper based dipstick assays.

1.3 Objectives

In the present work, nanocapsules should be equipped with a dye, which is capable of giving a color signal in the presence of lysozyme. Therefore, the beforementioned BCIP will be encapsulated in a chitosan shell. The over-all-goal was the creation of an infection detection kit, which would indicate the presence of lysozyme in a short time, to support and advance the development of real-time diagnostic materials in the detection of wound infections.

In theory, nanocapsules made from N-acetylated chitosan, equipped with BCIP on the one hand and alkaline phosphatase on the other hand should be used. When lysozyme would be present in a sample, e.g. in wound fluid of an infected wound, the chitosan-shell of the nanocapsules would be degraded by the wound enzyme under the release of the loaded BCIP and AP. When these substances are free in solution, (AP) should be able to cleave the phosphate group of the BCIP-molecule, leading to the formation of the resulting Indigo-dye. The blue colored Indigo complex would then act as indicator for the presence of lysozyme.

The possible application of the nanocapsules in solution, for clinical infection detection assays, and the reaction process is graphically described in Figure 14.In the second part of this work,

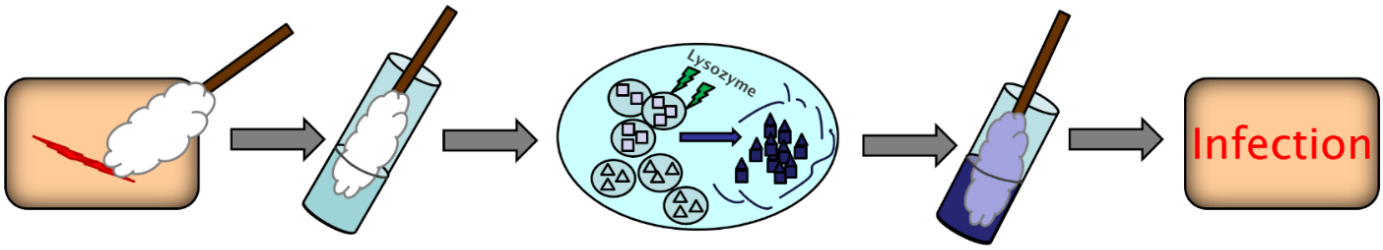

Figure 14: Graphical abstract of the color reaction mechanism used in this work. When lysozyme (lightning) is present in the wound and brought into the reaction mix, via the smear test, it would degrade the nanocapsule shell. Thus BCIP (squares) and alkaline phosphatase (triangles) can react and form the blue color, indicating the presence of lysozyme.

the possibility to bind the nanocapsules, as well as AP to paper, by EDC-NHS-coupling should be used to create a dipstick like assay. Here, it is expected, that the immobilization of nanocapsules leads to a more effective reaction and help decrease reaction time, to create a faster, more intense color signal, indicating the presence of lysozyme.

On the other hand, the solely binding of AP to paper, as described in the work of (Cao *et al.*, 2015), could help prepare a more precise dipstick-assay. When AP is effectively bound to a paper matrix, the paper could be coated with chitosan. When this type of paper is incubated in a solution of lysozyme and BCIP, the wound enzyme could degrade the chitosan-coat and BCIP could react with the isolated AP. This would lead to the conversion of BCIP into the blue colored indigo-molecule, indicating the presence of the wound enzyme.

2 Materials and Methods

2.1 Materials

Numerous devices, chemicals and different materials were used throughout the work. In this section types of used materials for the different experiments are listed in the following tables (Tables 1 to 6).

Table 1: List of used buffers

Buffer	Chemicals used	Specification
Acetic acid buffer	For 100 mL: 41 mL of 0.2 M acetic acid solution 9 mL of 0.2 M sodium acetate solution 50 mL of ultrapure water	0.2 M pH 4.0
KPO_4-buffer	For 1 L buffer: 8.98 g Potassium phosphate monobasic in 1 L UP-H_2O pH adjustment with 1 M KOH	66 mM pH 6.2
Potassium phosphate buffer	For 1 L buffer: 6.80 g potassium dihydrogen phosphate, pH adjustment if necessary	50 mM pH 4.5

Despite buffers, the materials for N-acetyl chitosan and nanocapsules preparation are mentioned in Table 2.

Table 2: Materials used to produce nanocapsules.

Material	Supplier	Specification
Shrimp chitosan	Sigma Aldrich	BCBQ3414V
Crab chitosan	Heppe Medical	90/50, DDA 89%
n-Dodecan	Sigma Aldrich	≥ 99%

All used color reagents and dyes are listed in Table 3.

Table 3: List of used color reagents.

Reagent	Supplier	Specification
BCIP	Sigma Aldrich	5-Bromo-4-chloro-3-indolyl phosphate disodium salt; ≥ 98% (HPLC)
Indigo	Sigma Aldrich	Analytical Grade ≥99%

The used enzymes were purchased by Sigma Aldrich and are described in Table 4

Table 4: Enzymes used throughout the project.

Enzyme	Supplier	Specification
Lysozyme	Sigma Aldrich	From chicken egg white Lot result 129103 U/mg
Alkaline phosphatase	Sigma Aldrich	From E. coli; 30-90 U/mg protein

All additionally used materials are listed in Table 5.

Table 5: Additionally, used materials

Name	Supplier	Specification
0.2 µm syringe filters	Whatman	Anotop 10 Plus
0.22 µm syringe filters	Whatman	PVDF-Filter
0.45 µm syringe filters	Marcherey-Nagel	Chromafil-PA
96Well-plate_UV-transparent	Eppendorf	UV-transparent
96 Well-plate- standard	Greiner	
Cuvettes for DLS	Wyatt	163255
Folded Capillary Cell for Zeta potential	Malvern	DTS 1061
Falcon Tubes	Greiner	15ml and 50ml
Microscope Slides	Sartorius	
Covering glass	Sartorius	
Syringes	Henke Sass Wolf	Norm-Ject 1ml
Needles	Becton, Dickinson and Co	BD Microlance 3

The instruments used throughout this work can be found in Table 6.

Table 6: instruments used in this work.

Device	Additional Information	Manufacturer
Balance	MSE1203S	Satorius
Balance	MSX (SD EE), Min: 1 mg, Max: 220g	Satorius
Camera (Microscope)	EOS 1300D	Canon
Centrifuge (for Reaction tubes)	5427 R	Eppendorf
Centrifuge (for Falcons)	5920 R	Eppendorf
Fourier transform infrared spectroscopy	Spectrum 100 FT-IR spectrometer	Perkin Elmer
Freeze dryer	FreeZone 2.5Plus	Labconco Corporation
Ice maker	Hoshizaki Ice Maker, Model number: FM-80KE-HC	Hoshizaki Europe Limited
Incubator	Innova44, incubator shaker series, Serial number: SI44FM103735	Eppendorf
Microscope	Olympus BX43, Model U-LHLEDC	Olympus Corporation
Nano Photometer	NP 80	Implen
pH electrode	Mettler Toledo	
Pipettes	2.5 µL, 20 µL, 100 µL, 200 µL, 1000 µL, 10 mL	Eppendorf
Platereader	Synergy HT	BioTek
Sonifier	SSE-1; Serial number: USW409213011-007	Branson
Wyatt DynaPro Nano Star detector	DynaPro Nano Star	Wyatt Technology Europe, Germany

2.2 Methods

The following methods belonged to certain parts of the project. For a better understanding, the affiliation of used techniques and the contributing part of the project is visualized in the following flowchart (Figure 15).

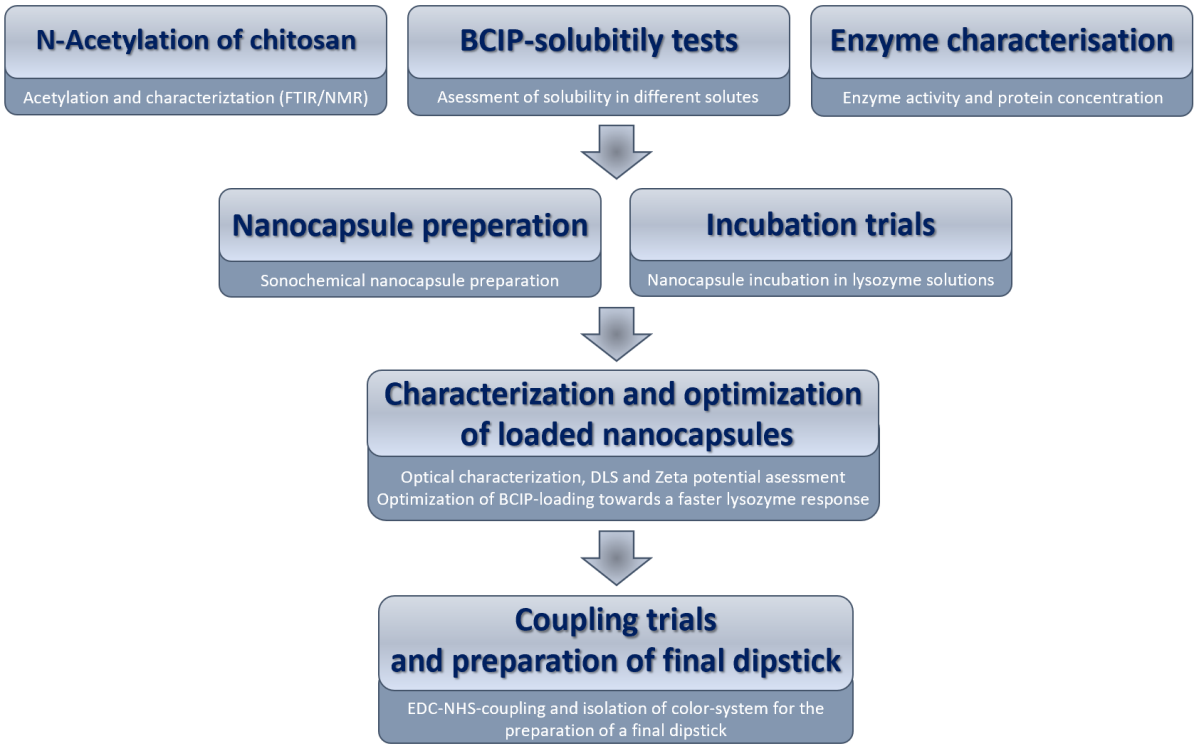

Figure 15: Organization chart of working packages leading to the development of a dipstick assay for the detection of Lysozyme.

2.2.1 N-Acetylation of chitosan

Based on the outcomes of pre-studies, 75% and 100% acetylated chitosan of different chitosan sources are among the most promising materials. Namely shrimp chitosan, and chitosan of crab shells, supplied by Heppe Medical (HMC) should be used for the experiments.

For this reason, 5 g of the native chitosan were mixed with 250 ml of 10% acetic acid and stirred at room temperature until everything was dissolved. Then the solution was slowly mixed with 500ml of absolute ethanol. In addition, acetic anhydride (Ac_2O) was added to the solution, the amount of Ac_2O added, was based on the pre-studies by (Tegl *et al.*, 2016) and can be found in Table 7. This solution was left for 1 h under ambient conditions and continuous stirring.

After 1 h, the pH of the solution was adjusted to pH 8 with 1 M and 10 M NaOH in order to precipitate the chitosan. The supernatant was separated from the acetylated chitosan by

centrifugation (3500 rpm for 10 min) and discarded, while the chitosan-pellet was washed with ultrapure water (UP-H_2O) until the supernatant showed a neutral pH value. For further experiments, the obtained N-acetylated chitosan was freeze dried and stored under ambient conditions.

As stated above, the used amount of acetic anhydride can be found in Table 7

Table 7: Calculated amount of acetic anhydride to be added to the solution in order to reach the desired acetylation degree

Acetylation degree [%]	Ac_2O added [ml]
75	2.25
100	3.0

2.2.2 Analysis of native and acetylated chitosan

2.2.2.1 Fourier Transmission Spectroscopy

All acetylated chitosan formulations were analyzed by FTIR in ATR mode and compared to the spectra of native chitosan by normalizing the spectra in the area of 1025 cm^{-1}. Additionally, a baseline correction was done to render the spectra comparable.

2.2.2.2 Nuclear Magnetic Resonance Spectroscopy

In order to characterize the acetylation and compare the acetylated chitosan with the native original, NMR-spectroscopy was performed and the degree of acetylation (DA) was calculated.

The sample was prepared by mixing10 mg of the chitosan with 10ml of deuterium oxide (D_2O), this mixture was then stirred for one hour. Here D_2O is used instead of water, to reduce the effect of Hydrogen on the NMR-spectra.

Afterwards acetic acid-D_4 was added, yielding a 1% (w/v) solution of acetic acid. This solution was stirred until all the chitosan was dissolved. In the final step, the solution was filtered through a 45 µm nylon filter into the NMR-tube. After this step a small spatula-tip of 4,4-dimethyl-4-silapentane-1-sulfonic acid (DSS) was added. This chemical was used as internal standard.

The prepared samples were analyzed using a Bruker Avance II 400 spectrometer (resonance frequencies 400.13 MHz) equipped with a 5 mm observe broadband probe head (BBFO) with z-gradients. The resulting ^1H measurement was used to calculate the DA by forming the integral of the proton peaks of H_2 of the native and the acetylated sample and calculated following Equation 7.

$$DA[\%] = \left(1 - \left(\frac{H_2D}{H_2D + \frac{HAc}{3}}\right)\right) * 100$$

Equation 7: Formula to calculate the DA

2.2.3 Preparation of chitosan based nanocapsules

After testing the degree of acetylation and the quality of the prepared chitosan-formulations, nanocapsules could be prepared following the optimized protocols of (Quadlbauer, 2018).

Therefore, 4.2 mg of the prepared chitosan was dissolved in 2 ml acetic acid buffer for several hours at 20°C. When it was ensured, that all the chitosan was dissolved, 1.3 ml of n-dodecan were slowly added to the solution, to create the organic phase, swimming on top of the chitosan-solution. This reaction mix could then be sonified according the conditions of Table *8* resulting from the pre-studies of this project.

After sonication, the resulting nanocapsule-suspension was stored in the fridge overnight to allow settling of the capsules. And washed with PBS-buffer by centrifuging 1ml aliquots (5000 rpm, 4 °C, 5 min) of the solution and exchanging the supernatant with PBS-buffer for 5 times. The aliquots were then stored at 4 °C for further experiments.

2.2.4 Sonication Method

The sonication conditions can be found in Table 8. A Branson 250 sonifier, equipped with a 12.7 mm disruptor horn was used for the sonication experiments. The total process had a limit of duration of 2 min. After the procedure was finished, and the nanocapsules were ready for further use.

Table 8: Sonication conditions for the preparation of nanocapsules depending on the type of chitosan used.

Chitosan Type	Amplitude [%]	Pulse On [sec]	Pulse Off [sec]
75% Shrimp	70	2	2,4
100% HMC	70	5	2

2.2.5 Loading of nanocapsules

In order to create nanocapsules carrying a lysozyme responsive color reaction-system, the BCIP dye molecules had to be loaded into the capsules. In order to do so, the solubility of BCIP had to be tested.

Therefore, the amounts, displayed in Table 9 were weighed into small glass vials and mixed with 1 ml of the respective phase for the solution. In this case, acetate buffer and n-dodecane were tried. Then the vials were left for stirring and in fixed time intervals, the vials were controlled for solid or dissolved BCIP-salt.

Table 9: BCIP amounts used for solubility experiments in Acetate buffer and Dodecane

Amount of BCIP [mg]	Solvent
1.0	n-dodecane/ acetate buffer 1 ml
2.5	
5.0	
10.0	
15.0	
25.0	
50.0	

After assessing the solubility, maximum amounts of BCIP were dissolved in the right phase and mixed with chitosan, to be used for the particle preparation according the procedure stated above.

2.2.6 Analysis of Nanocapsules

2.2.6.1 Dynamic Light Scattering

The aliquoted nanocapsule samples were diluted 15x in PBS-buffer and homogenized by vortexing. The DynaPro Nanostar system by Wyatt Technologies was programmed to measure the size for 30 minutes with an acquisition time of 2 seconds and 20 individual acquisitions. In addition, the size depending on the temperature was measured by setting a temperature gradient of 1 °C per minute from 25 °C to 80 °C with 10 acquisitions and an acquisition time of 2 seconds. For all measurements, 16 µl of the diluted sample were pipetted into a disposable cuvette by Wyatt and measured with a 90 °angle.

2.2.6.2 Zeta potential detection

A Malvern zetasizer Nano ZS was used to obtain the zeta potential (ζ) of the prepared nanocapsules. Therefore, the aliquoted samples were diluted 15x in PBS-buffer and injected into a folded, disposable capillary cell by Malvern. Every aliquot was measured in triplicates in automatic mode with 10-50 runs per measurement. The detailed settings can be found in Table 10.

Table 10: Conditions of zeta-potential measurements

Material	Dispersant	Viscosity [cp]	Scattering angle [°]	Mode
Chitosan RI 1,334	Water RI 1,330	0,8872	173	Automatic 10-50 runs

2.2.6.3 Visual characterization

In order to assess the quality optically, samples were diluted 10x in PBS-buffer and homogenized by short vortexing. The 15µl of the resulting dilution were transferred on microscope slides and the samples were visually qualified by 100x and 400x magnification. An Olympus Plan objective was used.

2.2.7 Enzyme characterization

2.2.7.1 Protein concentration detection

The protein concentration of enzymes used, was measured via a Bradford assay. The first step was the preparation of a calibration curve by the subsequent dilution of a BSA-standard of 2 mg/ml.

The dilutions were prepared with UP-H_2O and had following concentrations: 1; 0.5; 0.25; 0.2; 0.125; 0.1; 0.0625; 0.05; 0.03125; 0.025 mg/ml. The enzyme solutions were diluted 1:10; 1:100; 1:1000 with the appropriate buffer. In addition, a blank was created with the buffer used for the enzyme dilution and MQ-H_2O for the standard row.

For the measurement, 10 µl of each sample were mixed with 200 µl of a 1:5 diluted Bradford reagent solution in a 96 well plate. The plate was incubated at room temperature by shaking with 300 rpm for 5 min. Afterwards, the absorbance of each well was measured at 595 nm by a plate reader.

The protein concentration of the enzyme solutions was calculated by comparison of the absorbance values with the values for slope and intercept of the standard curve, following Equation 8. Before the calculation, all samples were corrected against the corresponding blank- value.

$$Protein\ concentration = \frac{(Abs.Sample - Abs.Blsnk) - Intercept}{Slope}$$

Equation 8: Adapted formula of the BSA- standard curve, to calculate the protein concentration of the sample.

2.2.7.2 Lysozyme activity measurement

The lysozyme activity assay was based on the degradation of *Micrococcus lysodeikticus.* In a first step a 0,01% (w/v) solution of the dried bacteria was prepared by dissolving it in potassium phosphate buffer (66 mM, pH 6.2 at 25 °C). Lysozyme solutions were done in different concentrations (0.1, 0.05, 0.0075, 0.005, 0.0025 and 0.001 mg/ml) in potassium phosphate buffer (KPO_4) In a 96 well plate, 290 µl of the substrate solution were mixed with 10 µl of enzyme solution and immediately measured at 450 nm for 10 min.

By plotting the decrease in absorbance against the time, a curve can be created. The slope of the resulting curve corresponded to the enzyme activity.

2.2.7.3 Activity assay of Alkaline Phosphatase

The activity assay for AP was purchased from Sigma Aldrich. Here, the reaction of the enzyme with the substrate, p-nitrophenyl phosphate, resulted in the formation of the yellow, dephosphorylated product. The absorbance of the yellow reaction product could be measured at 405 nm. By reading the increase in absorbance over a period of 5 min, after mixing the enzyme with the substrate, an external calibration curve could be created. The slope of the resulting curve was connected to the activity of the enzyme, as seen in Equation 9, Equation 10 and Equation11. The faster, the absorbance- intensity of the yellow product increased, the more active, the enzyme had to be.

For the activity measurement, the solutions of Table 11 had to be prepared.

Table 11: List of Solutions and their specifications, prepared for the activity measurement of AP.

Solution	Specification
A: Glycine buffer with MgCl and ZnCl	100mM Glycine buffer, supplemented with 1mM MgCl and 1mM ZnCl
B: Substrate solution	60mM P-Nitrophenyl phosphate solution
C: MgCL-solution	1mM MgCl
D: Sample solution	A solution of 0,1-0.2U/ml dissolved in reagent C

After preparation of the solutions, the reagents were combined in a microtiter plate according the protocol. The stepwise pipette scheme can be seen in Table 11.

Table 12: Pipette scheme for the measurement of AP-Activity

Step	Reagent solution	Blank [µL]	Sample [µL]
1	Reagent A (buffer)	260	260
2	Reagent B (substrate)	30	30
3	Mix by shaking		
4	Reagent C (MgCl-solution)	X	10
5	Reagent D (Enzyme Solution)	10	X

After mixing the reagents in the 96 well-plate, the samples were immediately measured at 405 nm for 5 min with a measuring interval of 20 sec. The absorbance values were then used to prepare a curve, which indicates the activity by the slope. In addition, the exact activity was calculated, following Equation 9, Equation 10 and

Equation ***11***.

$$U/ml_{Enzyme} = \frac{\Delta A_{405\ nm/min\ Sample} \Delta A_{405\ nm/min\ Blank} * 3 * df}{18.5 * 0.1}$$

Equation 9: Formula for the calculation of enzyme activity per ml of enzyme used. Whereby 3 is the total volume in ml, df is defined as the dilution factor, 18.5 is the corresponding extinction coefficient of the substrate and 0.1 is the sample volume in ml)

$$U/mg\ Solid\ sample = \frac{U/ml}{mg\ Solid/ml\ Enzyme}$$

Equation 10: Formula for the calculation of enzyme activity regarding the amount of solid sample.

$$U\ per\ mg\ of\ Protein\ used = \frac{\frac{U}{ml}}{mg\ Protein\ per\ ml\ Enzyme\ sample}$$

Equation 11: Formula for the calculation of enzyme activity regarding the protein concentration of the sample.

Here it should be mentioned that one unit of enzyme activity corresponds to the hydrolyzation of 1 µmol of P-nitrophenol phosphate per minute at pH 10.4 and 37 °C

2.2.8 Testing of lysozyme responsiveness

2.2.8.1 Incubation method

In order to control the lysozyme responsiveness, the nanocapsules were incubated, following a fixed method. To obtain comparable results, the incubation parameters had to be kept for all experiments. Epis containing the reaction mix, were incubated in a horizontal position, at 150 rpm and 37 °C In a standard experiment, the reaction mix consisted of, 250 µl of the nanocapsule sample solution mixed with 500 µl buffer and 1 µl/ml Alkaline Phosphatase. The volumes of the different components could be changed for optimization reasons, with respect to keeping the incubation conditions constant for a comparable output.

2.2.8.2 Optimization of Lysozyme responsiveness

To create a properly working detection mechanism for lysozyme, effective nanocapsules with the right load of BCIP had to be created. Therefore, different amounts of BCIP were dissolved in the aqueous phase of acetate buffer and dissolved N-acetylated chitosan.

The prepared nanocapsules were incubated according the before mentioned standard procedure for testing the lysozyme responsiveness. The results of these incubations were used for the creation of new nanocapsules with a corrected dye load, according the trend of the data resulting from the incubation. Thus, the amount of BCIP loaded into the capsules could be optimized, until no further improvement in response time was recognizable.

2.2.9 Dipstick assay preparation

After the nanocapsules were characterized and the lysozyme responsiveness was tested and optimized, the capsules should be immobilized on a filter paper-stripe to create a pilot of a user-friendly dipstick assay.

Therefore, the nanocapsules should be bound to the paper-stripe by an EDC-NHS coupling reaction. Hence, filter paper was cut into strips of 1.8 cm*7.5 mm and activated by dripping 20 µl of 0.05% Sodium alginate (Na-Alg) solution onto the paper stripe. This paper stripe was left for drying overnight.

After the activation step, the paper stripe was transferred into a wet box and the protocol for EDC/NHS coupling was applied. All necessary solutions are visualized in Table 13.

Table 13: All solutions necessary for the coupling experiments of nanocapsules

Solution	Specification	Work step
UP-H_2O	18,2 MΩcm	Basic solvent for buffer preparation
MES Buffer	0.1 M pH 4,6	Solution for EDC and NHS
EDC in MES	0.1 M	Crosslinking solution
NHS in MES	0.1 M	Crosslinking solution
Coupling buffer	1.5% (w/v) mannitol, 0.15% (v/v) glycerol, 0.01% (v/v) Tween 20 in PBS-buffer	Coupling buffer for the application of nanocapsules to be bound to paper
Wahing buffer	Tris-HCl buffer (50 mM pH 9.2) with additional 0.1% (v/v) Tween 20	Washing steps

At first, 2* 20 µl of 0.1 M EDC solution was dropped onto the paper, with a waiting period of 15 min in between the steps. Afterwards, 20 µl of 0.1 M NHS were applied and left for reacting for another 15 min. After the EDC/NHS-application, the nanocapsule solution was dripped onto the paper. In order to prepare the solution, a buffer exchange was required, therefore, the nanocapsules were centrifuged and washed with the coupling buffer, according the protocol for particle washing, described in 2.2.3. Here, 500 µl of nanocapsules in coupling buffer were applied, in order to have a saturating amount of nanocapsules on the paper. This mix was left on the paper for 2 h to allow the chitosan capsules to bind, to the crosslinking EDC/NHS. After the incubation, the paper stripes were taken out of the wet box and washed with 5x1 ml washing buffer on both sides, with a pipette, washing away everything unbound to the paper. Then, the stripes were left for drying under ambient conditions and a constant air flow under the fume hood. After 24 h, the paper stripes were washed one more time with 5 ml washing buffer on both sides. After drying in the fume hood, the paper stripes were ready for analysis and incubation experiments.

Additionally to the coupling of nanocapsules to filter paper stripes, the procedure of (Cao *et al.*, 2015) should be tested. Here, a zero-step functionalization for the coupling of AP was shown. In the experiment. AP should be coupled, and the paper should then be covered with a layer of chitosan. The expected outcome, was a lysozyme responsive dipstick assay, based on the principle of the developed nanocapsules. When lysozyme would be present in the sample solution, it would degrade the chitosan layer and the reaction solution, containing BCIP could react with the immobilized AP to form the blue Indigo-product, indicating the presence of lysozyme.

To create this dipstick like assay, the paper stripe was again activated with NaAlg overnight. Then, following the adapted protocol of (Cao *et al.*, 2015), stated above. Instead of applying the particle solution after the NHS-treatment step, here, 3 µl of 100 µg/ml AP in coupling buffer was applied and left for binding for 2 h in the wet box. After the binding period, the paper stripes were washed again with 5 times with 1 ml of washing buffer with a pipette and left for drying overnight. The resulting paper stripes were ready for analysis.

To create a lysozyme responsive dipstick, the paper stripes with coupled AP had to be coated with chitosan. Therefore, 4.2 mg/ml Chitosan were dissolved in acetic buffer and sprayed onto the paper, using a pump bottle. In order to create an isolating coat, this step was repeated 4 times for each side with a drying step, under ambient conditions, after each chitosan application step.

After the chitosan was applied four times and the paper stripes were dried completely and could be subsequently used for the incubation experiments under the conditions described in 2.2.8.1.

3 Results and Discussion

3.1 Reacetylation of Chitosan

3.1.1 FTIR-spectroscopy of n-acetylated chitosans

The first working steps were affiliated with the preparation of lysozyme responsive chitosan by re-acetylation. The graphs, seen below, show the FTIR-spectra of re-acetylated chitosan, using the technique of Tegl et al. In addition, the spectra of the native form of the sample is displayed, in order to compare the samples in one graph. Acetylated Chitosan is shown as orange graph, while the native form is displayed in blue. A change in distinctive bands is clearly visible throughout the graphs.

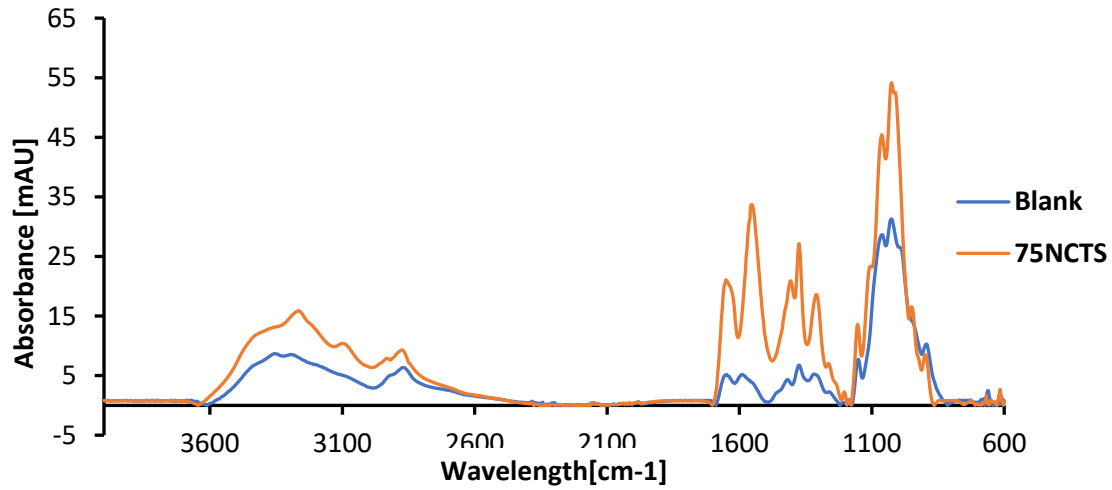

Figure 16: FTIR spectra of 75% N-acetylated shrimp chitosan. The spectra of native chitosan is displayed in blue, while N-Acetylated chitosan is shown as orange graph.

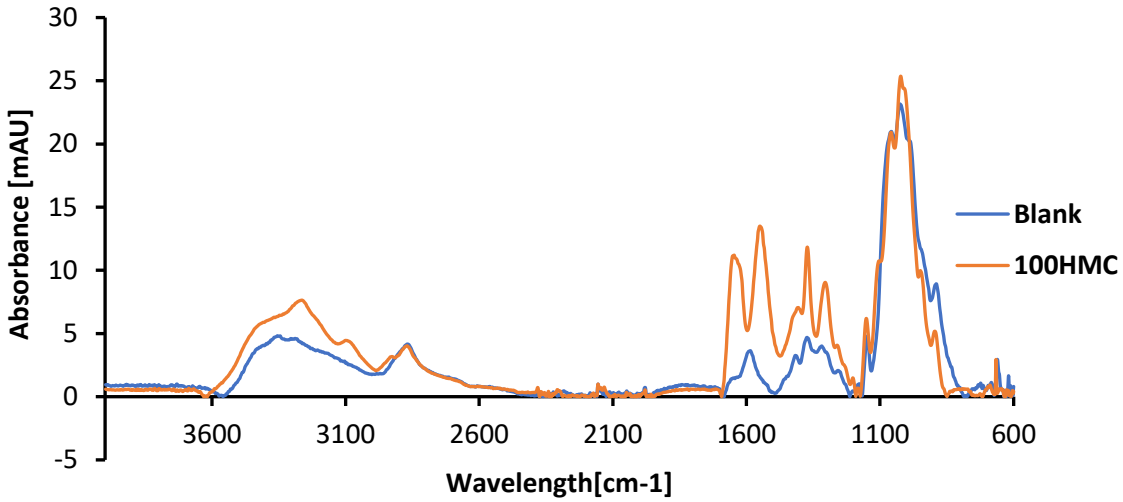

Figure 17: FTIR-spectra of 100% N-Acetylated chitosan by Heppe Medical. The obtained spectra for N-Acetylated chitosan is displayed in orange. The native chitosan is displayed in blue.

Despite the obvious change of the FTIR-spectra in general, it is important to illuminate the change of characteristic bands, confirming the re-acetylation of commercial chitosan. The characteristic peaks are listed in Table 14.

Table 14: Characteristic peaks in chitosan re-acetylation. The corresponding wavenumber to certain characteristic bands suggested by Tegl *et al.* is shown in this table.

Type	Band position
Amide stretching	1640 cm^{-1}
Carbonyl stretching	1540 cm^{-1}
NH_2 oscillation	1580 cm^{-1}

At a closer look, the decline in absorbance at 1580 cm^{-1} connected to the NH_2 oscillation, can be seen. This is decline is clearly connected to the acetylation and states a first proof for the proper re-acetylation.

The obtained FTIR data can be compared with the findings of Tegl *et al.* In this research on the re-acetylation of chitosan, the degree of acetylation was assigned to an increased absorbance in the bands of the Amide I (1640 cm^{-1}) and Amide II (1560 cm^{-1}). (Tegl *et al.*, 2016) Like in the preliminary project of Tegl *et al.* the re-acetylated chitosan of this work shows the typical change in characteristic bands in the FTIR-spectra.

In summary, it can be said, that the recorded FTIR-spectra show a distinctive change of the native chitosans, towards an acetylated form, giving a first proof, that the re-acetylation reaction worked.

3.1.2 NMR-spectroscopy

To confirm and quantify the acetylation of commercial chitosan, samples were analyzed via NMR-spectroscopy. The obtained NMR spectra were integrated and the obtained values for H_2D and HAc were used to calculate the degree of acetylation (DA) following formula of Equation 7. Both spectra can be found in the Appendix. The calculated DA was 79.08% for the 75% shrimp chitosan which is a promising result, indicating a very good acetylation reaction. For the 100% HMC chitosan, the obtained DA was calculated to be 87.17%, which is lower than the expected DA which should come close to 100%. Here it should be mentioned, that the acetylation process relies on a random reaction and DA-values in this range are already very satisfying, as significantly lower DA-values were obtained in previous works (Quadlbauer, 2018).

3.2 Characterization of Enzymes

3.2.1 Protein concentration

Despite the characterization of chitosan for the preparation of nanocapsules, the enzymes used throughout this work, had to be characterized. Therefore, the protein concentration of AP was measured. This analysis was not necessary for Lysozyme, because the enzyme was bought as freeze-dried powder of analytic purity.

The protein concentration of the AP-formulation was assessed, using the Bradford assay. The dilutions of AP were done in UP-H_2O. All measurements were corrected with a blank value for the ultrapure water. The resulting calibration curve can be seen in Figure 18, the calculated protein concentration and dilutions used, are visualized in Table 15.

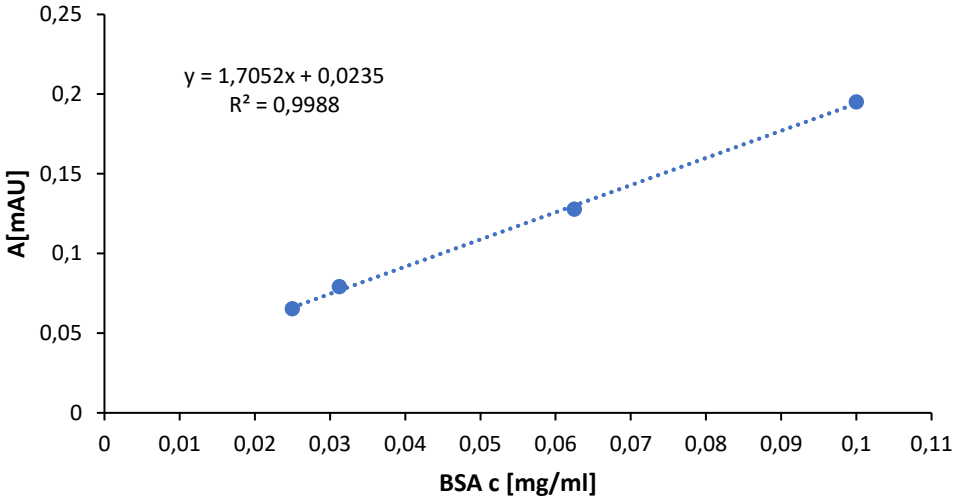

Figure 18: Calibration curve of diluted BSA standards for protein concentration measurement of enzyme dilutions.

Table 15: Protein concentration of Alkaline Phosphatase, calculated via Bradford assay.

Sample	Protein concentration [mg/ml]
AP 1:10	2.629
AP 1:100	2.225
AP 1:1000	-10.214

The protein concentration shows reliable values for the 1:10 and 1:100 dilutions. At the higher 1:1000 dilution, the samples were out of the measurable range, thus the value must be seen critically. In the following experiments, the average value of 2.43 mg/ml was used for further calculations.

3.2.2 Alkaline Phosphatase Activity

After assessing the protein concentration of enzyme formulations, the activity of lysozyme and AP should be measured with the respective activity assay.

With the data of these experiments, the performance of the enzymes used in this work could be assessed properly and the development of a lysozyme responsive assay could be done.

The activity of the enzyme formulation was measured following a protocol obtained by Sigma Aldrich. The reaction is visualized as curve, based on the absorbance of the reaction product. The slope of the curve displayed in Figure 19 was used to calculate the activity of the enzyme, following Equation 9.

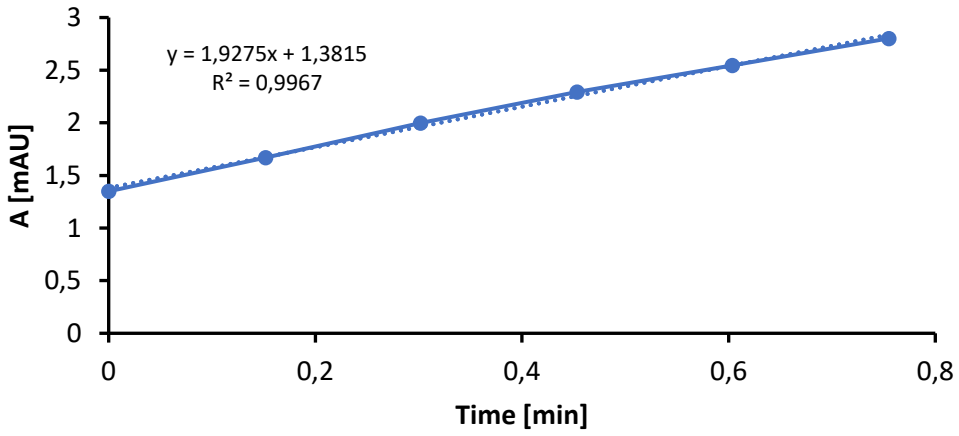

Figure 19: Reaction curve of the de-phosphorylated yellow product resulting from the reaction between AP and PNP.

The curve, resulting from the yellow reaction products indicates high enzyme activity, due to the low reaction time, until the curve leaves the linear range. The activity calculated by the recorded slope was 279.1 U/ml.

Although it is difficult to compare the measured activity with values of the literature, because different methods for the measurement are used, leading to various outcomes, which are hard to compare. However, Bowers *et al.* published AP-activities of a large group of healthy human probands, measured by the same method as it was used in this work. Here, the activity values of 258 participants ranged between 6 and 110 U/ml leading to a mean activity of 49 U/ml. (Bowers and McComb, 1966)

Because the effect of other enzymes brought into the developed assay by the samples of patients should be minimized, the AP used in the development of the assay should be highly active. The activity presented by Bowers *et al.* is by far lower than the activity measured for the Enzyme used throughout this work. Thus, it can be ensured, that if AP is brought into the

assay by the sample, the AP activity of the system is not heavily increased, leading to a distortion of the test result.

Following the protocol of the incubation and characterization of prepared nanocapsules, where 1µl of AP-solution was used, the reaction mix contained AP with an activity of 0,28 Units.

3.2.3 Lysozyme Activity

The lysozyme activity assessed by the degradation of freeze-dried *Micrococcus lysodeikticus* led to the reaction curves displayed in Figure20.

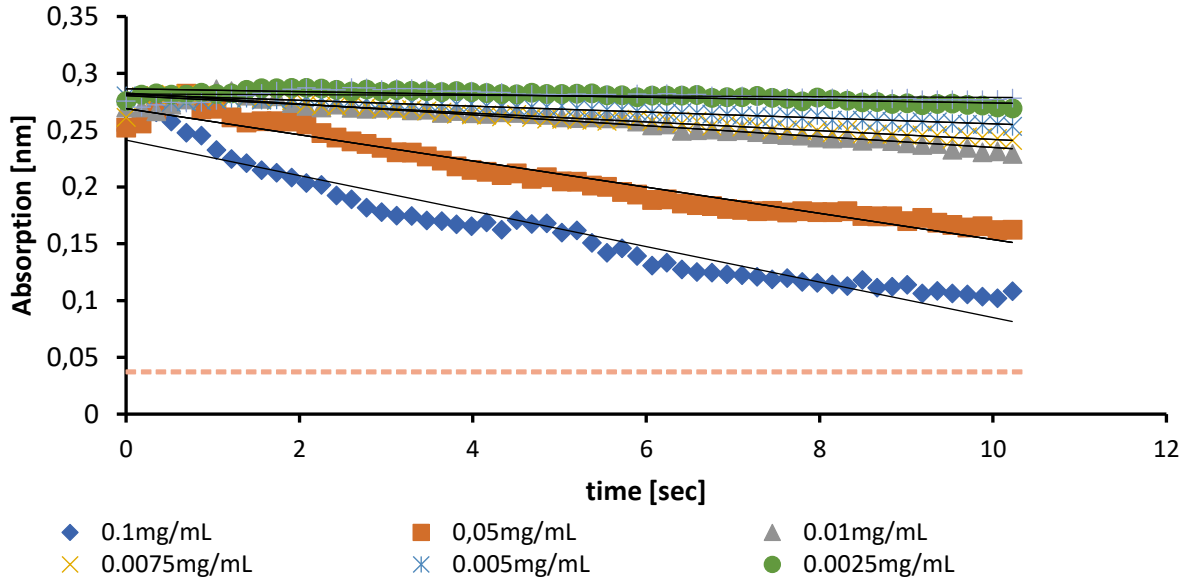

Figure 20: Curves resulting from the incubation of *Micrococcus lysodeikticus* with distinctive concentrations of Lysozyme solutions.

The slope of distinctive curves with a trustful linearity were used to create the calibration, seen in Figure 21.

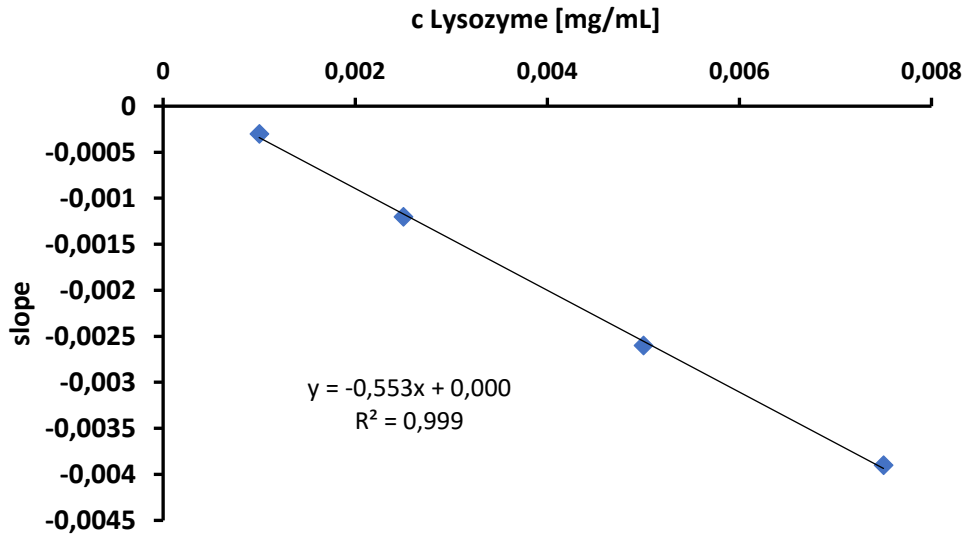

Figure 21: Calibration curve, created by the slopes of reactions with distinctive lysozyme solutions

Following the calculations of

Equation ***12***, the lysozyme activity was 55300 U/mg. This value was used for further experiments and the preparation of lysozyme solutions.

Equation 12: Calculation of the Lysozyme Activity, based on the calibration curve created.

$$y=-0.553+0.000$$

$$1\ U=0.001/min$$

$$1\ U=\Delta A=0.001/min$$

$$\Delta A=0.553 \Rightarrow 553\ U/min \Rightarrow 55300\ U/mg$$

In comparison to the previous work of (Quadlbauer, 2018), where the enzyme activity was calculated to be 50800 U/ml, the activity of this lysozyme batch was 4500 U/ml higher. This increased enzyme activity had to be respected and protocols had to be adapted to the higher activity.

3.3 Solubility experiments

After completing the characterization of the used enzymes and Chitosan, which should form the shell of the nanocapsule-carrier system, the solubility of BCIP should be tested. This experiment should help in planning the BCIP loading of the nanocapsules.

The solubility of the BCIP-salt should be characterized until 25mg/ml in acetate buffer. After weighing in the correct amounts of the salt, 1ml of acetate buffer was added and the samples were left on the stirring plate.

Table 16 shows the BCIP concentration and time until the salt was fully solubilized.

Table 16: Necessary time for the solubilization of BCIP, depending on the concentration.

BCIP concentration [mg/ml]	Time until solubilized [min]
1mg/ml	5 minutes
2.5mg/ml	5 minutes
5mg/ml	5 minutes
7.5mg/ml	5 minutes
10mg/ml	5 minutes
15mg/ml	7,5 minutes
25mg/ml	20 minutes

After assessing the solubility of BCIP in acetate buffer, the combination of this solution (BCIP in acetate buffer) with chitosan had to be tested. Therefore, 4,2 mg of chitosan were mixed into the reaction mix. After several hours, chitosan was dissolved, but a slight blue color of the solution could be observed in reaction mixes with higher BCIP concentrations. This leads to the assumption, that the dye was too long in solution and activated. The reaction of BCIP could be induced by the constant stirring, or by heat formation, which could be noticed on certain stirring plates. Still, no precipitation of BCIP or chitosan was visible.

In order to dissolve chitosan and BCIP effectively for the preparation of nanocapsules, the working steps were arranged in a new order. At first chitosan was dissolved in acetate buffer and after full solubilization, BCIP was added. After the salt was dissolved, the mix was ready for nanocapsule preparation.

3.4 Nanocapsule characterization

3.4.1 Particle Microscopy

The reaction mixes were sonified, following the conditions based on the type of used chitosan. After sonification, the typical appearance of nanoparticle emulsions could be observed.

After washing and aliquotation, the nanocapsules were assessed by the techniques described in 2.2.4. The results should be clearly visualized in tables. All measurement data connected to every sample can be found below.

A summary of microscopy pictures made of the different particle formulations can be seen in Figure 22 and Figure 23.

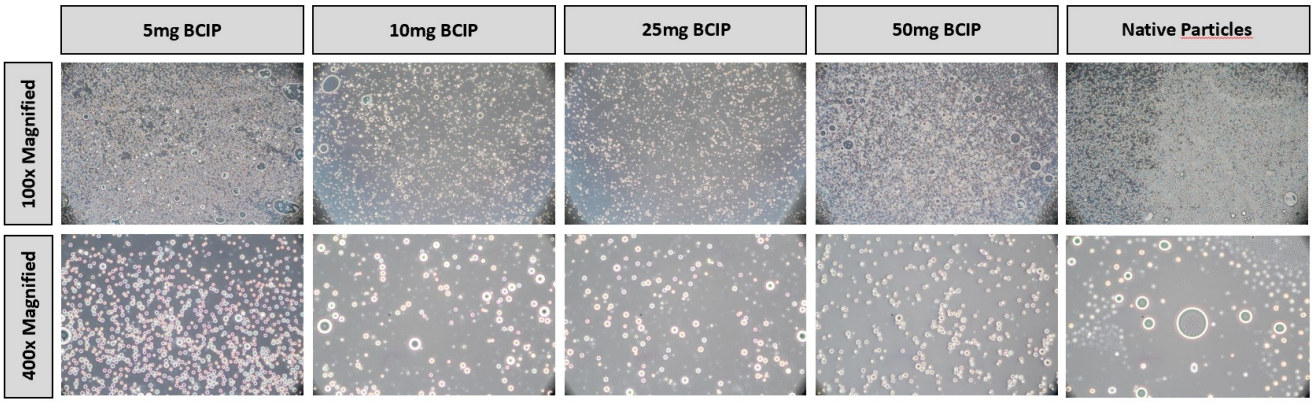

Figure 22: Microscopy Pictures of 75%NCTS-nanocapsules, loaded with different amounts of BCIP

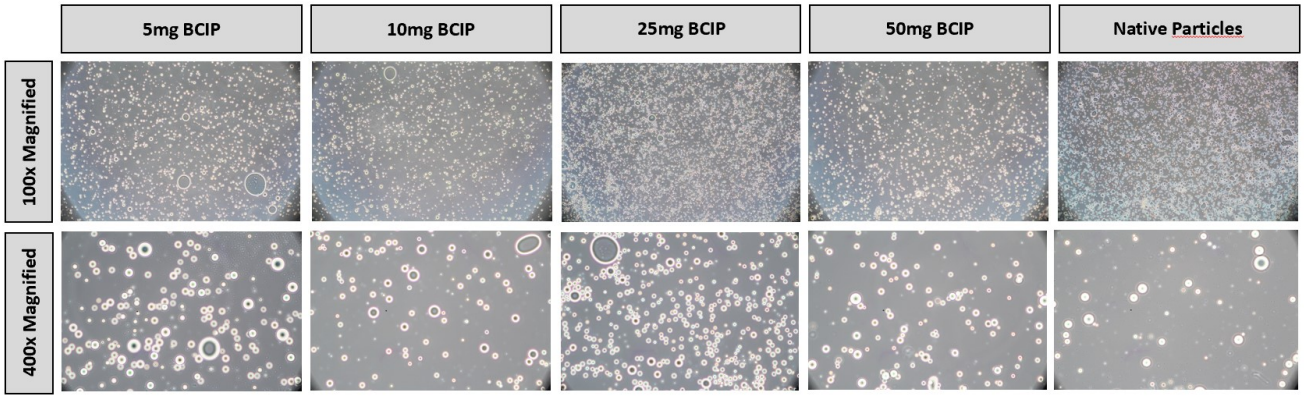

Figure 23: Microscopy Pictures of 100% HMC-nanocapsules, loaded with different amounts of BCIP

The microscopy analysis of nanocapsules is an appropriate tool to confirm the formulation of a nanocapsule emulsion and to assess the density of the emulsion. In order to define an exact difference between the formulations, analytics with more sophisticated tools are necessary. Therefore, the hydrodynamic radius and zeta potential of the nanocapsules were measured.

3.4.2 Nanocapsule size measurement via DLS

Unloaded nanocapsules of 75% acetylated shrimp chitosan and 100% acetylated Heppe Medical chitosan had a hydrodynamic radius of respectively 661.11 nm and 487.7 nm. Capsules loaded with different amounts of BCIP showed a slightly higher hydrodynamic radius. The measured values are displayed in Table 17.

Table 17: Hydrodynamic radius of different nanoparticle formulations.

Sample 75% Shrimp	Hydrodynamic radius [nm]
5 mg BCIP	766.17
10 mg BCIP	808.21
25 mg BCIP	1138.53
50 mg BCIP	1169.13
Sample 100% HMC	**Hydrodynamic radius [nm]**
5 mg BCIP	690.78
10 mg BCIP	587.44
25 mg BCIP	675.83
50 mg BCIP	1141.24

For better visualization, the distribution of sizes against the amount of BCIP, loaded into the capsule is shown in Figure 24 and Figure 25.

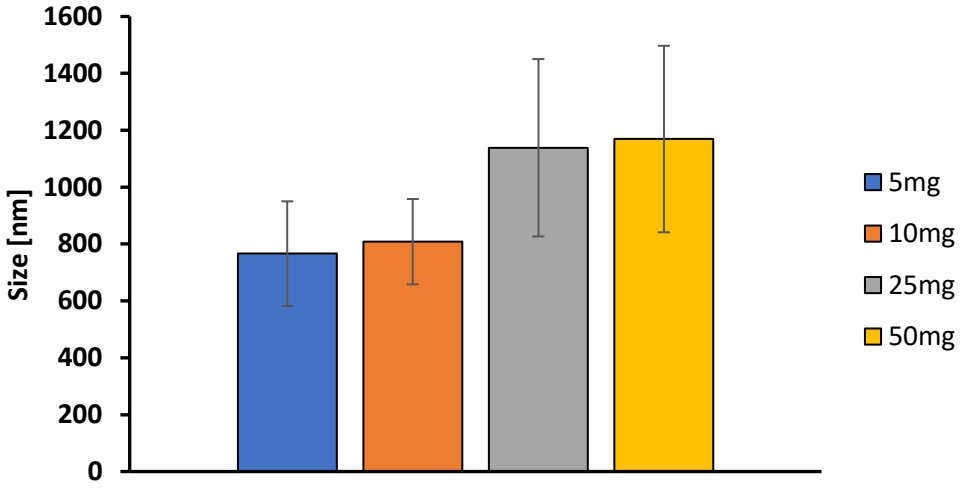

Figure 24: Average size of nanocapsules loaded with different amounts of BCIP, made of 75% acetylated Shrimp Chitosan.

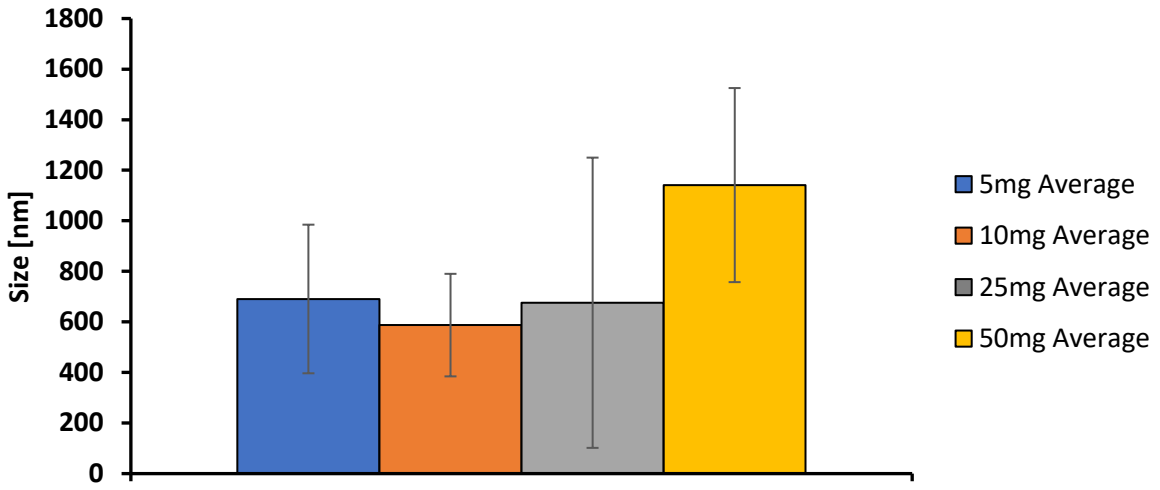

Figure 25: Average size of capsules loaded with different amounts of BCIP, made of 100% acetylated Chitosan by Heppe Medical

Compared to the preliminary work of (Quadlbauer, 2018), the nanocapsule sizes of unloaded samples are in a similar range. This shows that the optimization of nanocapsules and the protocol for the preparation of nanocapsules is reproducible. Also, the incorporation of the BCIP-salt does not lead to drastic changes in size, which indicates a high stability of the prepared nanocapsules.

3.4.3 Assessment of temperature dependent size changes

In order to investigate the stability of nanocapsules in a more precise manner and to obtain information on stability, the size of nanocapsules during a constant increase in temperature, should be measured over a time period of 30 minutes. The development of size during this temperature increase, for all nanocapsules created from 75% re-acetylated shrimp chitosan and 100% re-acetylated crab chitosan can be found in the following figures.

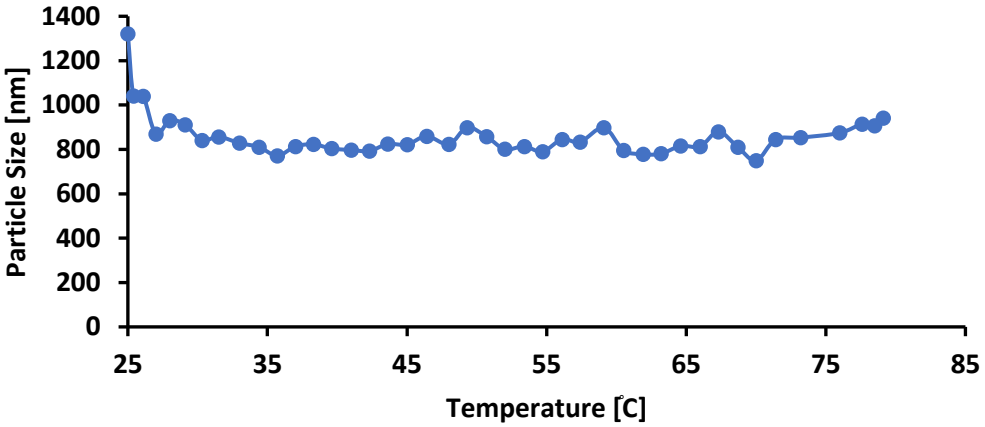

Figure 26: Size development of nanocapsules made from75% re- acetylated shrimp chitosan, loaded with 5mg BCIP, over a constant heat increase

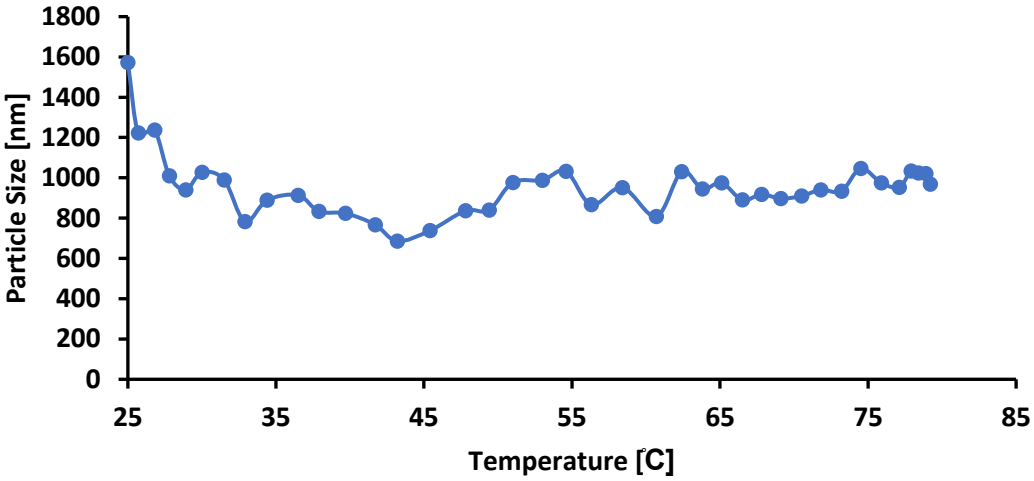

Figure 27: Size development of 75% Shrimp capsules, loaded with 10mg BCIP, over a constant heat increase

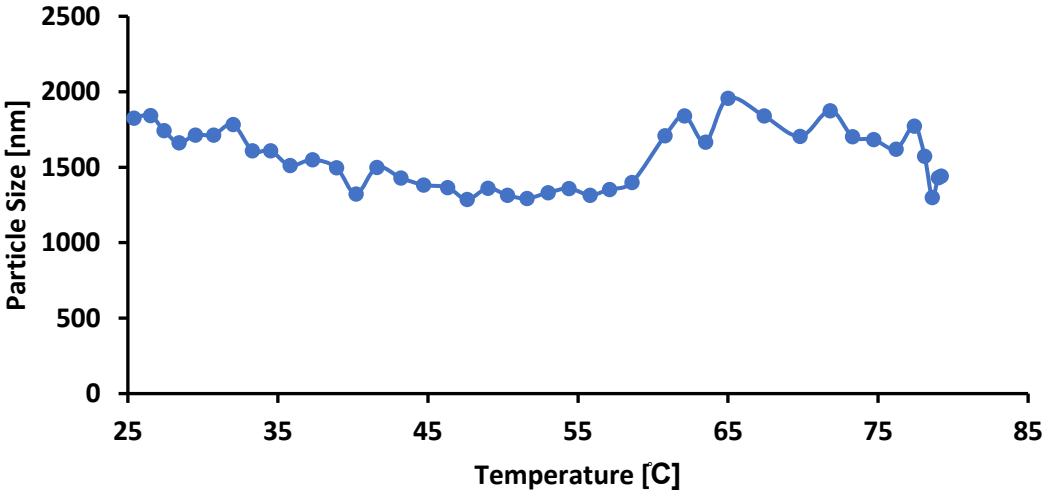

Figure 28: Size development of 75% Shrimp nanocapsules, loaded with 25mg BCIP, over a constant heat increase

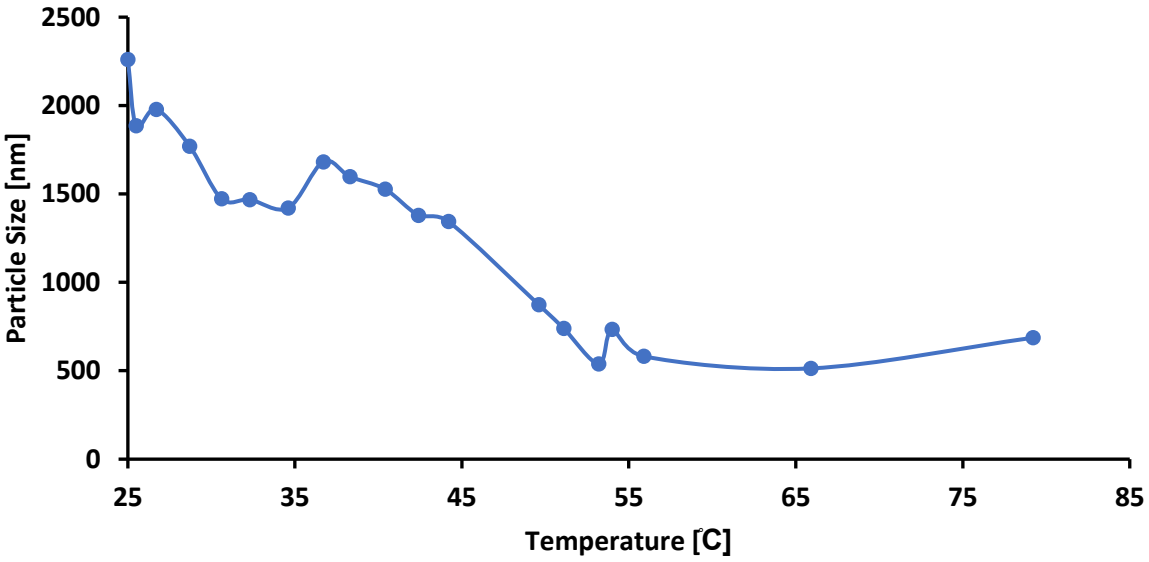

Figure 29: Size development of 75% Shrimp capsules, loaded with 50mg BCIP, over a constant heat increase

The temperature dependent size change of the prepared nanocapsules is behaving quite constant for dye loadings until 10 mg/ml. Nanocapsules loaded with a higher amount of BCIP, already show a different behavior. In respect to nanocapsules loaded with 25 mg/ml BCIP, the size is not as stable and the hydrodynamic radius seems to grow. The measurement of the sample loaded with 50 mg/ml BCIP, on the other side, shows a drastic decrease in size at 35 °C. This behavior could show a reduced stability of nanocapsules, loaded with a higher amount of substrate. In addition, the higher load of BCIP could lead to an interference with the optical principle of the measurement, resulting in measurements afflicted with a higher number of errors.

Respecting the nanocapsules made from 100% re- acetylated crab chitosan, the different measurements, displayed in the following figures, shows a more stable behavior. Only nanocapsules loaded with 50 mg/ml BCIP, show an increase in size, from 60 °C.

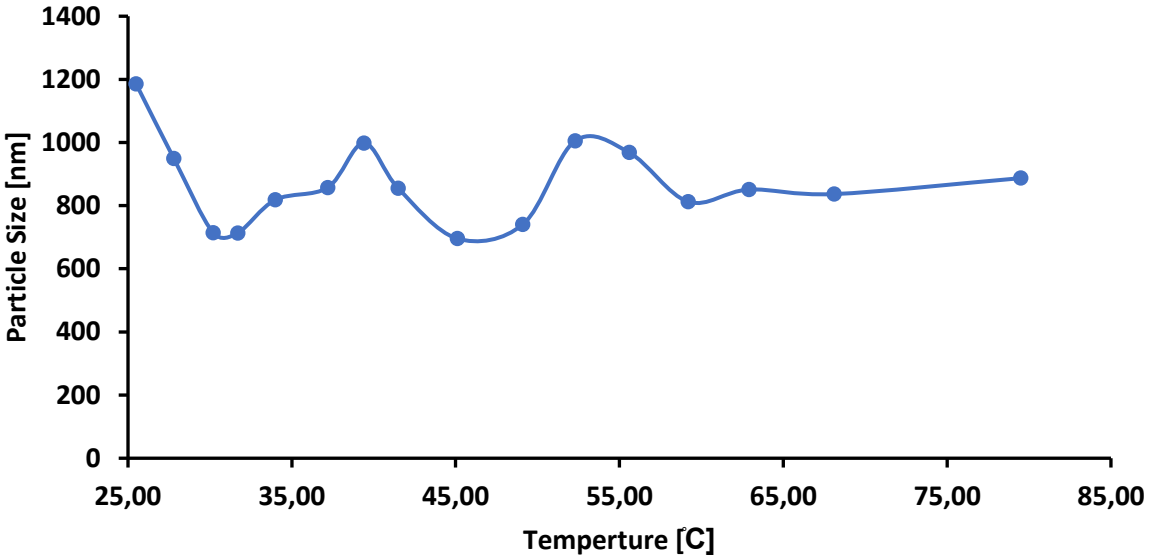

Figure 30: Size development of 100% re-acetylated crab chitosan nanocapsules, loaded with 5mg BCIP, over a constant temperature increase

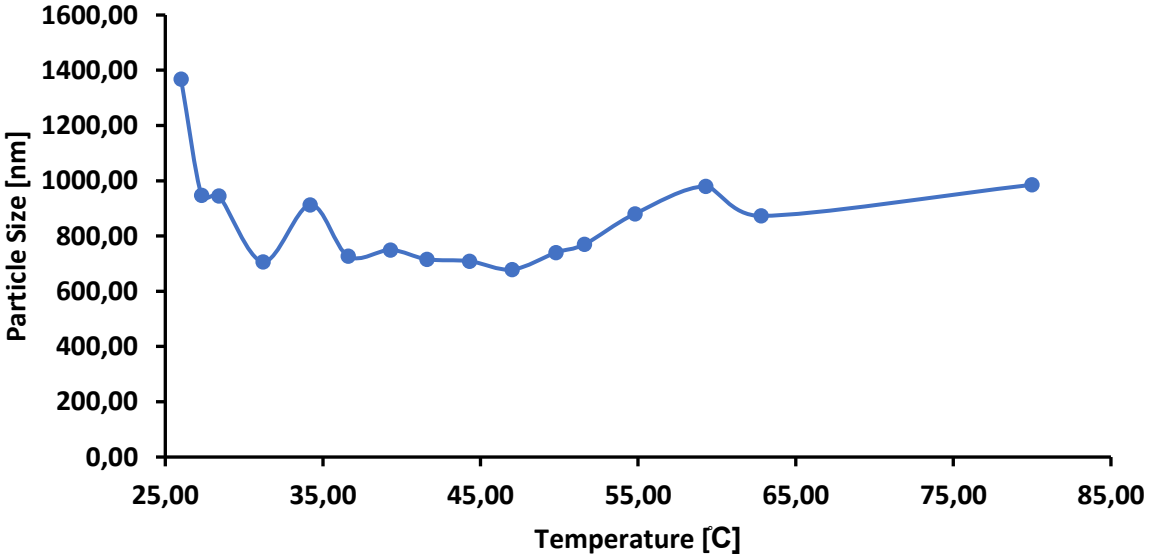

Figure 31: Size development of 100% HMC- nanocapsules, loaded with 10mg BCIP, over a constant temperature increase

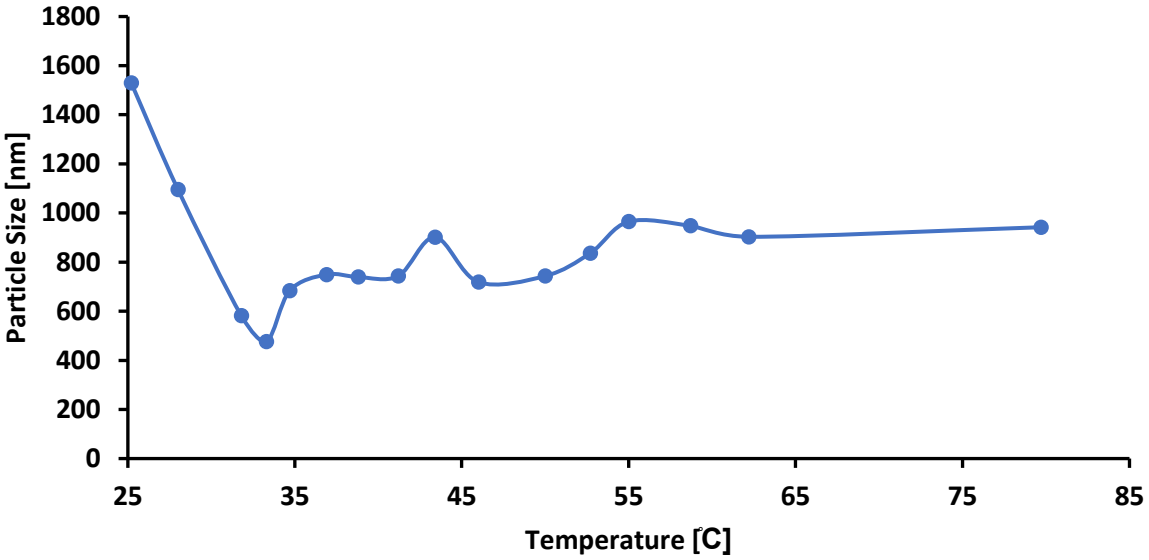

Figure 32: Size development of 100% HMC- nanocapsules, loaded with 25mg BCIP, over a constant temperature increase

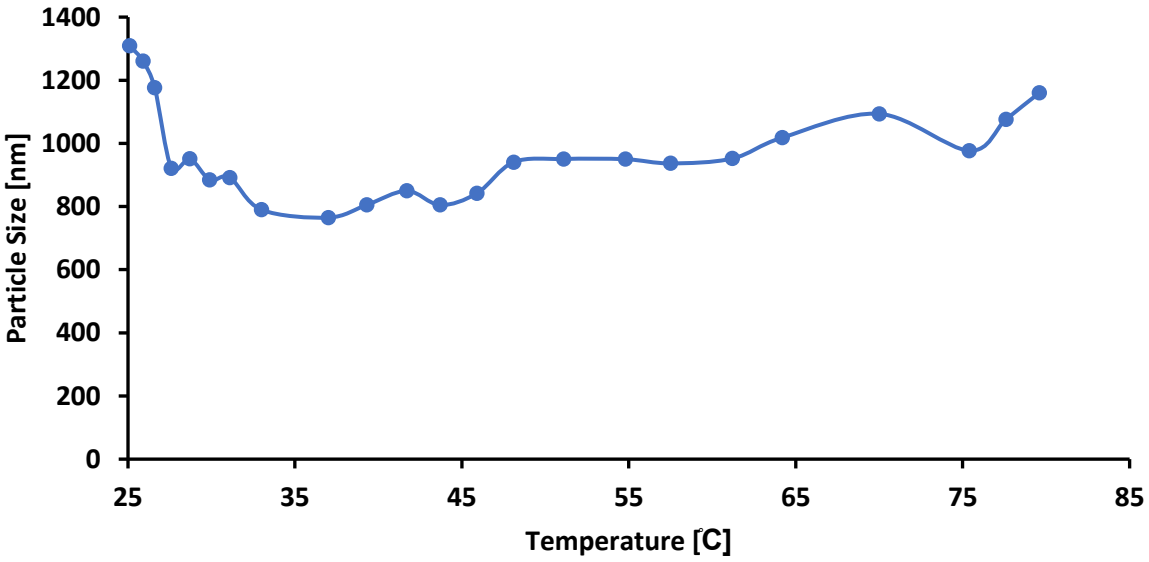

Figure 33: Size development of 100% HMC capsules, loaded with 50mg BCIP, over a constant temperature increase

3.4.4 Zeta potential measurement

The Zeta potential of all nanocapsule formulations was measured as triplicate, in order to assess the stability of the prepared nanocapsule emulsions. The measured values can be seen in Table 18.

Table 18: Average Zeta Potential of Nanoparticle formulations.

Nanocapsule type		Zeta potential [mV]	Standard deviation [mV]
75% Shrimp	5mg BCIP	22.64	1.09
	10mg BCIP	20.94	0.42
	25mg BCIP	21.87	0.78
	50mg BCIP	22.64	0.55
100% HMC	5mg BCIP	25,53	1.10
	10mg BCIP	23.57	0.99
	25mg BCIP	25	0.78
	50mg BCIP	23.17	1.46

Despite the first expectations, the amount of BCIP, loaded into the nanocapsules did not seem to have an impact on the Zeta potential. The Zeta potential of 100% HMC capsules was slightly higher, than the potential of 75% acetylated Shrimp chitosan nanocapsules, but throughout the BCIP concentrations, the Zeta potential was in the same range of about 22mV for 75% NCTS and about 24 mV for 100% HMC nanocapsules. This Zeta potential indicates high stability and non-agglomerating behavior. In addition, the measures Zeta potential was in the same range, as the Zeta potential of original, unloaded nanocapsules.

Here, the measured Zeta potential is comparable with the work of (Quadlbauer, 2018), respecting the nanocapsules made from 75% re-acetylated shrimp chitosan. For the samples made from 100% re-acetylated crab chitosan, the preliminary work suggests different values. A zeta potential of only 13.87 mV was measured in the pre-studies, while the measurements made in this work show a higher Zeta potential, indicating a higher stability. Also, the data is following the impression of the size measurements, respecting the dye loaded into the capsule. In addition, the amount of BCIP loaded into the nanocapsules is not changing the Zeta potential drastically, leading to the impression, that the prepared nanocapsules are highly stable.

3.5 Incubation experiments with dye-loaded nanocapsules

Nanocapsules from all types of chitosan were incubated with 5000 U/ml of lysozyme. The used nanocapsules were loaded with different amounts of BCIP. The type of particle with the BCIP concentration used in sample preparation and the time until color formation was visible, can be found in Table 19.

Table 19: Concentration dependent color change of nanocapsules carrying BCIP, when incubated with Lysozyme

Chitosan type	BCIP concentration [mg/ml]	Time until color change [min]
75% Shrimp	5mg/ml	100min
	10mg/ml	120min
	25mg/ml	No color change
100% Heppe Medical	5mg/ml	120min
	10mg/ml	150min
	25mg/ml	No color change

At a close look, it seems that higher BCIP-concentrations lead to longer reaction times, which could indicate a substrate inhibition of AP. This assumption correlates with results of other incubation experiments. At the beginning of this study, nanocapsules were loaded with BCIP concentrations, up to 50 mg/ml. Incubation of these samples never lead to the expected color reaction. Only after lowering the BCIP amount, color formation became visible.

It is important to mention, that the nanocapsules with enclosed AP did not work when incubated with lysozyme. This can be related to the localization of the enzyme in the nanocapsule. The measured zeta potential of AP-loaded nanocapsules showed negative values which indicates that AP is not encapsulated inside the nanocapsule but bound to the shell of the capsule. This could mean, that parts of the enzyme-structure are blocked, and that the enzyme is not free to react with BCIP, resulting in an uncatalyzed color reaction. No further experiments towards the encapsulation of AP could be made in this work and the findings should help the following project working on AP encapsulation.

3.6 Optimization of Dye-loaded nanocapsules

Following the results of the first incubation trials, the nanocapsules should be optimized, regarding the loaded BCIP concentrations. In contrast to the expectations, lowering the BCIP concentration below 5 mg/ml, did not lead to an improved reaction time. Thus, it was assumed that the optimal concentration must be close to 5 mg/ml of BCIP or between 5 and 10 mg/ml.

Therefore, nanocapsules were loaded with 4.5; 5.5 and 7.5 mg/ml. The outcome of the incubation trial of these samples was quite surprising again. The fastest reaction time was achieved with nanocapsules carrying an amount of 7.5 mg/ml of BCIP.

Because the lysozyme activity of 5000 U/ml should not be changed in the incubation trials, further optimization was restricted to the reaction conditions. The only possibility to improve the reaction time without changing the principle of the detection kit, was an improvement of the buffer. Respecting the information of initial trials, it was clear that the optimum in pH must be close to the conditions used in the activity assay of lysozyme. Thus, incubation trials were done using acetic buffer, KPO_4-buffer and PBS buffer. The results can be seen in the following table.

Table 20: Reaction time of BCIP nanocapsules incubated in different buffers.

Sample	Buffer	Reaction time
75% Shrimp chitosan	PBS	120 min
	Acetate	90 min
	KPO_4	80 min
100% Heppe Medical chitosan	PBS	120 min
	Acetate	100 min
	KPO_4	90 min

By changing the buffer used during incubation into a KPO_4-buffer, the reaction time could be improved once more. This result is following the expected outcome, due to the optimization towards the right conditions for lysozyme.

After this experiment, a change in the amount of AP should be tested. Therefore, the original concentration of 1µl/ml AP was raised respectively to 1.5-; 2-; 2.5- and 3µl/ml. The increased amount of Alkaline Phosphatase did not affect the reaction time drastically. Due to this and economic reasons, the original amount of 1 µl/ml AP was kept for all experiments.

To conclude this section, the optimal conditions for a fast detection reaction of 5000 U/ml lysozyme are listed in Table 21

Table 21: Optimal reaction conditions for lysozyme detection

Optimized lysozyme reaction detection			
Optimal capsule	BCIP concentration	AP concentration	Reaction buffer
75% Shrimp chitosan	7.5 mg/ml	1 µl/ml	KPO_4-Buffer

The outcome of incubating 1 µl/ml AP, 250 µl of 75% Shrimp nanocapsules loaded with 7,5 mg/ml BCIP and 500 µl of 5000 U/ml lysozyme in 66 mM KPO_4-Buffer (pH 6.2), results in a color reaction directly related to the present lysozyme. The resulting blue color was clearly visible after 60 min and can be seen in the following picture.

Figure 34: Photograph of optimized BCIP nanocapsules with 5000U/ml lysozyme (left reaction tube) and blank without lysozyme in the reaction mix (right reaction tube)

3.7 Characterization of optimized Nanocapsules

3.7.1 Microscopy of optimized Nanocapsules

The optimized nanocapsule formulation of 75% shrimp chitosan, loaded with 7.5 mg BCIP should be further analyzed, in order to create a complete picture of the developed nanocapsules formulations.

Therefore, the characterization experiments like size- and Zeta potential measurement were done. In addition, the Isoelectric Point (iP) of 75% NCTS nanocapsules, loaded with 7.5 mg BCIP should be assessed. The following microscopy pictures of optimized nanocapsules were prepared after nanocapsule preparation and washing.

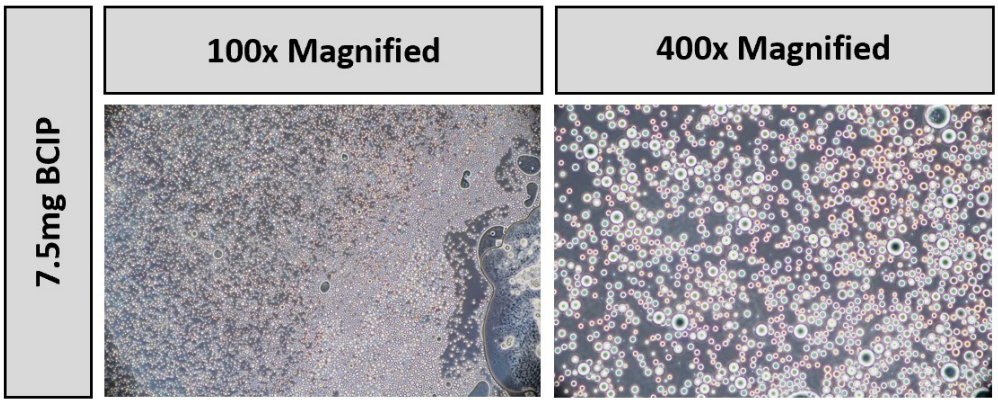

Figure 35: Microscopy pictures of 75% acetylated Shrimp chitosan nanocapsules, loaded with 7.5mg BCIP.

The microscopy shows an effective particle formulation, the prepared nanocapsules show a high density under the microscope. In addition, the decrease of sample density after 24 h of incubation in 5000 U lysozyme should be shown in Figure 36.

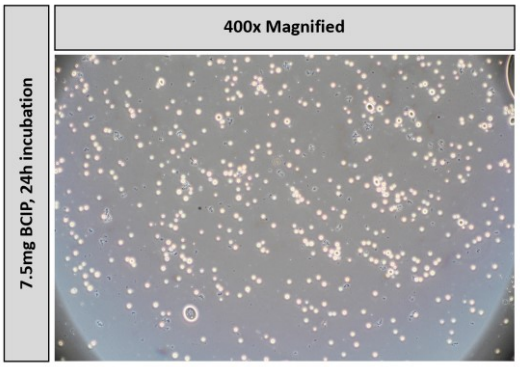

Figure 36: Decrease of particle density after Lysozyme incubation

3.7.2 DLS measurement of optimized nanocapsules

The size of 75% acetylated shrimp chitosan loaded with 7.5 mg BCIP was measured over a period of 30 min. The time profile can be seen in Figure 37. The average size acquired by the measurement was 710.8 nm.

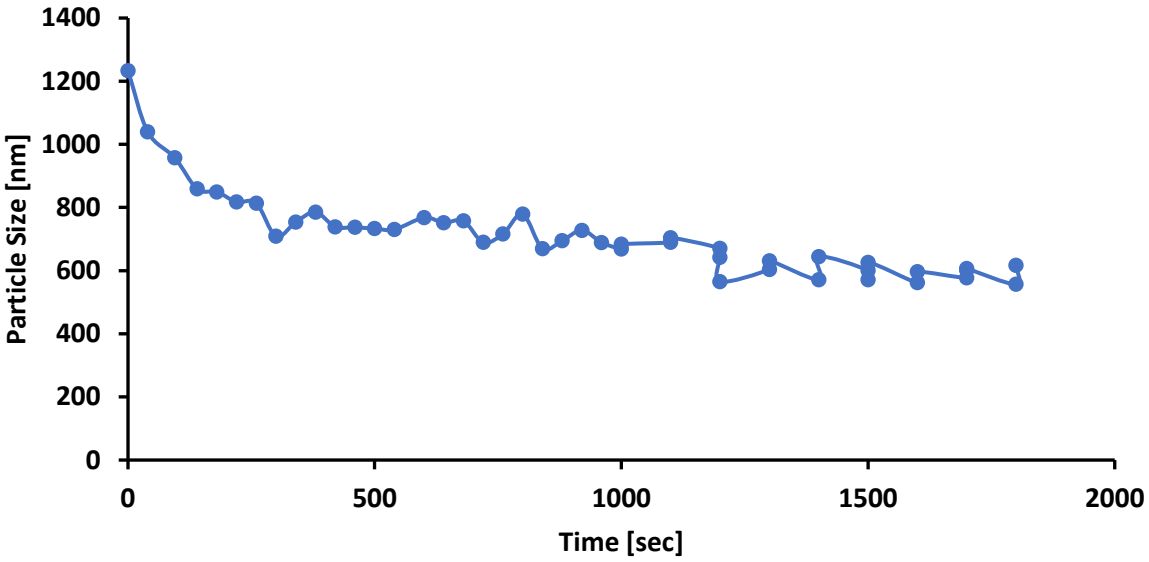

Figure 37: Measurement profile, of DLS- size measurement over a period of 30 min.

The temperature dependent change of size of optimized nanocapsules was measured as well and can be seen in the following figure. Throughout this measurement, the size of nanocapsules was outstandingly stable and the resulting curve, shows a constant hydrodynamic radius over the heat increase.

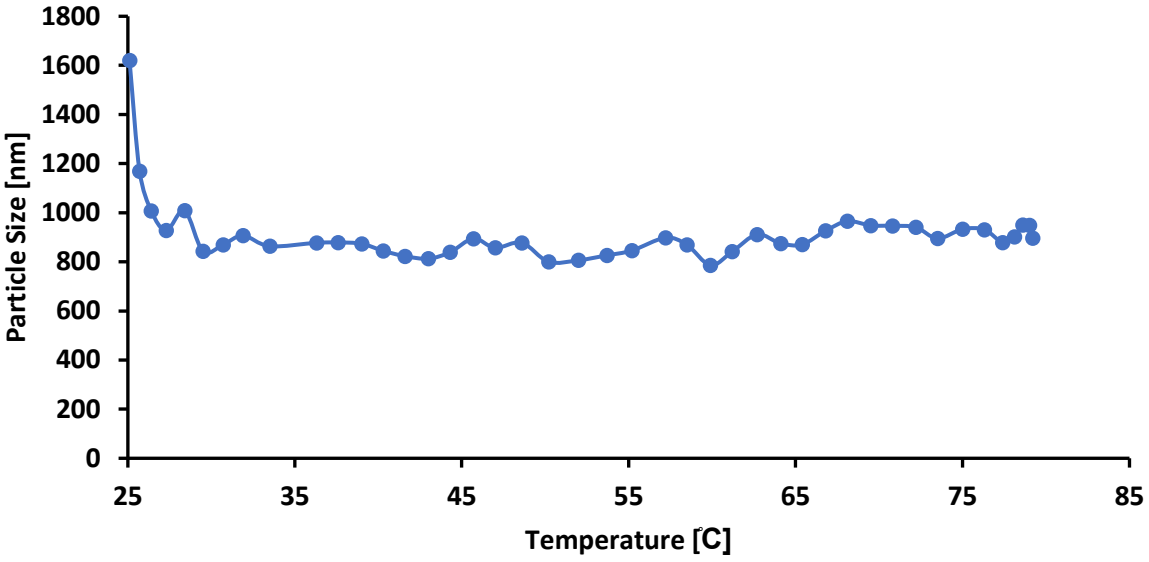

Figure 38: Size development of optimized nanocapsules throughout a constant heat increase.

The behavior of the nanocapsules throughout the temperature increase, leads to the assumption, that the sample must be very stable. This should be proved by the Zeta Potential measurement.

3.7.3 Zeta potential of optimized nanocapsule formulations

In order to proof the assumption, that the optimized nanocapsules are highly stable, the Zeta potential of the formulation should be measured. The results can be seen in the following table (Table 22).

Table 22: Zeta potential of optimized Nanoparticle formulations.

Nanocapsule Type	Zeta Potential [mV]	Average [mV]	Standard Deviation [mV]
75% acetylated Shrimp Chitosan 7.5mg BCIP	21.4	21.64	0.21
	21.8		
	21.7		

To create a better knowledge of the optimized nanocapsule formulation, the isoelectric point of the optimized formulation should be analyzed. Therefore, the nanocapsules were dissolved in buffer of different pH and the Zeta Potential of each solution was measured. The acquired data and the visualization of this experiment can be found below (Table 23).

Table 23: Data acquired throughout the measurements of nanocapsules, dissolved in buffer of different pH

Particle Type	pH	Size [nm]	Zeta Potential [mV]
Unloaded nanocapsules	6.2	450.96	16.77
	7.2	417.60	1.51
	8.2	415.84	-1.38
	9.2	386.77	-3.26
	10.2	368.82	-2.60
Optimized nanocapsules	6.2	592.01	14.12
	7.2	349.98	1.74
	8.2	549.37	-0.054
	9.2	368.82	-2.47
	10.2	438.35	-1.53

The data already shows a certain trend in size and Zeta potential of the nanocapsule formulations at different pH-values. Especially for the unloaded nanocapsules, the decrease in hydrodynamic radius and Zeta potential seems to go hand in hand with the increase in pH. The change of Zeta potential throughout the pH-increase should be visualized in the following graphs (Figure 39 to Figure 40).

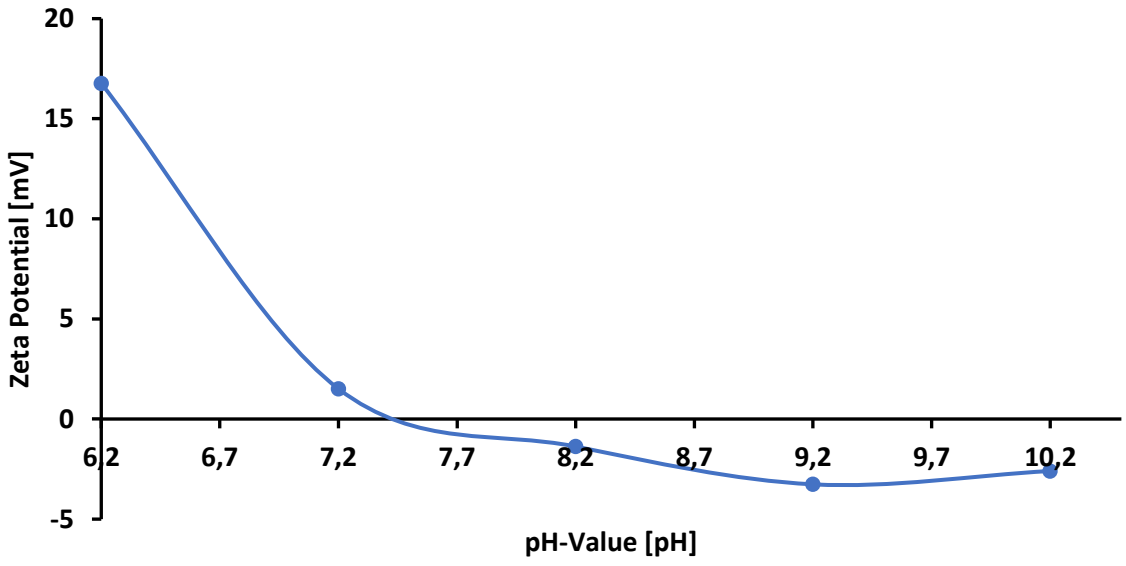

Figure 39: Zeta Potential change over pH increase of unloaded nanocapsules.

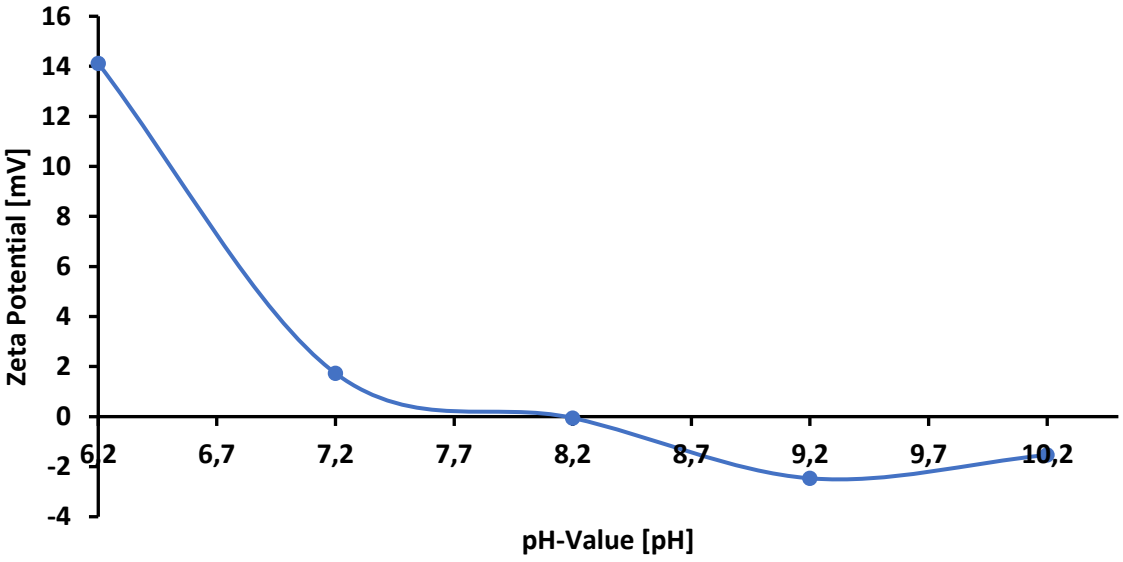

Figure 40: Zeta Potential change over pH increase of nanocapsules loaded with 7.5 mg of BCIP

The isoelectric Point of the nanocapsules formulations, at which the Zeta potential is zero, was calculated to be at pH 7.4, which corresponds to the iP, found in literature (Ma, Wang, Yang, 2019), for native nanocapsules and at pH 8.2 for the optimized nanocapsules formulation. This undeniable change of the iP can be correlated to the assumption, that the dye is not distributed in the core of the nanocapsules, but bound to the chitosan, forming the shell of the particle. If the dye would be distributed in the inside, it would be expected, that the isoelectric point would be closer to that, of unloaded nanocapsules.

3.8 Coupling experiments

3.8.1 Analysis of treated paper.

Although the optimized nanocapsule reaction already leads to a satisfying outcome, with a detection time of 60 minutes at a lysozyme concentration of 5000 U/ml, the nanocapsules emulsion cannot be classified as user friendly. Thus, the EDC/NHS-coupling system described above, should be used to isolate nanocapsules, carrying BCIP, on filter paper. It is expected, that nanocapsules bound to filter paper, can create a much faster response, when lysozyme is present in a solution to be tested.

By the immobilization of reactive nanocapsules, a paper-based biosensor could be designed, which can be used for the development of a dipstick like product for clinical applications.

The binding experiment can be separated in different parts, at which the chemical structure of the paper should be assessed. The structure of native filter paper, NaAlg-treated filter paper and paper with coupled nanocapsules was analyzed, using FTIR-spectroscopy in ATR-mode. The resulting spectra can be found in Figure 41.

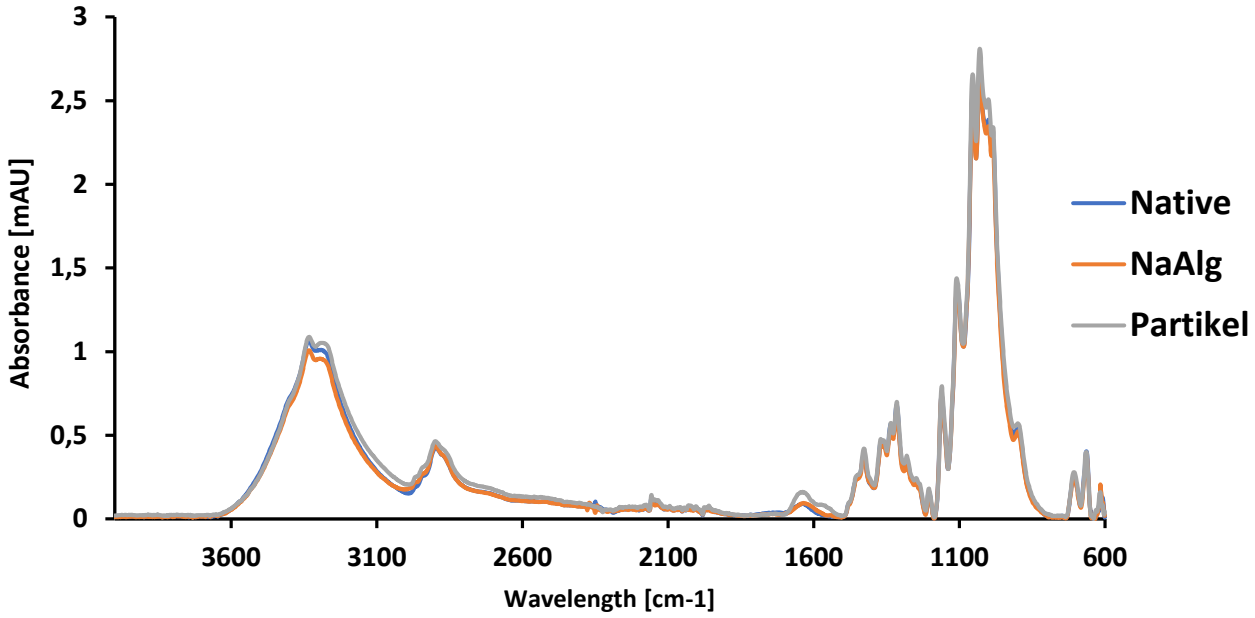

Figure 41: FTIR spectra of Filter paper throughout coupling experiments.

Considering the FTIR-spectra of the treated filter paper at different steps of the experiment, the characteristic change at about 1600 cm^{-1} after coupling of the nanocapsules can be seen as promising change, which can indicate the successful coupling of nanocapsules. (Sakai *et al.*, 2002; Lawrie *et al.*, 2007)

3.8.2 Incubation of filter paper with coupled BCIP-nanocapsules

The paper with coupled nanoparticles had to be tested for lysozyme responsiveness. The response mechanism should be tested by incubating the filter paper stripes with a lysozyme solution of 5000 U/ml and 1 µl/ml AP. In addition, a blank should be created by incubating a stripe in buffer without lysozyme but with the same amount of AP.

The reaction mixes were incubated under the same conditions, as the nanocapsules formulations (37 ℃, 150 rpm in a horizontal position).

The incubation did not lead to a color change in the first phase. Thus, the reaction tubes were left for incubation overnight, which did not lead to a visible color change as well.

In a further incubation experiment the lysozyme concentration was changed to 10.000 U/ml. Here, the incubation led to a slight change in color after overnight incubation. A picture of the resulting can be seen in the following picture.

Figure 42: Color reaction of BCIP nanocapsules after overnight incubation with 10.000U/ml of Lysozyme

The result of the incubation trial was not satisfying and led to the assumption, that the coupling reaction was not efficient enough. Due to the long time until color change, it can be expected that the number of nanocapsules bound to paper is not high enough.

On the other hand, it can be assumed, that nanocapsules are washed off the paper stripe during the incubation. And only the small number of washed off nanocapsules react with the lysozyme and AP present in the mixture. This assumption was made, due to the fact, that the solution turned blue, while the paper stripe did not show a change in color.

3.8.3 Transformation of the system into a dipstick assay

Because the nanocapsules seemed to float on the coupling reaction mix and the coupling mechanism turned out to be not efficient enough, the underlying color reaction system should be transferred to a system isolated on filter paper.

Therefore, the coupling mechanism of Cao et al. described in 2.2.8 was used to bind AP to the filter-paper. The filter paper stripe was then coated with chitosan, to create a dipstick like material, carrying the reaction mechanism of the developed nanocapsules.

The created paper stripes were tested by an incubation under the standard conditions for this assay. Paper stripes were placed in the reaction mix and incubated in a horizontal position at 37 ℃ and 150 rpm. The reaction mix included 5 mg/ml BCIP in 2ml KPO_4 Buffer. In addition, a blank was created by an incubation in pure buffer. The incubation led to a first color signal after 45minutes and a clear signal after 60minutes, showing the presence of lysozyme without a wrong positive signal in the blank reaction mix. The pictures, documenting the color reaction of the incubation, are shown below.

Figure 43: Color increase during incubation of the paper stripes with coupled AP, incubated with BCIP and lysozyme. Reaction tube on the left: Blank, reaction tube on the right: Sample.

Already after 45 min, a change in color, of the reaction mix was visible. The color-signal, resulting from the BCIP-reaction, under the formation of the blue indigo molecule got more intense and was clearly visible after one hour. The intensity of the blue color signal reached a maximum after 90 min. In addition, a test stripe was incubated in the reaction mix, without the presence of lysozyme. This stripe was used as negative control, and the stripe did not show a change in color over the whole incubation time of the experiment. Thus, the developed test-system can be seen as stable and reliable.

4. Discussion

Although research has already developed and optimized different lysozyme responsive materials (Öhlknecht *et al.*, 2017), and also the recognition of lysozyme by the usage of biosensors made from nanocapsules is already described by Jing *et al.*, 2010, the preparation of a bio based real time diagnostic tool for the detection of lysozyme has not been described yet. Also, the incorporation and localization of a chromogenic molecule in a chitosan based nanocapsules is rather novel and should be discussed here.

The obtained results contain valuable information for the preparation of real time diagnostic tools in wound infection detection. Also, lysozyme responsive nanocapsules and a pilot of a dipstick assay could be realized in this work, bringing bio-based lysozyme responsive materials closer to clinical application. Despite the satisfying response time of the developed

nanocapsules, the dye-system could be transferred into a dipstick like assay. This assay can be seen as a promising pilot for a clinical diagnostic tool in the detection of wound infections.

In addition, the developed method is more reliable than the established visual examination for infection indicators. Despite this, the assay is faster and simpler than the established measurement of other non-enzyme-based biomarkers. Hence, the acquired data contains a lot of knowledge, which should be discussed in the following section.

4.1 Particle characteristics

Although the prepared nanocapsule formulations seem to follow expected models, regarding size and Zeta potential, the assessment of the isoelectric point of BCIP-loaded nanocapsules, can help in estimasting the localization of the chromogenic reactant. While the Zeta potential of native and dye loaded nanocapsules seems to be similar, there is a distinctive change of the potential, when the pH of the solution is changed. The experiment shows a shift in the isoelectric point, when BCIP is loaded into the nanocapsule, which gives information on the localization of the color molecule. In contrast to the expectation, that the color-molecule is evenly distributed inside the core of the capsule, the data suggests a distribution in the shell. Another evidence for this assumption can be seen in Figure 32. When looking at this picture, a deep blue film, swimming on the surface of the reaction mix, can be seen. It is assumed, that this are nanocapsule shells with bound BCIP, transformed into indigo.

This assumption could lead to the suggestion that AP of the reaction mix could lead to the dye formation without the contribution of lysozyme. Still, the incubation experiments showed a failure proof reaction system. When the nanocapsules were incubated in a mix of AP without lysozyme, AP could not react with the bound BCIP and the color formation was suppressed. Thus, the lysozyme responsive reaction mechanism with a response time of about 60minutes until clearly detectable color formation, can be classified as satisfying and failure proof.

Despite the localization, also the amount of BCIP loaded into the nanocapsules might sound contradictory. When higher amounts of the dye molecule were applied, the reaction time could not be improved. In contrast to the expectations, the best response time was at a rather low amount of 7.5 mg BCIP. Since the effect of substrate inhibition can be seen at AP (Mazorra *et al.*, 2002), this can be a result of substrate inhibition of AP at BCIP amounts above 10 mg.

4.2 Coupling experiments

The experiments for the EDC-NHS-mediated binding of chitosan based nanocapsules to a filter paper stripe seemed to be satisfying as well. When the Nanocapsule solution was applied to the treated paper stripes, the FTIR-spectra of the resulting material showed a change at distinctive bands, after the coupling reaction. Although efficient washing steps were conducted,

the resulting impression, that the coupling reaction was successful was refuted by the incubation experiments.

Here the experiment led to the impression, that nanocapsules were washed off the paper and reacted with the enzymes after they were dissolved. In addition, the number of nanocapsules isolated on the paper seemed to be inefficient because of the high response time.

Although the coupling mechanism of nanocapsules, turned out to be inefficient, the work of Cao *et al*. on the coupling of AP sounded promising. The described protocol was used, to isolate the color- reaction mechanism of the nanocapsules and create an effective lysozyme responsive material. Here, AP was coupled to the filter paper stripe, which was then covered with a layer of Chitosan. When this material was incubated in a reaction mix of lysozyme and BCIP, the same mechanism, used for the lysozyme responsive nanocapsules, led to an indigo based color signal. When the wound enzyme degraded the chitosan shell, BCIP could react with the bound AP by the formation of a blue colored product.

5. Conclusion and Outlook

The goal of this work was the development of a lysozyme responsive material, which could be used in a user- friendly assay for the detection of lysozyme in infected wounds. The expectation was a system of lysozyme responsive nanocapsules, decorated with a chromogenic molecule for a color reaction system. The developed system should then be used for the preparation of a user-friendly dipstick-like assay.

In order to realize the goal, nanocapsules carrying the chromogenic reactant BCIP, were created and optimized towards the most effective response time, possible with this system. The reaction conditions were defined by a distinctive concentration of 1 µl/ml AP and 5000 U/ml lysozyme. The encapsulation of AP into the chitosan based nanocapsules was not possible, or at least the finalized nanocapsules did not work in a satisfying time period. Still, the optimized BCIP-capsules led to a color reaction, with a visible blue product, after 60minutes of incubation. In addition, it should be stated, that the developed nanocapsules were absolutely failure proof and a blue color signal was only visible, when lysozyme was present in the reaction mix. Therefore, this system can be seen as fully finalized, as the reaction system cannot be further improved without changing the preset parameters drastically. Respecting the discussion, the localization of the color-reactant BCIP, via the information of the isoelectric point, suggests that the dye is not located in the core but bound to the nanocapsules shell. Thus, the system could be further developed by the usage of a different color-system, which is distributed in the core and by minimizing the thickness of the nanocapsules shell.

In order to create a more user-friendly assay, the reaction system was used for the creation of a dipstick like assay. Here, AP was coupled to a filter paper stripe, which was coated with chitosan in a further step. The incubation experiments of this dipstick like assay, led to a response time of 45 min and a clear color signal after 60 min. Also, this system was safe, and the blank did not change the color when incubated without lysozyme. Here, further work can be done to optimize this pilot of a dipstick like assay. It is possible that the thickness of the chitosan layer could play an important role in the optimization of the response time. Thus, further steps towards a final product can be made by the optimization of this system.

The satisfying results of this work helped creating a user-friendly assay for the monitoring of the wound status of patients in clinic routine. The resulting pilots can be seen as failure proof and fully optimized respecting the available materials and methods in this stage of the project.

Still, this work was only a part of a bigger research project and further investigations must be made, to create a completely optimized and safe product for clinical use. The created nanocapsules seem to be efficient enough and here, only a drastic change of the reaction system (e.g. by the change of the color reaction mechanism) would lead to further optimization.

In addition, an incubation- experiment with real wound fluids would be necessary to receive a fully reliable statement on the performance of the nanocapsules and their future use.

Considering the formation of a paper-based dipstick like assay, more work is necessary for the safe application of this system in clinics. It is of very high importance to ensure a reliable and completely tight coating of chitosan. Here, tiny leaks in the coat could lead to a false positive answer. If the reaction mix can pass the chitosan barrier without lysozyme breaking it, an inflow of the reaction mix, containing BCIP could react with the isolated AP. This would lead to a false positive color signal and a potential danger for patients.

One possibility for the future design of the assay, is the combination of BCIP-loaded nanocapsules and the dipstick with AP bound to it. When lysozyme is degrading the chitosan of the nanocapsules and the chitosan layer on the dipstick, AP and BCIP could react and form the blue colored product. This system could ensure a failure proof reaction.

Also, the principle of the paper- based assay could be transferred to a polymer stripe to create an advanced carrier system for the dipstick assay. Furthermore, the addition of a positive control, and a negative control, like in state-of-the-art drug-tests should be considered for further evolution of this system.

However, the project led to the development of a promising and efficient lysozyme responsive assay, which can be further evolved to a user-friendly point of care device, helping in easing the suffering of patients, affected of wound infections.

References

Abdallah, E. A. A. *et al.* (2016) ‘Serial serum alkaline phosphatase as an early biomarker for osteopenia of prematurity’, *Medicine (United States)*, 95(37), pp. 1–5. doi: 10.1097/MD.0000000000004837.

Bart, J. *et al.* (2009) ‘Room-temperature intermediate layer bonding for microfluidic devices’, *Lab on a Chip*, 9(24), pp. 3481–3488. doi: 10.1039/b914270c.

Behera, B. C. *et al.* (2017) ‘Spreadability studies of metal working fluids on tool surface and its impact on minimum amount cooling and lubrication turning’, *Journal of Materials Processing Technology*. doi: 10.1016/j.jmatprotec.2017.01.016.

Bhattacharjee, S. (2016) ‘DLS and zeta potential - What they are and what they are not?’, *Journal of Controlled Release*. doi: 10.1016/j.jconrel.2016.06.017.

Bowers, G. N. and McComb, R. B. (1966) *A Continuous Spectrophotometric Method for Measuring the Activity of Serum Alkaline Phosphatase*.

Bradford, M. M. (1976) ‘A rapid and sensitive method for the quantitation of microgram quantities of protein utilizing the principle of protein-dye binding’, *Analytical Biochemistry*. Academic Press, 72(1–2), pp. 248–254. doi: 10.1016/0003-2697(76)90527-3.

C.W.N.C. (1977) ‘Principles of physical chemistry’, *Journal of Molecular Structure*, 42, p. 279. doi: 10.1016/0022-2860(77)87062-2.

Cammann, K. (2001) ‘Instrumentelle Analytische Chemie’, *Springer spektrum*, p. 622.

Cao, R. *et al.* (2015) ‘A zero-step functionalization on paper-based biosensing platform for covalent biomolecule immobilization’, *Sensing and Bio-Sensing Research*. Elsevier, 6, pp. 13–18. doi: 10.1016/j.sbsr.2015.09.002.

Coleman (1992) ‘STRUCTURE AND MECHANISM OF ALKALINE PHOSPHATASE’, *Annu: Rev. Biomol. Struct.*, 21, pp. 441–481. doi: 10.1016/S1570-9639(03)00156-0.

Diegelmann Robert F. and Evans Melissa C. (2004) ‘WOUND HEALING: AN OVERVIEW OF ACUTE, FIBROTIC AND DELAYED HEALING’, *Frontiers in Bioscience*, 9, pp. 283–289. doi: 10.2741/1184.

Dutta, P., Dutta, J. and Tripathi, V. (2003) ‘Chitin and chitosan: Chemistry, properties and applications’, *J Sci Indus Res*, 63.

Gorgieva, S. and Kokol, V. (2012) ‘Preparation, characterization, and in vitro enzymatic degradation of chitosan-gelatine hydrogel scaffolds as potential biomaterials’, *Journal of*

Biomedical Materials Research - Part A, 100 A(7), pp. 1655–1667. doi: 10.1002/jbm.a.34106.

Häggström, M. (2014) 'Medical gallery of Mikael Häggström 2014', *WikiJournal of Medicine*, 1(2). doi: 10.15347/wjm/2014.008.

Harish Prashanth, K. V. and Tharanathan, R. N. (2007) 'Chitin/chitosan: modifications and their unlimited application potential-an overview', *Trends in Food Science and Technology*. doi: 10.1016/j.tifs.2006.10.022.

Hasmann, A. *et al.* (2011) 'Novel peptidoglycan-based diagnostic devices for detection of wound infection', *Diagnostic Microbiology and Infectious Disease*. doi: 10.1016/j.diagmicrobio.2010.09.009.

Hilscher, M. *et al.* (2016) 'Alkaline phosphatase normalization is a biomarker of improved survival in primary sclerosing cholangitis', *Annals of Hepatology*. Elsevier, 15(2), pp. 246–253. doi: 10.5604/16652681.1193721.

Huang, P. *et al.* (2011) 'Characterization and expression of HLysG2, a basic goose-type lysozyme from the human eye and testis', *Molecular Immunology*. doi: 10.1016/j.molimm.2010.10.008.

Hudson, D. and Margaritis, A. (2014) 'Biopolymer nanoparticle production for controlled release of biopharmaceuticals', *Critical Reviews in Biotechnology*, 34(2), pp. 161–179. doi: 10.3109/07388551.2012.743503.

Irwin, D. M., Biegel, J. M. and Stewart, C. B. (2011) 'Evolution of the mammalian lysozyme gene family', *BMC Evolutionary Biology*, 11(1). doi: 10.1186/1471-2148-11-166.

Jing, T. *et al.* (2010) 'Magnetic molecularly imprinted nanoparticles for recognition of lysozyme', *Biosensors and Bioelectronics*. Elsevier B.V., 26(2), pp. 301–306. doi: 10.1016/j.bios.2010.08.044.

De Jong, A. S. H., Van Kessel-Van Vark, M. and Raap, A. K. (1985) 'Sensitivity of various visualization methods for peroxidase and alkaline phosphatase activity in immunoenzyme histochemistry', *The Histochemical Journal*, 17(10), pp. 1119–1130. doi: 10.1007/BF01002537.

Kawasumi, A. *et al.* (2013) 'Wound Healing in Mammals and Amphibians: Toward Limb Regeneration in Mammals', in Heber-Katz, E. and Stocum, D. L. (eds) *New Perspectives in Regeneration*. Berlin, Heidelberg: Springer Berlin Heidelberg, pp. 33–49. doi: 10.1007/82_2012_305.

Kazarian, S. G. and Chan, K. L. A. (2013) 'ATR-FTIR spectroscopic imaging: Recent advances and applications to biological systems', *Analyst*, 138(7), pp. 1940–1951. doi:

10.1039/c3an36865c.

Kirby, B. J. and Hasselbrink, E. F. (2004) ‘Zeta potential of microfluidic substrates: 1. Theory, experimental techniques, and effects on separations’, *Electrophoresis*, 25(2), pp. 187–202. doi: 10.1002/elps.200305754.

Lawrie, G. *et al.* (2007) ‘Interactions between alginate and chitosan biopolymers characterized using FTIR and XPS’, *Biomacromolecules*, 8(8), pp. 2533–2541. doi: 10.1021/bm070014y.

Ma, F., Wang, Y. and Yang, G. (2019) ‘The modulation of chitosan-DNA interaction by concentration and pH in solution’, *Polymers*, 11(4). doi: 10.3390/polym11040646.

Mazorra, M. T., Rubio, J. A. and Blasco, J. (2002) ‘Acid and alkaline phosphatase activities in the clam Scrobicularia plana: Kinetic characteristics and effects of heavy metals’, *Comparative Biochemistry and Physiology - B Biochemistry and Molecular Biology*, 131(2), pp. 241–249. doi: 10.1016/S1096-4959(01)00502-4.

Millán, J. L. (2006a) ‘Alkaline phosphatases’, *Purinergic Signalling*, 2(2), pp. 335–341. doi: 10.1007/s11302-005-5435-6.

Millán, J. L. (2006b) *Mammalian Alkaline Phosphatase*.

Nagpal, K., Singh, S. K. and Mishra, D. N. (2010) ‘Chitosan nanoparticles: A promising system in novel drug delivery’, *Chemical and Pharmaceutical Bulletin*, 58(11), pp. 1423–1430. doi: 10.1248/cpb.58.1423.

Öhlknecht, C. *et al.* (2017) ‘Cellobiose dehydrogenase and chitosan-based lysozyme responsive materials for antimicrobial wound treatment’, *Biotechnology and Bioengineering*, 114(2), pp. 416–422. doi: 10.1002/bit.26070.

Pechkova, E., Tripathi, S. K. and Nicolini, C. (2010) ‘Comparison of lysozyme crystals grown by APA and classical hanging drop method’. doi: 10.2210/PDB3IJV/PDB.

Pillai, C. K. S., Paul, W. and Sharma, C. P. (2009) ‘Chitin and chitosan polymers: Chemistry, solubility and fiber formation’, *Progress in Polymer Science (Oxford)*. doi: 10.1016/j.progpolymsci.2009.04.001.

Quadlbauer, L. (2018) *Enzyme-Responsive Chitosan Nanoparticles for the Detection of Wound Infection and Targeted Drug Delivery*.

Hesse, M.; Meier, H.; Zeeh, B. (1989) ‘Spektroskopisehe Methoden in der organischen Chemie. 3. über-arb. Aufl. VIII, 318 S., 199 Abb., 94 Tab., 19,3 × 23,8 cm. Stuttgart, New York: G. Thieme Verlag 1987. Kartoniert, 49,80 DM’, *Journal für Praktische Chemie*. John

Wiley & Sons, Ltd, 331(2), p. 211. doi: 10.1002/prac.19893310207.

Rao, J. P. and Geckeler, K. E. (2011) ‘Polymer nanoparticles: Preparation techniques and size-control parameters’, *Progress in Polymer Science (Oxford)*. doi: 10.1016/j.progpolymsci.2011.01.001.

Rollett, A. *et al.* (2012) ‘Folic acid-functionalized human serum albumin nanocapsules for targeted drug delivery to chronically activated macrophages’, *International Journal of Pharmaceutics*. doi: 10.1016/j.ijpharm.2012.02.028.

Sakai, Y. *et al.* (2002) ‘Chitosan-coating of cellulosic materials using an aqueous chitosan-CO2 solution’, *Polymer Journal*, 34(3), pp. 144–148. doi: 10.1295/polymj.34.144.

Schiffer Doris *et al.* (2015) ‘Enzyme-responsive polymers for microbial infection detection’, *Expert Review of Molecular Diagnostics*, 15, pp. 1125–1131. doi: 10.1586/14737159.2015.1061935.

Schmidt, H. (1997) ‘Indigo - 100 jahre industrielle synthese’, *Chemie in Unserer Zeit*, 31(3), pp. 121–128. doi: 10.1002/ciuz.19970310304.

Schultz, G. S. and Wysocki, A. (2009) ‘Interactions between extracellular matrix and growth factors in wound healing’, *Wound Repair and Regeneration*, 17(2), pp. 153–162. doi: 10.1111/j.1524-475X.2009.00466.x.

Sigma-Aldrich (2008) *-glucosamine residues in peptidoglycan and between N-acetyl-*.

Sigma-Aldrich Inc. (1994a) *ProductInformation SIGMA QUALITY CONTROL TEST PROCEDURE Enzymatic Assay of PHOSPHATASE, ALKALINE 1 (EC 3.1.3.1) Glycine with Zinc Assay PRINCIPLE: p-Nitrophenyl Phosphate + H 2 O*.

Sigma-Aldrich Inc. (1994b) *SIGMA QUALITY CONTROL TEST PROCEDURE Enzymatic Assay of LYSOZYME 1 (EC 3.2.1.17)*.

Singh, R. and Lillard, J. W. (2009) ‘Nanoparticle-based targeted drug delivery’, *Experimental and Molecular Pathology*. doi: 10.1016/j.yexmp.2008.12.004.

Stokke, B. T. *et al.* (1995) ‘ Sequence specificities for lysozyme depolymerization of partially N -acetylated chitosans ’, *Canadian Journal of Chemistry*, 73(11), pp. 1972–1981. doi: 10.1139/v95-244.

Tallian, C. *et al.* (2018) ‘Structural insights into pH-responsive drug release of self-assembling human serum albumin-silk fibroin nanocapsules’, *European Journal of Pharmaceutics and Biopharmaceutics*. Elsevier, 133, pp. 176–187. doi: 10.1016/J.EJPB.2018.10.002.

Tegl, G. *et al.* (2015) ‘Biomarkers for infection: enzymes, microbes, and metabolites’, *Applied Microbiology and Biotechnology*, 99(11), pp. 4595–4614. doi: 10.1007/s00253-015-6637-7.

Tegl, G. *et al.* (2016) ‘Chitosan based substrates for wound infection detection based on increased lysozyme activity’, *Carbohydrate Polymers*. doi: 10.1016/j.carbpol.2016.05.069.

Thermo Fisher (2012) ‘Chemical Reactivity of Crosslinkers and Modification Reagents’, *Crosslinking technology Reactivity chemistries, applications and structure references*, pp. 3–4.

Vollhardt P. and Schore N. (2015) *Organic Chemistry: Structure and Function BT - Organic Chemistry: Structure and Function*.

Weinhold, M. X. *et al.* (2009) ‘Studies on acetylation patterns of different chitosan preparations’, *Carbohydrate Polymers*. doi: 10.1016/j.carbpol.2009.06.001.

Wu, L., Zhang, J. and Watanabe, W. (2011) ‘Physical and chemical stability of drug nanoparticles’, *Advanced Drug Delivery Reviews*. Elsevier B.V., 63(6), pp. 456–469. doi: 10.1016/j.addr.2011.02.001.

Yetisen, A. K., Akram, M. S. and Lowe, C. R. (2013) ‘Paper-based microfluidic point-of-care diagnostic devices’, *Lab on a Chip*, 13(12), pp. 2210–2251. doi: 10.1039/c3lc50169h.

Yikrazuul (2008) *BCIP-AP-Reaction*.

Zargar, V., Asghari, M. and Dashti, A. (2015) ‘A Review on Chitin and Chitosan Polymers: Structure, Chemistry, Solubility, Derivatives, and Applications’, *ChemBioEng Reviews*, 2(3), pp. 204–226. doi: 10.1002/cben.201400025.

Appendix

List of Figures

List of Tables

Obtained Data

FTIR Data

Selected data of native and acetylated chitosan

Chitosan					
Native chitosan		75 NCTS		100 HMC	
Wavenumber [cm-1]	Absorbance	Wavenumber [cm-1]	A	Wavenumber [cm-1]	A
4000	-0,8261	4000	-0,7937	4000	0,5949
3900	-0,8398	3900	-0,7921	3900	0,5722
3800	-0,8014	3800	-0,7931	3800	0,5584
3700	-0,7863	3700	-0,7296	3700	0,551
3600	0,325	3600	1,5481	3600	0,4374
3500	3,5971	3500	7,0758	3500	3,1631
3400	7,4827	3400	12,3942	3400	5,9798
3300	8,4881	3300	14,6275	3300	7,1867
3200	6,8493	3200	12,7331	3200	5,8117
3100	5,0782	3100	10,3884	3100	4,4475
3000	3,0657	3000	6,4637	3000	2,2007
2900	5,3884	2900	8,3353	2900	3,3576
2800	3,6003	2800	4,8306	2800	2,1362
2700	2,542	2700	3,0444	2700	1,3497
2600	1,5894	2600	1,7333	2600	0,8057
2500	1	2500	1	2500	0,5627
2400	0,4621	2400	0,3013	2400	0,3332
2300	0,4481	2300	0,0713	2300	0,4524
2200	-0,0061	2200	-0,0265	2200	0,02
2100	-0,1064	2100	-0,0991	2100	0,0052
2000	-0,3472	2000	-0,351	2000	0,0128
1900	-0,6194	1900	-0,731	1900	0,384
1800	-0,8351	1800	-0,7702	1800	0,5978
1700	-0,6495	1700	0,3026	1700	0,2509
1600	4,7769	1600	11,8719	1600	5,2465
1500	0,6208	1500	10,7937	1500	4,7228
1400	3,4907	1400	19,7895	1400	6,8232
1300	4,6372	1300	16,5114	1300	8,5355
1200	-0,3276	1200	1,8256	1200	1,2259
1100	16,1414	1100	23,2024	1100	10,7009
1000	26,5838	1000	45,6068	1000	22,4645
900	9,8826	900	8,3721	900	5,086
800	0,4133	800	0,7918	800	0,5583
700	0,4939	700	0,1518	700	0,7615
600	0,784	600	0,6847	600	0,4464

Selected Data of nanocapsule-coupling experiment

Native Paper		NaAlg		Nanocapsules	
cm-1	A	cm-1	A	cm-1	A
4000	0,0122	4000	0,0107	4000	0,0199
3900	0,0112	3900	0,0109	3900	0,0225
3800	0,0161	3800	0,0138	3800	0,0226
3700	0,0154	3700	0,0143	3700	0,0225
3600	0,061	3600	0,0558	3600	0,0629
3500	0,2813	3500	0,2631	3500	0,2664
3400	0,7236	3400	0,6805	3400	0,7117
3300	1,0097	3300	0,9558	3300	1,0457
3200	0,5782	3200	0,5486	3200	0,6465
3100	0,2855	3100	0,2781	3100	0,3497
3000	0,1537	3000	0,1765	3000	0,2075
2900	0,4267	2900	0,4362	2900	0,4653
2800	0,1923	2800	0,1911	2800	0,2295
2700	0,1458	2700	0,1443	2700	0,1763
2600	0,1081	2600	0,1067	2600	0,1332
2500	0,0981	2500	0,0933	2500	0,1204
2400	0,0751	2400	0,0746	2400	0,0954
2300	0,0506	2300	0,0512	2300	0,0552
2200	0,0502	2200	0,0582	2200	0,0723
2100	0,0583	2100	0,0556	2100	0,0667
2000	0,0576	2000	0,0544	2000	0,0657
1900	0,0273	1900	0,0302	1900	0,0367
1800	0,0246	1800	0,0209	1800	0,0214
1700	0,036	1700	0,0313	1700	0,0284
1600	0,048	1600	0,0664	1600	0,099
1500	0,0125	1500	0,0114	1500	0,02
1400	0,1968	1400	0,1953	1400	0,2185
1300	0,3669	1300	0,3492	1300	0,3976
1200	0,1368	1200	0,1291	1200	0,1525
1100	1,2835	1100	1,2672	1100	1,3164
1000	2,3866	1000	2,3469	1000	2,508
900	0,5452	900	0,519	900	0,5703
800	0,0184	800	0,0192	800	0,0306
700	0,2264	700	0,2143	700	0,254
600	0,0165	600	0,0187	600	0,0442

Integrated NMR Spectra

75% Acetylated shrimp chitosan:

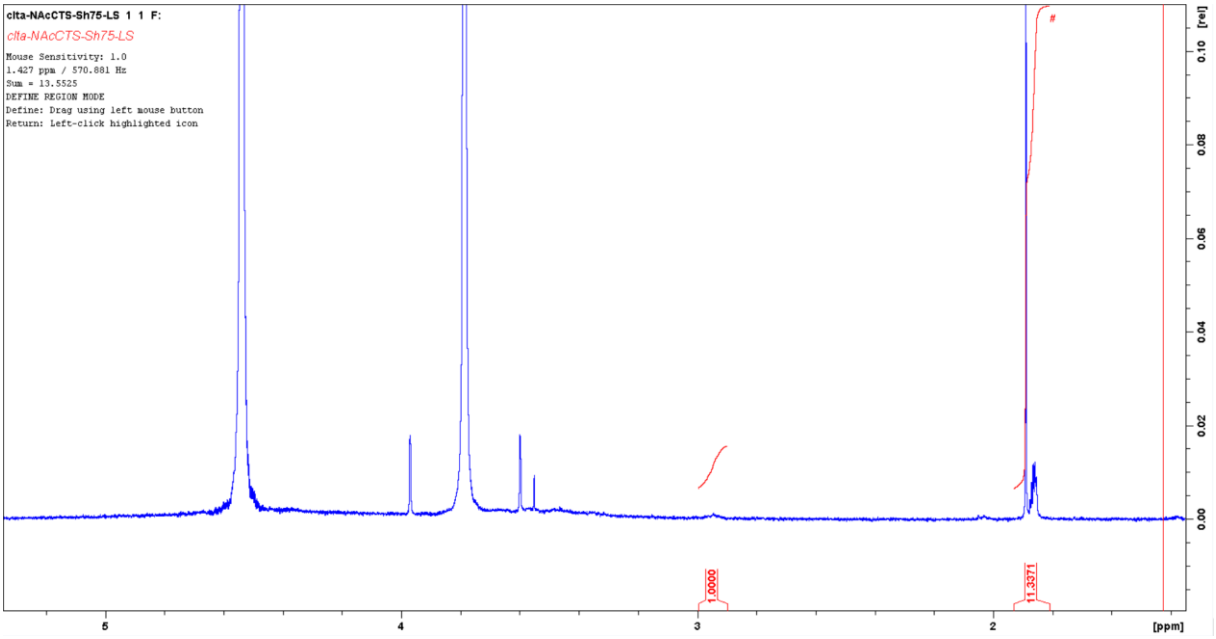

100% Acetylated HMC-chitosan:

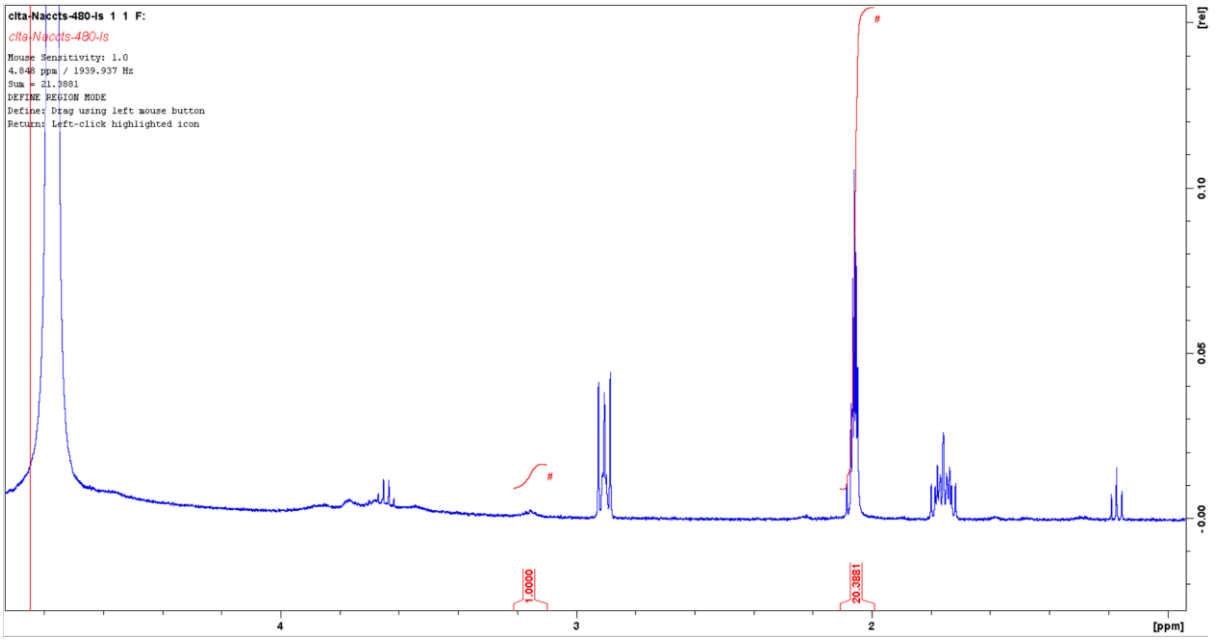

BSA-calibration

BSA-Standard	Average (blk corrected)	Replicate 1	Replicate 2	Replicate 3	BLK
Concentration [mg]	Absorbance	Absorbance	Absorbance	Absorbance	Absorbance
0,025	0,034400016	0,340200007	0,333600014	0,336900011	
0,03125	0,043650001	0,342999995	0,349299997	0,346149996	
0,05	0,087750003	0,395999998	0,384499997	0,390249997	0,302499995
0,0625	0,125599995	0,425399989	0,430799991	0,42809999	
0,1	0,213400021	0,50120002	0,530600011	0,515900016	

AP-activity measurement

Cycle Nr.	1	2	3	4	5	6
Time [s]	0	9,1	18,1	27,2	36,2	45,3
	0	0,15166667	0,30166667	0,45333333	0,60333333	0,755
Temp. [°C]	25,6	25,8	25,8	25,9	25,7	25,9
Blank 1	0,1767	0,17659999	0,17560001	0,17479999	0,17460001	0,17479999
1:100	1,52559996	1,84640002	2,17379999	2,46729994	2,71819997	2,97659993
	1,34889996	1,66980003	1,99819998	2,29249994	2,54359996	2,80179994

Lysozyme activity measurement

Cycle Nr.	1	2	3	4	5	6	7	8	9	10	11	12	13	14	15	16	17	18	19	20	21	22	23	24	25	26	27	28	29	30
Time [s]	0	10,5	20,9	31,3	41,7	52,1	62,4	72,9	83,2	93,6	104	114,4	124,8	135,2	145,6	156	166,4	176,8	187,2	197,6	208	218,4	228,7	239,1	249,5	259,9	270,3	280,7	291,1	301,5
	0	0,175	0,348333	0,521667	0,695	0,868333	1,04	1,215	1,386667	1,56	1,733333	1,906667	2,08	2,253333	2,426667	2,6	2,773333	2,946667	3,12	3,293333	3,466667	3,64	3,811667	3,985	4,158333	4,331667	4,505	4,678333	4,851667	5,025
Temp. [°C]	21	21,2	21,6	22,1	22,5	23	23,6	24	24,8	25	25,2	25,5	25,1	25,3	25,3	25,1	24,9	25	25,1	24,9	24,9	24,6	24,7	24,6	24,5	24,5	24,4	24,4	24	24,2
A1	0,2752	0,2807	0,2656	0,2574	0,2475	0,2449	0,2323	0,2244	0,2208	0,2145	0,2122	0,2082	0,2032	0,2017	0,1924	0,189	0,1815	0,1776	0,1746	0,1743	0,1703	0,1697	0,167	0,1653	0,1686	0,1623	0,1706	0,1672	0,1678	0,1596
B1	0,2752	0,2807	0,2656	0,2574	0,2475	0,2449	0,2323	0,2244	0,2208	0,2145	0,2122	0,2082	0,2032	0,2017	0,1924	0,189	0,1815	0,1776	0,1746	0,1743	0,1703	0,1697	0,167	0,1653	0,1686	0,1623	0,1706	0,1672	0,1678	0,1596
0.1mg/mL	0,2752	0,2807	0,2656	0,2574	0,2475	0,2449	0,2323	0,2244	0,2208	0,2145	0,2122	0,2082	0,2032	0,2017	0,1924	0,189	0,1815	0,1776	0,1746	0,1743	0,1703	0,1697	0,167	0,1653	0,1686	0,1623	0,1706	0,1672	0,1678	0,1596
A2	0,2502	0,2616	0,2669	0,2717	0,2834	0,2677	0,274	0,2635	0,257	0,2571	0,2594	0,258	0,2577	0,2484	0,2489	0,243	0,2446	0,2368	0,2351	0,2305	0,2341	0,2258	0,222	0,2182	0,2181	0,2147	0,2153	0,2102	0,2095	0,2071
B2	0,2539	0,2501	0,2686	0,2849	0,2804	0,2688	0,2636	0,2588	0,2559	0,2583	0,2558	0,2571	0,2521	0,2463	0,2377	0,2368	0,2306	0,2318	0,2256	0,2297	0,2193	0,2202	0,2137	0,2116	0,2083	0,2059	0,2085	0,2038	0,2075	0,2022
0.05mg/ml	0,25205	0,25585	0,26775	0,2783	0,2819	0,26825	0,2688	0,26115	0,25645	0,2577	0,2576	0,25755	0,2549	0,24735	0,2433	0,2399	0,2376	0,2343	0,23035	0,2301	0,2267	0,223	0,21785	0,2149	0,2132	0,2103	0,2119	0,207	0,2085	0,20465
A3	0,2767	0,281	0,282	0,2909	0,289	0,2921	0,2915	0,2889	0,2838	0,2791	0,2816	0,2752	0,2762	0,2736	0,2734	0,2713	0,2707	0,2684	0,2686	0,2656	0,2669	0,2608	0,2646	0,2595	0,2593	0,2594	0,2605	0,2583	0,2564	0,2544
B3	0,2631	0,2588	0,2508	0,2537	0,2645	0,2725	0,2801	0,2792	0,2765	0,276	0,278	0,2725	0,2662	0,2661	0,2713	0,2677	0,2669	0,2706	0,2702	0,2691	0,2688	0,2693	0,2691	0,2701	0,2692	0,2715	0,2696	0,2695	0,2704	0,2679
0.01mg/ml	0,2699	0,2699	0,2664	0,2723	0,27675	0,2823	0,2858	0,28405	0,28015	0,27755	0,2798	0,27385	0,2712	0,26985	0,27235	0,2695	0,2688	0,2695	0,2694	0,26735	0,26785	0,26505	0,26685	0,2648	0,26425	0,26545	0,26505	0,2639	0,2634	0,26115
A4	0,2548	0,2748	0,2759	0,2801	0,2838	0,284	0,2804	0,2777	0,2769	0,2767	0,2744	0,2757	0,2725	0,2722	0,2714	0,2723	0,2718	0,2698	0,2686	0,2697	0,2686	0,2671	0,266	0,2643	0,2645	0,263	0,2651	0,2619	0,2618	0,2601
B4	0,2671	0,2839	0,2848	0,2826	0,2796	0,2772	0,2768	0,2782	0,2787	0,2798	0,2779	0,2761	0,2726	0,2703	0,2712	0,2713	0,2692	0,2668	0,2664	0,2665	0,2647	0,2639	0,2617	0,2624	0,2616	0,2602	0,262	0,2604	0,2578	0,2585
0.0075mg/	0,26095	0,27935	0,28035	0,28135	0,2817	0,2806	0,2786	0,27795	0,2778	0,27825	0,27615	0,2759	0,27255	0,27125	0,2713	0,2718	0,2705	0,2683	0,2675	0,2681	0,26665	0,2655	0,26385	0,26335	0,26305	0,2616	0,26355	0,26115	0,2598	0,2593
A5	0,2888	0,2877	0,291	0,2914	0,2885	0,2857	0,2841	0,2816	0,2811	0,2792	0,2802	0,2795	0,2799	0,2794	0,278	0,2768	0,2772	0,2751	0,2768	0,2755	0,2756	0,2733	0,2744	0,2757	0,2735	0,2715	0,2702	0,2706	0,2714	0,2733
B5	0,2711	0,2697	0,2644	0,2574	0,2615	0,2658	0,2689	0,2737	0,2749	0,2735	0,2732	0,2764	0,2789	0,2772	0,2762	0,2775	0,2771	0,2751	0,2737	0,2725	0,2736	0,2731	0,2709	0,2701	0,269	0,2699	0,2698	0,2694	0,2694	0,2692
0.005mg/m	0,27995	0,2787	0,2777	0,2744	0,275	0,27575	0,2765	0,27765	0,278	0,27635	0,2767	0,27795	0,2794	0,2783	0,2771	0,27715	0,27715	0,2751	0,27525	0,274	0,2746	0,2732	0,27265	0,2729	0,27125	0,2707	0,27	0,27	0,2704	0,27125
A6	0,273	0,2787	0,2802	0,2789	0,2794	0,2811	0,2816	0,28	0,2788	0,2793	0,2806	0,2826	0,2856	0,2839	0,2828	0,2802	0,2845	0,2833	0,2847	0,2843	0,2832	0,2837	0,2843	0,2837	0,2807	0,2817	0,2811	0,2826	0,2812	0,2812
B6	0,278	0,2836	0,2843	0,2832	0,283	0,2844	0,2817	0,2843	0,292	0,294	0,293	0,2913	0,2886	0,289	0,2879	0,2876	0,2865	0,2842	0,2853	0,2849	0,2852	0,2831	0,2838	0,2829	0,2842	0,2818	0,2817	0,2832	0,282	0,2821
0.0025mg/	0,2755	0,28115	0,28225	0,28105	0,2812	0,28275	0,28165	0,28215	0,2854	0,28665	0,2868	0,28695	0,2871	0,28645	0,28535	0,2839	0,2855	0,28375	0,285	0,2846	0,2842	0,2834	0,28405	0,2833	0,28245	0,28175	0,2814	0,2829	0,2816	0,28165
A7	0,2771	0,2684	0,2718	0,2772	0,2751	0,2674	0,2693	0,2789	0,2779	0,28	0,2833	0,2862	0,289	0,286	0,2846	0,2875	0,2883	0,287	0,2864	0,2876	0,2882	0,2852	0,2856	0,2861	0,2844	0,2848	0,2828	0,2821	0,2808	0,2798
B7	0,2737	0,2717	0,2726	0,2713	0,2722	0,281	0,2826	0,2835	0,2823	0,2843	0,2848	0,2856	0,2848	0,286	0,2863	0,2868	0,2859	0,2843	0,2862	0,2851	0,2841	0,2829	0,2826	0,2825	0,282	0,2814	0,2807	0,2806	0,2821	0,2825
0.0001mg/	0,2754	0,27005	0,2722	0,27425	0,27365	0,2742	0,27595	0,2812	0,2801	0,28215	0,28405	0,2859	0,2869	0,286	0,28545	0,28715	0,2871	0,28565	0,2863	0,28635	0,28615	0,28405	0,2841	0,2843	0,2832	0,2831	0,28175	0,28135	0,28145	0,28115
A8	0,0367	0,0367	0,0367	0,0367	0,0367	0,0367	0,0367	0,0367	0,0367	0,0367	0,0367	0,0367	0,0367	0,0367	0,0367	0,0367	0,0367	0,0367	0,0367	0,0367	0,0367	0,0367	0,0367	0,0367	0,0367	0,0367	0,0367	0,0367	0,0367	0,0367
B8	0,0375	0,0375	0,0375	0,0375	0,0375	0,0375	0,0375	0,0375	0,0375	0,0375	0,0375	0,0375	0,0375	0,0375	0,0375	0,0375	0,0375	0,0375	0,0375	0,0375	0,0375	0,0375	0,0375	0,0375	0,0375	0,0375	0,0375	0,0375	0,0375	0,0375
Blank	0,0371	0,0371	0,0371	0,0371	0,0371	0,0371	0,0371	0,0371	0,0371	0,0371	0,0371	0,0371	0,0371	0,0371	0,0371	0,0371	0,0371	0,0371	0,0371	0,0371	0,0371	0,0371	0,0371	0,0371	0,0371	0,0371	0,0371	0,0371	0,0371	0,0371

31	32	33	34	35	36	37	38	39	40	41	42	43	44	45	46	47	48	49	50	51	52	53	54	55	56	57	58	59	60
311,9	322,3	332,7	343,1	353,5	363,9	374,2	384,6	395	405,4	415,8	426,2	436,6	447	457,4	467,8	478,2	488,6	499	509,4	519,7	530,1	540,5	550,9	561,3	571,7	582,1	592,5	602,9	613,3
5,198333	5,371667	5,545	5,718333	5,891667	6,065	6,236667	6,41	6,583333	6,756667	6,93	7,103333	7,276667	7,45	7,623333	7,796667	7,97	8,143333	8,316667	8,49	8,661667	8,835	9,008333	9,181667	9,355	9,528333	9,701667	9,875	10,04833	10,22167
24	23,9	24,4	23,9	24,4	24,2	24,3	24,1	24,1	24	23,9	24,3	24,2	24	24,1	24,4	24,1	24,4	24,4	24,3	24,5	24,2	24,1	24,1	24,3	24,4	24,1	24	24,2	24
0,1616	0,1505	0,1418	0,1458	0,1391	0,1305	0,133	0,1272	0,1251	0,1244	0,123	0,1221	0,1207	0,1186	0,1196	0,1163	0,1153	0,1141	0,1125	0,1178	0,1112	0,1119	0,1137	0,106	0,1083	0,106	0,1051	0,1034	0,1019	0,108
0,1616	0,1505	0,1418	0,1458	0,1391	0,1305	0,133	0,1272	0,1251	0,1244	0,123	0,1221	0,1207	0,1186	0,1196	0,1163	0,1153	0,1141	0,1125	0,1178	0,1112	0,1119	0,1137	0,106	0,1083	0,106	0,1051	0,1034	0,1019	0,108
0,1616	0,1505	0,1418	0,1458	0,1391	0,1305	0,133	0,1272	0,1251	0,1244	0,123	0,1221	0,1207	0,1186	0,1196	0,1163	0,1153	0,1141	0,1125	0,1178	0,1112	0,1119	0,1137	0,106	0,1083	0,106	0,1051	0,1034	0,1019	0,108
0,2074	0,2071	0,2099	0,2029	0,1997	0,1948	0,1952	0,1919	0,1905	0,1893	0,1863	0,1838	0,184	0,1841	0,182	0,1826	0,1811	0,1811	0,1823	0,1803	0,18	0,1801	0,1798	0,182	0,1792	0,1757	0,1755	0,175	0,1731	0,1732
0,2017	0,1952	0,1897	0,1879	0,1869	0,182	0,1826	0,1784	0,1773	0,1768	0,1744	0,1754	0,173	0,1735	0,1725	0,1745	0,1742	0,1744	0,1747	0,1681	0,1681	0,1679	0,1597	0,163	0,1576	0,1569	0,153	0,1553	0,1505	0,1511
0,20455	0,20115	0,1998	0,1954	0,1933	0,1884	0,1889	0,18515	0,1839	0,18305	0,18035	0,1796	0,1785	0,1788	0,17725	0,17855	0,17765	0,17775	0,1785	0,1742	0,17405	0,174	0,16975	0,1725	0,1684	0,1663	0,16425	0,16515	0,1618	0,16215
0,2535	0,2538	0,2547	0,2537	0,2499	0,2484	0,2518	0,246	0,2474	0,2465	0,2459	0,2461	0,2443	0,2424	0,2411	0,2411	0,2381	0,2376	0,2377	0,2352	0,2373	0,2348	0,2327	0,2311	0,2318	0,2271	0,2293	0,2255	0,2259	0,2237
0,2674	0,2681	0,2659	0,2669	0,2647	0,2595	0,2579	0,2527	0,2521	0,2542	0,2522	0,2537	0,2517	0,2505	0,2498	0,2492	0,2485	0,2473	0,2486	0,2459	0,2478	0,2457	0,2439	0,2428	0,2438	0,2381	0,2394	0,2353	0,2364	0,2342
0,26045	0,26095	0,2603	0,2603	0,2573	0,25395	0,25485	0,24935	0,24975	0,25035	0,24905	0,2499	0,248	0,24645	0,24545	0,24515	0,2433	0,24245	0,24315	0,24055	0,24255	0,24025	0,2383	0,23695	0,2378	0,2326	0,23435	0,2304	0,23115	0,22895
0,2607	0,2595	0,2585	0,2599	0,2611	0,2584	0,26	0,2564	0,26	0,2549	0,2573	0,254	0,2557	0,2517	0,2507	0,2507	0,2503	0,2478	0,2506	0,2475	0,2472	0,2464	0,2472	0,2463	0,2468	0,2435	0,2449	0,2436	0,2432	0,2425
0,2567	0,2573	0,2569	0,2577	0,2579	0,257	0,2558	0,2548	0,2555	0,252	0,254	0,2513	0,2503	0,2487	0,2495	0,2483	0,2486	0,2473	0,25	0,2454	0,2455	0,2456	0,2436	0,2446	0,2439	0,2405	0,2427	0,2429	0,2416	0,239
0,2587	0,2584	0,2577	0,2588	0,2595	0,2577	0,2579	0,2556	0,25775	0,25345	0,25565	0,25265	0,253	0,2502	0,2501	0,2495	0,24945	0,24755	0,2503	0,24645	0,24635	0,246	0,2454	0,24545	0,24535	0,242	0,2438	0,24325	0,2424	0,24075
0,2708	0,2687	0,2694	0,2706	0,2684	0,2669	0,2668	0,2669	0,2667	0,2662	0,2673	0,2658	0,2651	0,2638	0,2637	0,2634	0,2642	0,2602	0,2604	0,2611	0,2607	0,2592	0,2578	0,2579	0,2578	0,2565	0,2555	0,2548	0,2558	0,2534
0,2678	0,2687	0,266	0,2659	0,2644	0,2641	0,2631	0,2639	0,2635	0,2618	0,2605	0,2597	0,2599	0,259	0,2605	0,2578	0,2613	0,2567	0,2567	0,2562	0,2561	0,2557	0,2548	0,2561	0,2562	0,2548	0,2545	0,2552	0,2544	0,2528
0,2693	0,2687	0,2677	0,26825	0,2664	0,2655	0,26495	0,2654	0,2651	0,264	0,2639	0,26275	0,2625	0,2614	0,2621	0,2606	0,26275	0,25845	0,25855	0,25865	0,2584	0,25745	0,2563	0,257	0,257	0,25565	0,255	0,255	0,2551	0,2531
0,2823	0,283	0,2821	0,2809	0,2794	0,2798	0,2797	0,2786	0,2797	0,2777	0,278	0,277	0,2772	0,2762	0,275	0,2747	0,2756	0,275	0,2737	0,2728	0,2728	0,2723	0,2717	0,2708	0,2708	0,271	0,2695	0,2689	0,2682	0,267
0,2817	0,2817	0,2792	0,2803	0,2785	0,2806	0,2807	0,2817	0,2819	0,2788	0,2797	0,2808	0,2827	0,2806	0,28	0,2758	0,2816	0,2786	0,2777	0,2758	0,2762	0,2736	0,2753	0,2729	0,2751	0,2754	0,2747	0,274	0,2715	0,2708
0,282	0,28235	0,28065	0,2806	0,27895	0,2802	0,2802	0,28015	0,2808	0,27825	0,27885	0,2789	0,27995	0,2784	0,2775	0,27525	0,2786	0,2768	0,2757	0,2743	0,2745	0,27295	0,2735	0,27185	0,27295	0,2732	0,2721	0,27145	0,26985	0,2689
0,2814	0,2797	0,281	0,2802	0,282	0,28	0,2822	0,2811	0,2811	0,2792	0,2791	0,2804	0,2792	0,2795	0,2797	0,2789	0,2787	0,28	0,2795	0,2792	0,2804	0,2808	0,2793	0,2788	0,2774	0,2785	0,2784	0,2784	0,2786	0,2795
0,2817	0,2826	0,282	0,2805	0,2813	0,2817	0,2818	0,2804	0,2815	0,2805	0,2785	0,2795	0,2793	0,2775	0,2772	0,2774	0,2765	0,2767	0,2758	0,2758	0,2747	0,274	0,2769	0,2745	0,2759	0,2749	0,275	0,2749	0,275	0,2765
0,28155	0,28115	0,2815	0,28035	0,28165	0,28085	0,282	0,28075	0,2813	0,27985	0,2788	0,27995	0,27925	0,2785	0,27845	0,27815	0,2776	0,27835	0,27765	0,2775	0,27755	0,2774	0,2781	0,27665	0,27665	0,2767	0,2767	0,27665	0,2768	0,278
0,0367	0,0367	0,0367	0,0367	0,0367	0,0367	0,0367	0,0367	0,0367	0,0367	0,0367	0,0367	0,0367	0,0367	0,0367	0,0367	0,0367	0,0367	0,0367	0,0367	0,0367	0,0367	0,0367	0,0367	0,0367	0,0367	0,0367	0,0367	0,0367	0,0367
0,0375	0,0375	0,0375	0,0375	0,0375	0,0375	0,0375	0,0375	0,0375	0,0375	0,0375	0,0375	0,0375	0,0375	0,0375	0,0375	0,0375	0,0375	0,0375	0,0375	0,0375	0,0375	0,0375	0,0375	0,0375	0,0375	0,0375	0,0375	0,0375	0,0375
0,0371	0,0371	0,0371	0,0371	0,0371	0,0371	0,0371	0,0371	0,0371	0,0371	0,0371	0,0371	0,0371	0,0371	0,0371	0,0371	0,0371	0,0371	0,0371	0,0371	0,0371	0,0371	0,0371	0,0371	0,0371	0,0371	0,0371	0,0371	0,0371	0,0371

Nanocapsule size measurements

BCIP loaded nanocapsules

75% re-acetylated shrimp chitosan 5mg BCIP

	Item		Time (s)		Intensity (C	Normalizec	DLS Temp (	Diffusion C	Radius (nm	%PD	SOS	
	Meas 1		0		1437077	1,02E+08	25	1,53E-09	1578,2	Multimoda	22,204	
Item	Time (s)		Intensity (Cnt/s)		Normalized	DLS Temp (	Diffusion C	Radius (nm	%PD	SOS	% Acqs Unr	
Meas 1	0	0	1437077		1,02E+08	25	1,53E-09	1578,2	Multimoda	22,204	100	
Meas 2	65	1,083333	968890		33946458	25	1,83E-09	1320,5	Multimoda	21,861	100	
Meas 3	1,10E+02	1,833333	1501987		52624295	25	2,34E-09	1030,7	46,1	9,796	100	
Meas 4	1,60E+02	2,666667	1581089		20578107	25	2,51E-09	961,3	Multimoda	34,48	100	
Meas 5	2,00E+02	3,333333	1638250		21322058	25	2,70E-09	894,2	41,8	16,422	100	
Meas 6	2,40E+02	4	1295444		16860390	25	2,64E-09	913,4	Multimoda	14,718	100	
Meas 7	2,90E+02	4,833333	1249281		16259577	25	2,96E-09	817,2	21,7	9,406	100	
Meas 8	3,30E+02	5,5	1543147		20084275	25	2,78E-09	868,5	31,6	7,811	100	
Meas 9	3,70E+02	6,166667	1283907		16710233	25	2,84E-09	852	30,3	6,94	100	
Meas 10	4,10E+02	6,833333	1224881		15942005	25	3,05E-09	792,9	55	20,633	100	
Meas 11	4,50E+02	7,5	1384427		18018511	25	2,89E-09	835,2	12,6	7,033	100	
Meas 12	4,90E+02	8,166667	1097054		14278322	25	3,15E-09	765,9	30,9	19,361	100	
Meas 13	5,30E+02	8,833333	1142124		14864904	25	2,83E-09	853,8	35,7	6,476	100	
Meas 14	5,70E+02	9,5	933362		12147847	25	3,34E-09	722,7	40,3	11,625	100	
Meas 15	6,10E+02	10,16667	1011004		13158362	25	3,26E-09	740,7	26,1	7,565	100	
Meas 16	6,50E+02	10,83333	912531		11876727	25	3,14E-09	768,2	26,5	12,687	100	
Meas 17	6,90E+02	11,5	941768		12257242	25	3,37E-09	715,9	41,2	28,146	100	
Meas 18	7,30E+02	12,16667	843446		10977574	25	3,17E-09	760,8	10,4	10,655	100	
Meas 19	7,80E+02	13	996685		12971999	25	3,19E-09	756,2	Multimoda	15,331	100	
Meas 20	8,20E+02	13,66667	900487		11719967	25	3,33E-09	726,3	26,4	5,307	100	
Meas 21	8,60E+02	14,33333	846870		11022134	25	3,12E-09	773,3	31,7	7,68	100	
Meas 22	9,00E+02	15	849557		11057105	25	3,30E-09	731,9	34,6	9,918	100	
Meas 23	9,40E+02	15,66667	894208		11638251	25	3,43E-09	705,2	21,4	6,196	100	
Meas 24	9,80E+02	16,33333	1055892		13742580	25	3,09E-09	782,1	42,5	10,04	100	
Meas 25	1,00E+03	16,66667	789567		10276328	25	3,57E-09	676	17,1	22,568	100	
Meas 26	1,10E+03	18,33333	1676997		8232798	25	3,69E-09	654,4	34,1	9,996	100	
Meas 27	1,10E+03	18,33333	1940998		9528842	25	3,38E-09	715,3	51,1	4,669	100	
Meas 28	1,20E+03	20	1968347		9663107	25	3,26E-09	740,8	42,7	18,741	100	
Meas 29	1,20E+03	20	1697691		8334391	25	3,69E-09	655	Multimoda	68,229	100	
Meas 30	1,20E+03	20	1782571		8751088	25	3,43E-09	705	27,8	35,258	100	
Meas 31	1,30E+03	21,66667	1692658		8309683	25	3,42E-09	707	45,2	27,174	100	
Meas 32	1,30E+03	21,66667	1736152		8523202	25	3,48E-09	694,7	13,3	50,756	100	
Meas 33	1,40E+03	23,33333	1594804		7829293	25	3,72E-09	648,9	49,3	34,908	100	
Meas 34	1,40E+03	23,33333	1912022		9386592	25	3,67E-09	657,7	4,6	19,996	100	
Meas 35	1,40E+03	23,33333	1747939		8581070	25	4,11E-09	587,6	54,6	134,712	100	
Meas 36	1,50E+03	25	1572259		7718612	25	3,72E-09	650,2	23,8	18,477	100	
Meas 37	1,50E+03	25	1728241		8484366	25	3,81E-09	633,9	22,7	24,03	100	
Meas 38	1,60E+03	26,66667	1883602		9247071	25	3,77E-09	640,7	26	33,367	100	
Meas 39	1,60E+03	26,66667	1610782		7907729	25	4,13E-09	585,3	30,7	43,9	100	
Meas 40	1,60E+03	26,66667	1408247		6913434	25	3,74E-09	646,7	31,8	26,035	100	
Meas 41	1,70E+03	28,33333	1336126		6559378	25	3,84E-09	628,7	22,4	86,269	100	
Meas 42	1,70E+03	28,33333	1121460		5505527	25	4,20E-09	575,2	34,3	133,144	100	
Meas 43	1,80E+03	30	1511473		7420197	25	3,87E-09	623,9	14,6	12,624	100	
Meas 44	1,80E+03	30	1730535		8495626	25	3,91E-09	617,7	17,9	29,753	100	

75% re-acetylated shrimp chitosan 10mg BCIP

Item	Time (s)		Intensity (C	Normalized	DLS Temp (	Diffusion C	Radius (nm	%PD	SOS	% Acqs Unr
Meas 1	0	0	1431514	1,72E+08	25	1,92E-09	1260,6	Multimoda	10,298	100
Meas 2	82	1,366667	1447703	44439785	25	2,25E-09	1074,8	48,2	19,852	100
Meas 3	1,20E+02	2	1343466	41240031	25	2,46E-09	982,9	27,5	54,443	100
Meas 4	1,60E+02	2,666667	1562869	47974997	25	2,44E-09	990,4	1,4	14,199	100
Meas 5	2,00E+02	3,333333	1512485	46428357	25	2,34E-09	1030,1	27,2	1,879	100
Meas 6	2,40E+02	4	1208412	37094309	25	2,34E-09	1031,2	24,8	46,114	100
Meas 7	2,90E+02	4,833333	800830	24582888	25	2,97E-09	812,8	42	61,029	100
Meas 8	3,30E+02	5,5	1043717	32038729	25	2,58E-09	935	23,9	27,871	100
Meas 9	3,70E+02	6,166667	1034215	31747051	25	2,50E-09	965,4	42,6	66,325	100
Meas 10	4,10E+02	6,833333	843104	25880547	25	2,80E-09	861,2	41	56,127	100
Meas 11	4,60E+02	7,666667	919339	28220723	25	2,74E-09	880,3	19,7	55,366	100
Meas 12	5,00E+02	8,333333	1386556	42562764	25	2,98E-09	809,8	42,7	161,446	100
Meas 13	5,70E+02	9,5	1316875	28575234	25	3,54E-09	682,7	53,1	444,316	100
Meas 14	6,20E+02	10,33333	1401684	20598785	25	3,24E-09	745,8	47,4	141,659	100
Meas 15	6,60E+02	11	1259904	18515224	25	2,70E-09	893,3	16,3	81,691	100
Meas 16	7,00E+02	11,66667	1882974	27671694	25	3,28E-09	735,8	Multimoda	1120,272	100
Meas 17	7,40E+02	12,33333	1816286	26691657	25	3,04E-09	793,9	32,9	76,067	100
Meas 18	7,80E+02	13	1568813	23054862	25	2,55E-09	945,6	2	42,981	100
Meas 19	8,20E+02	13,66667	1030842	15148988	25	5,50E-09	438,7	Multimoda	13262,08	100
Meas 20	8,70E+02	14,5	1600846	23525617	25	4,75E-09	508,9	Multimoda	17643,29	100
Meas 21	9,10E+02	15,16667	1142505	16789949	25	2,83E-09	853,2	Multimoda	233,926	100
Meas 22	9,50E+02	15,83333	1503272	17942593	25	2,80E-09	864,1	17,7	22,788	100
Meas 23	1,00E+03	16,66667	1365733	16300971	25	3,15E-09	767,7	25,7	8,727	100
Meas 24	1,00E+03	16,66667	1527884	18236353	25	3,29E-09	734,8	28,1	10,072	100
Meas 25	1,10E+03	18,33333	1246383	14876446	25	3,10E-09	778,2	41,7	21,941	100
Meas 26	1,10E+03	18,33333	1148132	13703748	25	3,08E-09	785,3	27,9	6,032	100
Meas 27	1,20E+03	20	1334812	15931902	25	3,09E-09	782,7	50,5	109,564	100
Meas 28	1,20E+03	20	1430046	17068590	25	2,56E-09	945,3	12,5	18,251	100
Meas 29	1,20E+03	20	1126309	13443282	25	2,74E-09	881,6	44,6	14,22	100
Meas 30	1,30E+03	21,66667	837968	10001727	25	3,36E-09	719,1	27,6	31,351	100
Meas 31	1,30E+03	21,66667	964883	11516551	25	3,60E-09	670,1	14,1	55,507	100
Meas 32	1,40E+03	23,33333	1243486	14841871	25	3,41E-09	707,4	31,4	27,621	100
Meas 33	1,40E+03	23,33333	1377311	16439163	25	3,26E-09	742	12,2	21,324	100
Meas 34	1,40E+03	23,33333	1540300	18384551	25	3,24E-09	746,4	21,9	3,672	100
Meas 35	1,50E+03	25	1217903	14536511	25	3,09E-09	782,7	8,7	6,792	100
Meas 36	1,50E+03	25	1313705	15679984	25	3,21E-09	751,8	12,8	9,532	100
Meas 37	1,60E+03	26,66667	1025263	12237227	25	3,46E-09	697,1	12,3	8,773	100
Meas 38	1,60E+03	26,66667	905630	10809322	25	3,47E-09	696,1	0,8	13,583	100
Meas 39	1,60E+03	26,66667	835411	9971210	25	3,59E-09	672,9	29	33,113	100
Meas 40	1,70E+03	28,33333	820163	9789211	25	3,65E-09	662,5	32,8	101,911	100
Meas 41	1,70E+03	28,33333	816646	9747237	25	3,44E-09	701,2	16,6	52,551	100
Meas 42	1,80E+03	30	1145185	13668581	25	3,35E-09	720	3,6	51,077	100
Meas 43	1,80E+03	30	1271699	15178613	25	3,39E-09	711,4	6,1	25,937	100

75% re-acetylated shrimp chitosan 25mg BCIP

Item	Time (s)		Intensity (C	Normalized	DLS Temp (	Diffusion C	Radius (nm	%PD	SOS	% Acqs Unr
Meas 1	0	0	1625500	8508423	25	1,23E-09	1960,3	Multimoda	74,586	100
Meas 2	71	1,183333	1393159	7813945	25	1,51E-09	1602,7	Multimoda	182,106	100
Meas 3	1,90E+02	3,166667	2416619	4500708	25	1,88E-09	1284,8	Multimoda	43,32	100
Meas 4	2,70E+02	4,5	1745773	4234029	25	3,00E-09	804,4	Multimoda	36,579	100
Meas 5	3,10E+02	5,166667	1708164	4142816	25	1,25E-09	1929	Multimoda	101,54	100
Meas 6	4,60E+02	7,666667	1664255	3083780	25	2,28E-09	1057,1	Multimoda	32,165	100
Meas 7	5,10E+02	8,5	1039353	1942150	25	2,31E-09	1046,4	Multimoda	18,13	100
Meas 8	5,90E+02	9,833333	1722573	2750339	25	2,01E-09	1202,2	Multimoda	6,805	100
Meas 9	6,60E+02	11	951484	3983003	25	2,76E-09	874,5	37,6	15,5	100
Meas 10	7,10E+02	11,83333	1876896	3445484	25	1,79E-09	1352,2	Multimoda	32,208	100
Meas 11	7,90E+02	13,16667	2085003	7794814	25	1,98E-09	1221,7	46,8	16,063	100
Meas 12	8,40E+02	14	1079201	2637981	25	1,92E-09	1256,6	Multimoda	37,726	100
Meas 13	9,10E+02	15,16667	1151775	2087351	25	2,44E-09	988,4	51,4	28,48	100
Meas 14	9,60E+02	16	962678	1698105	25	2,49E-09	969,8	Multimoda	16,449	100
Meas 15	1,00E+03	16,66667	1531523	2701513	25	2,64E-09	916,3	Multimoda	30,315	100
Meas 16	1,00E+03	16,66667	1250295	2205444	25	2,31E-09	1046,3	Multimoda	19,795	100
Meas 17	1,10E+03	18,33333	982149	1732450	25	2,47E-09	979,2	Multimoda	18,731	100
Meas 18	1,10E+03	18,33333	1525223	2690401	25	2,08E-09	1159	Multimoda	17,736	100
Meas 19	1,20E+03	20	1569554	2512496	25	1,80E-09	1342,3	Multimoda	61,66	100
Meas 20	1,30E+03	21,66667	896902	2011122	25	2,76E-09	875,4	Multimoda	19,657	100
Meas 21	1,30E+03	21,66667	1266415	1266415	25	3,59E-09	672,6	Multimoda	29,278	100
Meas 22	1,40E+03	23,33333	2051983	2051983	25	1,96E-09	1233,7	Multimoda	28,327	100
Meas 23	1,40E+03	23,33333	1055830	3783198	25	3,60E-09	670,6	Multimoda	40,29	100
Meas 24	1,50E+03	25	1558509	2702438	25	3,90E-09	619,3	Multimoda	19,281	100
Meas 25	1,50E+03	25	1350873	2342399	25	1,85E-09	1305	Multimoda	27,984	100
Meas 26	1,60E+03	26,66667	1070972	3688466	25	1,82E-09	1326,5	Multimoda	12,636	100
Meas 27	1,60E+03	26,66667	1283181	4419322	25	2,71E-09	892	49,4	14,553	100
Meas 28	1,70E+03	28,33333	2400396	4035935	25	2,19E-09	1101,7	Multimoda	30,525	100
Meas 29	1,80E+03	30	935099	1504926	25	1,86E-09	1300,6	Multimoda	27,814	100
Meas 30	1,80E+03	30	879585	1415583	25	2,09E-09	1153,4	Multimoda	37,287	100
Meas 31	1,90E+03	31,66667	1320178	2025966	25	2,10E-09	1150,4	Multimoda	36,269	100

75% re-acetylated shrimp chitosan 50mg BCIP

Item	Time (s)		Intensity (C	Normalized	DLS Temp (	Diffusion C	Radius (nm	%PD	SOS	% Acqs Unr
Meas 1	0	0	1425442	27084102	24,8	1,2E-09	2043,5	Multimoda	12,226	100
Meas 2	40	0,666667	1716534	32614993	24,9	1,2E-09	2047,5	Multimoda	130,847	100
Meas 3	120	2	1758575	29842217	24,9	1,31E-09	1874,2	Multimoda	168,332	100
Meas 4	160	2,666667	1390932	23603478	24,9	1,53E-09	1611,5	Multimoda	40,546	100
Meas 5	220	3,666667	1390392	9861554	25	1,38E-09	1787	Multimoda	7,423	100
Meas 6	260	4,333333	1209188	8576340	25	1,62E-09	1521,3	Multimoda	14,887	100
Meas 7	300	5	1527682	10835303	25	1,58E-09	1557,3	Multimoda	13,065	100
Meas 8	340	5,666667	841253	5966704	25	1,98E-09	1244,7	Multimoda	9,783	100
Meas 9	400	6,666667	1340646	6295506	25	2,04E-09	1204,9	Multimoda	41,209	100
Meas 10	450	7,5	1570038	8199670	25	2,03E-09	1209,4	Multimoda	44,027	100
Meas 11	490	8,166667	1360691	7106334	25	2,32E-09	1062,9	Multimoda	12,15	100
Meas 12	570	9,5	1356735	7850628	25	2,08E-09	1183,4	42,5	20,736	100
Meas 13	610	10,16667	994031	5751874	25	2,22E-09	1110,6	47,3	10,851	100
Meas 14	650	10,83333	970102	5613413	25	2,22E-09	1109,7	53,7	4,873	100
Meas 15	700	11,66667	1466630	8486527	25	2,37E-09	1037,8	54,8	11,661	100
Meas 16	740	12,33333	1733866	10032863	25	2,09E-09	1179,7	Multimoda	20,073	100
Meas 17	780	13	1079626	6247162	25	2,52E-09	975,9	44,4	23,524	100
Meas 18	840	14	1404354	4026589	25	2,45E-09	1004,1	Multimoda	70,168	100
Meas 19	880	14,66667	1319549	3783434	25	2,28E-09	1079,6	Multimoda	9,572	100
Meas 20	920	15,33333	1124799	3225045	25	2,53E-09	973,8	Multimoda	39,789	100
Meas 21	960	16	1247691	3577401	25	2,32E-09	1059,8	54,3	47,704	100
Meas 22	1000	16,66667	971655	2785946	25	2,26E-09	1087,5	14,4	22,28	100
Meas 23	1000	16,66667	1728691	4956534	25	1,92E-09	1284,6	45,3	14,554	100
Meas 24	1100	18,33333	1074231	3080055	25	2,11E-09	1165,2	27,9	17,444	100
Meas 25	1100	18,33333	782959	2244914	25	3,13E-09	786,7	Multimoda	31,677	100
Meas 26	1200	20	868431	2489980	25	2,85E-09	863,2	34,1	30,514	100
Meas 27	1200	20	991653	2843287	25	2,7E-09	911,6	39	26,936	100
Meas 28	1200	20	1078871	3093359	25	2,04E-09	1204	Multimoda	17,753	100
Meas 29	1300	21,66667	1160435	3327221	25	1,73E-09	1424	Multimoda	15,361	100
Meas 30	1300	21,66667	1199150	3438225	25	2,01E-09	1223,8	Multimoda	16,545	100
Meas 31	1400	23,33333	754111	2162200	25	2,4E-09	1027,2	Multimoda	20,012	100
Meas 32	1400	23,33333	1694459	4858385	25	2,81E-09	875,4	20,6	7,773	100
Meas 33	1500	25	1803866	3323542	25	2,57E-09	957,2	20,9	5,853	100
Meas 34	1500	25	1156229	2142363	25	2,43E-09	1011,2	40,5	3,593	100
Meas 35	1600	26,66667	1330029	2464395	25	2,8E-09	879,5	35,2	11,561	100
Meas 36	1600	26,66667	1082048	2004915	25	2,93E-09	838,8	42,6	15,232	100
Meas 37	1600	26,66667	924200	1712438	25	3,08E-09	800,4	46,7	8,349	100
Meas 38	1700	28,33333	1006800	1865488	25	3,03E-09	813,4	25,7	14,661	100
Meas 39	1700	28,33333	1736966	3218404	25	2,24E-09	1101,1	50,8	12,009	100
Meas 40	1800	30	1453393	2692975	25	2,26E-09	1091,4	23,6	14,688	100
Meas 41	1800	30	1344429	1344429	25	3,47E-09	709,6	24,4	9,355	100

100% re-acetylated HMC chitosan 5mg BCIP

	Item		Time (s)		Intensity (C	Normalizec	DLS Temp (	Diffusion C	Radius (nm	%PD	SOS
	Meas 1		0		1437077	1,02E+08	25	1,53E-09	1578,2	Multimoda	22,204
Item	Time (s)		Intensity (C	Normalized	DLS Temp (	Diffusion C	Radius (nm	%PD	SOS	% Acqs Unr	% Acqs Unr
Meas 1 (Inc	0	0	1519140	22342255	25	1,32E-09	1,86E+03	Multimoda	31,581	100	100
Meas 2 (Inc	63	1,05	537710	20352530	25	1,58E-09	1,56E+03	Multimoda	383,96	100	100
Meas 3	1,00E+02	1,666667	1305368	4277177	25	2,6E-09	9,48E+02	Multimoda	33,776	100	100
Meas 4	1,80E+02	3	1028052	1890643	25	3,47E-09	7,10E+02	Multimoda	17,819	100	100
Meas 5	2,20E+02	3,666667	1435170	2639354	25	2,46E-09	9,99E+02	Multimoda	19,534	100	100
Meas 6	2,70E+02	4,5	1333961	2365459	25	4,76E-09	5,17E+02	Multimoda	30,221	100	100
Meas 7	3,50E+02	5,833333	1404851	1404851	25	3,17E-09	7,77E+02	Multimoda	9,1	100	100
Meas 8	3,90E+02	6,5	1409212	1409212	25	3,05E-09	8,08E+02	Multimoda	13,154	100	100
Meas 9	4,30E+02	7,166667	1063071	1063071	25	3,4E-09	7,25E+02	Multimoda	10,678	100	100
Meas 10	4,70E+02	7,833333	1291873	1291873	25	4,05E-09	6,07E+02	47,2	3,877	100	100
Meas 11	5,60E+02	9,333333	891528	1416700	25	3,61E-09	6,81E+02	Multimoda	21,089	100	100
Meas 12	6,40E+02	10,66667	898325	898325	25	3,56E-09	6,92E+02	Multimoda	36,065	100	100
Meas 13	6,90E+02	11,5	886185	886185	25	4,19E-09	5,88E+02	Multimoda	131,323	100	100
Meas 14	7,80E+02	13	795361	1305739	25	4,88E-09	5,05E+02	40,1	68,438	100	100
Meas 15	8,50E+02	14,16667	1041133	1041133	25	4,15E-09	5,93E+02	Multimoda	20,302	100	100
Meas 16	8,90E+02	14,83333	841616	841616	25	4,72E-09	5,21E+02	Multimoda	67,748	100	100
Meas 17	9,50E+02	15,83333	1249584	1249584	25	4,79E-09	5,13E+02	Multimoda	22,288	100	100
Meas 18	9,90E+02	16,5	1739525	1739525	25	4,35E-09	5,66E+02	Multimoda	6,995	100	100
Meas 19	1,00E+03	16,66667	1566430	1566430	25	3,72E-09	6,62E+02	19,2	2,872	100	100
Meas 20	1,10E+03	18,33333	833057	833057	25	4,96E-09	4,97E+02	42	4,271	100	100
Meas 21	1,10E+03	18,33333	1392542	1392542	25	3,2E-09	7,68E+02	Multimoda	7,846	100	100
Meas 22	1,20E+03	20	465207	465207	25	5,09E-09	4,84E+02	Multimoda	17,584	100	100
Meas 23	1,20E+03	20	877651	877651	25	4,41E-09	5,58E+02	Multimoda	27,58	100	100
Meas 24	1,30E+03	21,66667	1493818	1493818	25	3,87E-09	6,36E+02	Multimoda	12,982	100	100
Meas 25	1,40E+03	23,33333	1037728	1037728	25	5,25E-09	4,69E+02	Multimoda	58,309	100	100
Meas 26	1,40E+03	23,33333	1284657	1284657	25	3,98E-09	6,18E+02	29,9	33,449	100	100
Meas 27	1,50E+03	25	1355663	1355663	25	3,9E-09	6,31E+02	45,6	26,783	100	100
Meas 28	1,50E+03	25	833157	833157	25	4,51E-09	5,45E+02	42,6	58,629	100	100
Meas 29	1,60E+03	26,66667	930255	930255	25	4,38E-09	5,62E+02	42,4	52,547	100	100
Meas 30	1,70E+03	28,33333	754069	754069	25	4,96E-09	4,96E+02	Multimoda	14,583	100	100
Meas 31	1,70E+03	28,33333	828490	828490	25	4,5E-09	5,47E+02	23,9	12,44	100	100
Meas 32	1,80E+03	30	1080884	1080884	25	4,26E-09	5,77E+02	Multimoda	12,73	100	100
Meas 33	1,90E+03	31,66667	1467802	1467802	25	4,26E-09	5,77E+02	Multimoda	8,879	100	100

100% re-acetylated HMC chitosan 10mg BCIP

Item	Time (s)		Intensity (C	Normalized	DLS Temp (	Diffusion C	Radius (nm	%PD	SOS	% Acqs Unr
Meas 1	0	0	1278065	2534483	25	1,63E-09	1479,3	Multimoda	24,137	100
Meas 2 (Inc	88	1,466667	--	--	--	--	--	--	--	100
Meas 3	88	1,466667	817253	1321300	25	3,90E-09	619,7	Multimoda	37,17	100
Meas 4	1,80E+02	3	286145	286145	25	6,91E-09	349,5	47,4	6,377	100
Meas 5	2,20E+02	3,666667	382584	382584	25	5,13E-09	471	Multimoda	18,953	100
Meas 6	3,00E+02	5	466364	466364	25	4,01E-09	601,8	41,9	3,064	100
Meas 7	3,50E+02	5,833333	200246	200246	25	5,01E-09	482	Multimoda	3,718	100
Meas 8	3,90E+02	6,5	328257	328257	25	4,66E-09	518,6	47,3	9,627	100
Meas 9	4,30E+02	7,166667	970778	970778	25	2,84E-09	849,3	32,9	2,847	100
Meas 10	4,70E+02	7,833333	409155	409155	25	4,34E-09	556,2	22,8	5,121	100
Meas 11	5,30E+02	8,833333	541937	541937	25	3,73E-09	648	Multimoda	2,249	100
Meas 12	5,70E+02	9,5	464731	464731	25	3,38E-09	714,5	51,7	2,717	100
Meas 13	6,70E+02	11,16667	303006	303006	25	3,93E-09	614,6	26,9	3,276	100
Meas 14	7,10E+02	11,83333	793391	793391	25	3,44E-09	701,8	37,2	4,186	100
Meas 15	7,90E+02	13,16667	870481	870481	25	3,61E-09	669,6	34,6	11,653	100
Meas 16	8,50E+02	14,16667	427250	427250	25	4,08E-09	592,2	28,6	6,288	100
Meas 17	8,90E+02	14,83333	268691	268691	25	3,93E-09	614,3	39,8	7,26	100
Meas 18	9,70E+02	16,16667	215271	215271	25	5,37E-09	449,7	Multimoda	8,601	100
Meas 19	1,00E+03	16,66667	287741	287741	25	4,69E-09	514,7	42,9	8,24	100
Meas 20	1,00E+03	16,66667	511261	511261	25	4,21E-09	573,6	48,5	3,917	100
Meas 21	1,20E+03	20	384655	384655	25	4,65E-09	519,3	40,1	4,443	100
Meas 22	1,20E+03	20	204269	204269	25	5,57E-09	433,5	49,3	7,229	100
Meas 23	1,30E+03	21,66667	419342	419342	25	5,01E-09	481,7	22,9	9,548	100
Meas 24	1,40E+03	23,33333	407985	407985	25	4,34E-09	556,8	47,2	3,024	100
Meas 25	1,50E+03	25	286011	286011	25	6,08E-09	397	Multimoda	8,234	100
Meas 26	1,50E+03	25	1082262	1082262	25	2,79E-09	866,4	Multimoda	42,206	100
Meas 27	1,60E+03	26,66667	457013	457013	25	4,73E-09	510,2	42,4	11,37	100
Meas 28	1,60E+03	26,66667	493182	493182	25	5,03E-09	479,7	37	7,334	100
Meas 29	1,70E+03	28,33333	273174	273174	25	4,59E-09	525,8	Multimoda	10,217	100
Meas 30	1,70E+03	28,33333	245883	245883	25	5,29E-09	456,2	Multimoda	11,692	100
Meas 31	1,80E+03	30	374047	374047	25	4,78E-09	504,8	Multimoda	10,132	100
Meas 32	1,90E+03	31,66667	198284	198284	25	5,26E-09	458,9	Multimoda	22,16	100

100% re-acetylated HMC chitosan 25mg BCIP

Item	Time (s)		Intensity (C	Normalized	DLS Temp (	Diffusion C	Radius (nm	%PD	SOS	% Acqs Unr
Meas 1	0	0	916344	937024	25	4,00E-09	604,2	Multimoda	29,082	100
Meas 2	110	1,833333	808308	808308	25	3,01E-09	801,7	Multimoda	47,696	100
Meas 3	2,00E+02	3,333333	1844896	1844896	25	2,17E-09	1114,1	Multimoda	10,221	100
Meas 4	2,90E+02	4,833333	1417572	2356187	25	3,56E-09	678,3	Multimoda	7,329	100
Meas 5	3,50E+02	5,833333	395376	395376	25	4,01E-09	601,8	Multimoda	56,7	100
Meas 6	4,00E+02	6,666667	1293307	1293307	25	1,58E-09	1524,3	Multimoda	60,013	100
Meas 7	4,40E+02	7,333333	466343	466343	25	4,24E-09	569,4	Multimoda	21,488	100
Meas 8	5,20E+02	8,666667	261194	261194	25	9,73E-09	248,3	Multimoda	9,613	100
Meas 9	5,60E+02	9,333333	242445	242445	25	8,63E-09	279,8	Multimoda	11,549	100
Meas 10	6,00E+02	10	651661	651661	25	4,61E-09	523,8	Multimoda	41,54	100
Meas 11	6,50E+02	10,83333	1349216	1725239	25	7,44E-10	3247,1	Multimoda	43,419	100
Meas 12	7,60E+02	12,66667	849508	849508	25	2,83E-09	853,3	Multimoda	15,463	100
Meas 13	8,80E+02	14,66667	421780	421780	25	4,72E-09	511,4	Multimoda	19,499	100
Meas 14	9,30E+02	15,5	365470	365470	25	6,35E-09	380,2	Multimoda	84,28	100
Meas 15	9,80E+02	16,33333	266743	266743	25	6,12E-09	394,9	Multimoda	14,847	100
Meas 16	1,00E+03	16,66667	327185	327185	25	9,45E-09	255,6	Multimoda	21,766	100
Meas 17	1,10E+03	18,33333	384969	384969	25	6,20E-09	389,5	Multimoda	17,473	100
Meas 18	1,10E+03	18,33333	324311	324311	25	5,08E-09	475,6	Multimoda	11,043	100
Meas 19	1,20E+03	20	955229	955229	25	4,37E-09	552,2	51,6	6,702	100
Meas 20	1,20E+03	20	685864	685864	25	6,14E-09	393,2	35,9	7,238	100
Meas 21	1,30E+03	21,66667	321710	321710	25	5,35E-09	451	Multimoda	25,861	100
Meas 22	1,30E+03	21,66667	170125	170125	25	6,60E-09	365,7	Multimoda	12,548	100
Meas 23	1,40E+03	23,33333	207978	207978	25	1,01E-08	239,5	Multimoda	12,591	100
Meas 24	1,40E+03	23,33333	258020	258020	25	7,48E-09	322,7	Multimoda	45,924	100
Meas 25	1,40E+03	23,33333	496502	496502	25	4,87E-09	496,2	Multimoda	18,876	100
Meas 26	1,50E+03	25	2217757	2217757	25	2,62E-09	922,9	Multimoda	19,846	100
Meas 27	1,50E+03	25	394782	394782	25	2,74E-09	880,4	Multimoda	29,041	100
Meas 28	1,60E+03	26,66667	227948	227948	25	4,31E-09	559,9	Multimoda	36,552	100
Meas 29	1,60E+03	26,66667	251111	251111	25	7,34E-09	329	Multimoda	19,649	100
Meas 30	1,70E+03	28,33333	1318022	1318022	25	1,38E-09	1753,9	Multimoda	213,924	100
Meas 31	1,80E+03	30	533385	675878	25	3,47E-09	697	Multimoda	139,498	100
Meas 32	1800	30	154861	154861	25	5,45E-09	442,7	Multimoda	24,053	100
			154861	154861	25	5,45E-09	442,7	Multimoda	24,053	100

100% re-acetylated HMC chitosan 25mg BCIP

Item	Time (s)		Intensity (C	Normalized	DLS Temp (	Diffusion C	Radius (nm	%PD	SOS	% Acqs Unr
Meas 1	0	0	1229023	10108085	25	9,79E-10	2467,8	Multimoda	17,013	100
Meas 2	78	1,3	1965356	9147956	25	1,1E-09	2199	Multimoda	7,655	100
Meas 3	140	2,333333	1163590	6108425	25	1,4E-09	1727,4	Multimoda	42,243	100
Meas 4	180	3	1033242	5424144	25	1,76E-09	1370,2	Multimoda	14,322	100
Meas 5	240	4	1143473	3289083	25	1,59E-09	1521,5	Multimoda	10,553	100
Meas 6	280	4,666667	1500511	4316066	25	1,82E-09	1326,9	Multimoda	16,067	100
Meas 7	320	5,333333	838272	2411203	25	1,98E-09	1219,8	44,1	28,468	100
Meas 8	410	6,833333	937652	2416098	25	2,45E-09	986,9	43,4	36,828	100
Meas 9	470	7,833333	1334341	1638790	25	2,12E-09	1141,3	36,2	10,345	100
Meas 10	510	8,5	1305369	1603208	25	2,18E-09	1110,2	45,1	12,236	100
Meas 11	550	9,166667	838566	1029897	25	2,6E-09	928,4	Multimoda	20,991	100
Meas 12	590	9,833333	1259663	1547074	25	1,93E-09	1254,3	Multimoda	10,424	100
Meas 13	630	10,5	886019	1088178	25	2,46E-09	981,2	Multimoda	20,476	100
Meas 14	670	11,16667	1054300	1294855	25	2,31E-09	1045,4	32	11,305	100
Meas 15	720	12	1729599	2124233	25	1,8E-09	1344	43,5	16,214	100
Meas 16	760	12,66667	1332436	1636451	25	2,25E-09	1071,3	45,9	7,386	100
Meas 17	800	13,33333	1055848	1296755	25	2,47E-09	976,4	Multimoda	12,598	100
Meas 18	840	14	1213879	1490844	25	2,27E-09	1063,7	31,2	7,534	100
Meas 19	880	14,66667	814778	1000681	25	2,47E-09	977,1	18,3	25,34	100
Meas 20	930	15,5	925441	1136594	25	2,23E-09	1085,1	36	6,693	100
Meas 21	970	16,16667	734147	901654	25	2,48E-09	975,4	Multimoda	8,519	100
Meas 22 (Ir	1000	16,66667	722143	722143	25	2,53E-09	956,6	Multimoda	12,284	100
Meas 23	1200	20	1014242	1014242	25	2,25E-09	1073,4	23,1	6,146	100
Meas 24	1300	21,66667	769752	769752	25	2,34E-09	1034,1	Multimoda	4,114	100
Meas 25	1300	21,66667	801889	801889	25	2,77E-09	870,9	Multimoda	6,473	100
Meas 26	1400	23,33333	876914	876914	25	2,86E-09	844,4	41,3	14,24	100
Meas 27	1400	23,33333	504251	504251	25	2,87E-09	842,9	Multimoda	18,313	100
Meas 28	1500	25	339584	339584	25	3,31E-09	729,7	Multimoda	23,608	100
Meas 29	1500	25	620157	620157	25	3,07E-09	785,7	41,6	10,574	100
Meas 30	1600	26,66667	754760	754760	25	2,36E-09	1022,2	42,4	17,741	100
Meas 31	1700	28,33333	588899	588899	25	3,11E-09	777,8	Multimoda	24,517	100
Meas 32	1800	30	815659	815659	25	2,99E-09	808,7	Multimoda	13,776	100

Nanocapsule size during temperature increase:

75% re-acetylated shrimp chitosan 5mg BCIP

Item	Time (s)		Intensity (C	DLS Temp (	Radius (nm	Amplitude	%PD	Mw-R (kDa	Baseline	SOS
25.0C	0	0	1446454	25	1320	0,309	Multimoda	67409916	1	23,686
25.4C	54	0,9	1293269	25,4	1041,5	0,294	45,9	38713810	0,994	26,085
26.1C	94	1,566667	1124536	26,1	1039,9	0,339	39,6	38578693	0,999	19,97
27.0C	140	2,333333	771310	27	869,6	0,305	26,7	25389142	0,999	19,702
28.0C	180	3	894632	28	930,4	0,366	37,4	29737142	0,998	15,652
29.1C	220	3,666667	901893	29,1	911,2	0,337	27,2	28321468	0,998	8,308
30.3C	260	4,333333	1037750	30,3	840,9	0,365	35,4	23467013	0,998	14,924
31.5C	300	5	829231	31,5	856,8	0,371	Multimoda	24523299	0,986	16,26
33.0C	340	5,666667	1839521	33	828,4	0,385	38,1	22658534	0,999	8,428
34.4C	390	6,5	1970522	34,4	810,3	0,388	22,9	21516533	1,001	6,729
35.7C	430	7,166667	1978922	35,7	771,5	0,401	10,9	19187281	1	7,709
37.0C	470	7,833333	1898540	37	813,1	0,375	14	21692192	1,006	8,139
38.3C	510	8,5	2238582	38,3	822,6	0,387	27,3	22294292	0,998	5,934
39.6C	550	9,166667	2009804	39,6	803,6	0,381	20	21103634	0,997	6,325
41.0C	590	9,833333	1787413	41	797,2	0,376	18,7	20712356	0,999	2,8
42.3C	640	10,66667	1927341	42,3	792,8	0,393	13,1	20445975	1,001	7,417
43.6C	680	11,33333	2129878	43,6	823,7	0,424	15,5	22359504	0,996	8,218
45.0C	720	12	2001563	45	822	0,4	9	22252493	1,001	6,099
46.4C	760	12,66667	2314012	46,4	859,1	0,415	19,8	24674506	1,004	11,247
48.0C	810	13,5	1649782	48	823,3	0,43	31,4	22333176	0,998	17,195
49.3C	850	14,16667	1906500	49,3	898,2	0,438	31,9	27383082	0,995	12,926
50.7C	890	14,83333	1775489	50,7	857,7	0,402	19,5	24580103	1,008	20,589
52.0C	930	15,5	1421352	52	801	0,426	18,7	20948894	1,003	21,848
53.4C	970	16,16667	1616229	53,4	813,5	0,449	23,4	21717420	1	12,631
54.7C	1000	16,66667	1453469	54,7	790,2	0,446	34,2	20289517	0,999	12,752
56.1C	1100	18,33333	1670190	56,1	844,9	0,449	19,2	23728203	1,003	15,072
57.4C	1100	18,33333	1441094	57,4	833,7	0,445	16,4	23001503	1,001	22,357
59.1C	1100	18,33333	1941411	59,1	897,8	0,442	21,3	27356902	1,009	3,277
60.5C	1200	20	1321877	60,5	796,2	0,422	28,6	20653462	1,006	7,744
61.9C	1200	20	1307138	61,9	777,7	0,431	13,2	19549239	1,013	12,389
63.2C	1300	21,66667	1016190	63,2	780,7	0,43	32,5	19727536	1,008	10,376
64.6C	1300	21,66667	1336914	64,6	815,3	0,431	14,9	21829767	1,018	8,92
66.0C	1300	21,66667	1036974	66	813,5	0,444	15	21720517	1,013	15,221
67.3C	1400	23,33333	1592733	67,3	879,4	0,436	26,2	26061804	1,016	11,589
68.7C	1400	23,33333	1293431	68,7	810,6	0,42	25,6	21536788	1,022	19,288
70.0C	1500	25	1284196	70	749,2	0,434	25,7	17910415	1,015	26,744
71.4C	1500	25	1759495	71,4	844,4	0,404	30,5	23700461	1,011	28,053
73.2C	1600	26,66667	1664034	73,2	853,2	0,402	14,9	24282673	1,021	35,578
76.0C	1600	26,66667	2063373	76	874,2	0,368	15,8	25698379	1,02	24,01
77.6C	1700	28,33333	2226498	77,6	914,4	0,397	25,5	28550511	1,026	20,247
78.5C	1800	30	1914439	78,5	906,9	0,379	20,3	28008110	1,023	7,418
79.1C	1800	30	1822317	79,1	941,5	0,402	9,3	30574608	1,019	14,268

75% re-acetylated shrimp chitosan 10mg BCIP

Item	Time (s)		Intensity (C	DLS Temp (	Radius (nm	Amplitude	%PD	Mw-R (kDa	Baseline	SOS
25.0C	0	0	1078634	25	1572,5	0,402	45,1	1,02E+08	1,005	17,57
25.7C	58	0,966667	1552291	25,7	1222,6	0,363	Multimoda	56336698	1,004	75,143
26.8C	130	2,166667	1370253	26,8	1237,8	0,36	Multimoda	57993812	0,994	34,818
27.8C	170	2,833333	1068369	27,8	1010,3	0,364	Multimoda	36054887	1,003	91,943
28.9C	210	3,5	981724	28,9	940	0,411	Multimoda	30458641	0,988	227,162
30.0C	250	4,166667	1131794	30	1027,1	0,375	Multimoda	37479188	0,999	46,27
31.5C	290	4,833333	1685084	31,5	990	0,387	55,1	34381186	0,998	56,301
32.9C	350	5,833333	1466884	32,9	783,5	0,365	51,3	19889712	1,002	132,443
34.4C	390	6,5	1659779	34,4	889	0,353	40,6	26731290	0,999	53,044
36.5C	450	7,5	1895668	36,5	913,7	0,297	Multimoda	28502909	1,003	29,069
37.9C	500	8,333333	1719999	37,9	833,4	0,299	38,7	22978995	1,003	105,75
39.7C	540	9	1731310	39,7	823,5	0,38	Multimoda	22347390	1,005	108,393
41.7C	620	10,33333	1265730	41,7	767,4	0,434	Multimoda	18949686	0,996	541,941
43.2C	660	11	1238995	43,2	685,9	0,407	Multimoda	14571297	1,007	557,979
45.4C	710	11,83333	1697068	45,4	737,6	0,373	Multimoda	17268105	1,005	265,029
47.8C	800	13,33333	1863312	47,8	836,5	0,299	Multimoda	23180498	1,007	183,605
49.4C	850	14,16667	1675328	49,4	839,9	0,344	47,7	23400815	1	46,966
51.0C	890	14,83333	1500415	51	977,3	0,317	38,9	33358643	1,003	29,406
53.0C	950	15,83333	1197627	53	988,2	0,368	37,1	34242540	1,002	40,159
54.6C	1000	16,66667	982900	54,6	1032,9	0,42	17,8	37973078	1,004	27,996
56.3C	1000	16,66667	1251200	56,3	866,6	0,343	37,3	25182025	1,006	38,814
58.4C	1100	18,33333	1240738	58,4	951,8	0,379	42,5	31363030	1,01	21,523
60.7C	1200	20	1408042	60,7	808,7	0,303	28,9	21420195	1,01	8,186
62.4C	1200	20	1928335	62,4	1030	0,337	43,4	37727780	1,009	18,967
63.8C	1300	21,66667	1364276	63,8	944,9	0,314	18,3	30833401	1,008	13,402
65.1C	1300	21,66667	1499474	65,1	975,3	0,318	24,2	33203487	1,009	13,786
66.5C	1400	23,33333	1256324	66,5	890,6	0,341	29,8	26842369	1,011	22,637
67.8C	1400	23,33333	1513810	67,8	917,5	0,336	39,9	28781200	1,017	19,049
69.1C	1400	23,33333	1571369	69,1	897,4	0,334	48	27325270	1,015	25,881
70.5C	1500	25	1573877	70,5	909,4	0,337	30,7	28187809	1,013	35,613
71.8C	1500	25	1535927	71,8	940,5	0,324	39,4	30498794	1,018	25,571
73.2C	1600	26,66667	1684748	73,2	934	0,321	46	30008854	1,016	22,818
74.5C	1600	26,66667	1578641	74,5	1046,1	0,33	12	39120813	1,021	22,086
75.9C	1600	26,66667	2180426	75,9	974,5	0,345	39,7	33141259	1,023	32,615
77.1C	1700	28,33333	1865248	77,1	953	0,326	56,5	31454080	1,025	15,918
77.9C	1700	28,33333	2064434	77,9	1034,5	0,327	27,7	38110604	1,024	23,219
78.4C	1800	30	2187104	78,4	1023,9	0,324	37,5	37203016	1,022	30,829
78.9C	1800	30	1923534	78,9	1020,9	0,299	13,4	36947132	1,018	10,019
79.2C	1900	31,66667	1885997	79,2	969,1	0,339	Multimoda	32709204	1,018	36,531

75% re-acetylated shrimp chitosan 25mg BCIP

Item	Time (s)		Intensity (C	DLS Temp (	Radius (nm	Amplitude	%PD	Mw-R (kDa	Baseline	SOS
25.4C	0	0	1528964	25,4	1826,1	0,305	Multimoda	1,44E+08	0,998	18,967
26.5C	110	1,833333	1326726	26,5	1843,4	0,339	Multimoda	1,47E+08	1,001	65,822
27.4C	150	2,5	1449205	27,4	1742,7	0,331	Multimoda	1,29E+08	0,997	50,297
28.4C	190	3,166667	1213468	28,4	1662,3	0,368	Multimoda	1,16E+08	0,993	13,92
29.5C	230	3,833333	1291246	29,5	1714	0,379	Multimoda	1,24E+08	0,99	35,733
30.7C	270	4,5	1163687	30,7	1713,7	0,327	Multimoda	1,24E+08	0,999	45,377
32.0C	310	5,166667	1279492	32	1782,8	0,355	Multimoda	1,36E+08	1,01	32,781
33.3C	350	5,833333	932760	33,3	1609,3	0,371	Multimoda	1,07E+08	1,009	30,338
34.5C	400	6,666667	1073036	34,5	1609,6	0,399	Multimoda	1,07E+08	0,998	14,112
35.8C	440	7,333333	1069369	35,8	1512,2	0,4	Multimoda	92642050	0,991	14,838
37.3C	480	8	1114217	37,3	1549,2	0,371	Multimoda	98035880	1,003	21,844
38.9C	530	8,833333	2066938	38,9	1496,6	0,372	Multimoda	90423517	0,989	14,671
40.2C	570	9,5	2097778	40,2	1322,3	0,358	Multimoda	67680171	1,002	47,356
41.6C	610	10,16667	1976113	41,6	1500	0,374	Multimoda	90909741	1,001	30,707
43.2C	660	11	1733246	43,2	1429	0,361	Multimoda	81152834	0,995	16,154
44.7C	700	11,66667	1735048	44,7	1382,5	0,39	55,2	75108389	0,995	31,973
46.3C	750	12,5	1732606	46,3	1365,8	0,377	Multimoda	72999895	0,993	29,095
47.6C	800	13,33333	1359996	47,6	1286,9	0,355	Multimoda	63522236	1	33,104
49.0C	840	14	1714767	49	1360,9	0,353	53,7	72394625	1	28,658
50.3C	880	14,66667	1700521	50,3	1313,4	0,335	Multimoda	66624967	1,001	64,832
51.6C	920	15,33333	1574942	51,6	1293,7	0,355	Multimoda	64301920	1,002	84,302
53.0C	960	16	1785331	53	1330,8	0,354	Multimoda	68704601	1,001	126,021
54.4C	1000	16,66667	1718095	54,4	1359,1	0,362	Multimoda	72176039	1,003	245,658
55.8C	1000	16,66667	1696110	55,8	1315,5	0,345	Multimoda	66874894	0,997	83,944
57.1C	1100	18,33333	1544044	57,1	1353,3	0,376	Multimoda	71451635	1,004	36,577
58.6C	1100	18,33333	2050905	58,6	1400,2	0,355	44,9	77378684	1,007	17,054
60.8C	1200	20	1754542	60,8	1708,5	0,41	Multimoda	1,23E+08	1	37,415
62.1C	1200	20	1941357	62,1	1840	0,391	Multimoda	1,47E+08	1,007	31,604
63.5C	1300	21,66667	1804187	63,5	1666,2	0,393	Multimoda	1,16E+08	1,002	16,316
65.0C	1300	21,66667	2027486	65	1957,1	0,381	Multimoda	1,69E+08	1,001	33,311
67.4C	1400	23,33333	1609115	67,4	1839,4	0,394	25,9	1,47E+08	1,017	20,287
69.8C	1400	23,33333	1693854	69,8	1704,8	0,399	Multimoda	1,23E+08	1,022	35,119
71.8C	1500	25	2007184	71,8	1875,4	0,351	4,5	1,53E+08	1,018	19,048
73.3C	1600	26,66667	1844464	73,3	1702,8	0,37	4,9	1,22E+08	1,019	22,559
74.7C	1600	26,66667	1952639	74,7	1683,6	0,367	25,9	1,19E+08	1,019	19,58
76.2C	1600	26,66667	1755643	76,2	1620,8	0,365	28,3	1,09E+08	1,014	12,59
77.4C	1700	28,33333	1940377	77,4	1772,6	0,38	38,1	1,34E+08	1,018	20,593
78.1C	1700	28,33333	1947828	78,1	1574	0,369	27,7	1,02E+08	1,026	17,705
78.6C	1800	30	1701277	78,6	1299,9	0,37	42,4	65027797	1,015	197,636
79.0C	1800	30	1713029	79	1431,8	0,38	33,6	81525733	1,02	46,256
79.2C	1900	31,66667	1502767	79,2	1442,6	0,415	41,1	82974397	1,021	19,64

75% re-acetylated shrimp chitosan 50mg BCIP

Item	Time (s)		Intensity (C	DLS Temp (	Radius (nm	Amplitude	%PD	Mw-R (kDa	Baseline	SOS
25.0C	0	0	1050256	25	2261,4	0,297	Multimoda	2,38E+08	0,988	9,855
25.5C	42	0,7	874008	25,5	1886,7	0,301	Multimoda	1,55E+08	0,986	12,988
26.7C	99	1,65	786749	26,7	1979	0,308	Multimoda	1,74E+08	0,996	9,811
28.7C	190	3,166667	1227627	28,7	1770,4	0,352	Multimoda	1,34E+08	0,994	7,266
30.6C	270	4,5	987958	30,6	1473,4	0,374	Multimoda	87182082	0,999	5,596
32.3C	310	5,166667	1021697	32,3	1467,9	0,359	44,9	86420035	1,005	6,766
34.6C	390	6,5	1120394	34,6	1420,7	0,349	32,8	80061562	0,995	22,325
36.7C	450	7,5	1226749	36,7	1682,1	0,408	39,9	1,19E+08	0,99	14,375
38.3C	500	8,333333	1121474	38,3	1597,8	0,37	Multimoda	1,05E+08	0,989	8,014
40.4C	580	9,666667	1078200	40,4	1527	0,335	18	94781216	0,999	8,943
42.4C	620	10,33333	2080623	42,4	1379,6	0,283	52,8	74739167	1,002	1,508
44.2C	680	11,33333	1641673	44,2	1343,9	0,293	28,8	70294644	1,009	12,063
N/A	790	13,16667	1274357	49,6	873,7	0,397	36,6	25664106	1,044	227,736
49.6C	840	14	1042395	51,1	739,6	0,306	0	17380834	1,032	238,827
51.1C	900	15	559435	53,2	538,4	0,385	0	8266870	1,033	372,34
53.2C	940	15,66667	870529	54	734,5	0,397	33,2	17099120	1,037	156,538
54.0C	990	16,5	703357	55,9	581,5	0,351	0	9901105	1,045	199,193
55.9C	1000	16,66667	1048679	65,9	513,3	0,421	0	7393884	1,049	465,129
79.2C	1200	20	1410942	79,2	686,6	0,384	0	14607248	1,04	279,581

100% re-acetylated HMC chitosan 5mg BCIP

Item	Time (s)	Intensity (Cnt/s)	DLS Temp (C)	Radius (nm)	Amplitude	%PD	Mw-R (kDa)	Baseline	SOS
25.5C	0	1483678	25.5	1185.1	0.308	Multimodal	52375886.6	1.004	45.739
27.8C	1200	1398755	27.8	949.1	0.276	Multimodal	31150236.8	0.999	28.894
30.2C	2400	1113301	30.2	714.4	0.275	Multimodal	16024021.7	1.009	23.912
31.7C	3100	1600469	31.7	713.5	0.247	Multimodal	15978384.4	1.004	19.675
34.0C	3600	1446960	34.0	818.6	0.317	Multimodal	22036019.0	1.008	10.182
37.2C	4300	1589804	37.2	857.5	0.396	Multimodal	24568220.5	0.998	17.796
39.4C	5300	2033295	39.4	997.5	0.258	45.4	34999797.2	1.006	11.163
41.5C	600	1618391	41.5	854.6	0.295	42.6	24370393.5	1.012	14.985
45.1C	6700	1921543	45.1	695.6	0.260	48.5	15059137.4	1.004	10.698
49.1C	800	1660558	49.1	740.5	0.303	Multimodal	17428926.6	1.010	10.616
52.3C	9200	1786985	52.3	1005.4	0.321	Multimodal	35645990.4	1.012	14.319
55.6C	1000	1422189	55.6	968.1	0.273	Multimodal	32635023.1	1.016	18.697
59.2C	11000	1507892	59.2	812.4	0.333	Multimodal	21648762.4	1.018	8.653
62.9C (Incomplete)	12000	2015228	62.9	851.0	0.324	Multimodal	24132350.3	1.018	22.809
68.1C (Incomplete)	14000	997224	68.1	436.6	0.274	51.4	5064095.6	1.022	38.704
79.5C	18000	773039	79.5	887.1	0.268	Multimodal	26598217.1	1.030	47.363

100% re-acetylated HMC chitosan 10mg BCIP

Item	Time (s)	Intensity (Cnt/s)	DLS Temp (C)	Radius (nm)	Amplitude	%PD	Mw-R (kDa)	Baseline	SOS
26.0C	0	1401757	26.0	1367.9	0.240	Multimodal	73274137.7	1.009	21.725
27.3C	1500	1203242	27.3	946.9	0.183	Multimodal	30985269.4	1.015	5.848
28.4C	1900	1346449	28.4	1145.4	0.251	Multimodal	48364816.6	1.017	4.210
31.2C	2400	1238590	31.2	706.6	0.266	Multimodal	15618874.7	1.008	5.453
34.2C	3400	1458579	34.2	912.8	0.273	Multimodal	28433107.7	1.009	14.952
36.6C	4300	1011441	36.6	727.1	0.248	Multimodal	16700492.1	1.008	10.079
39.3C	5300	1817148	39.3	949.5	0.292	Multimodal	31186188.0	1.020	34.579
41.6C	600	1296199	41.6	715.8	0.301	50.6	16099157.9	1.007	11.588
44.3C	6600	1440916	44.3	1009.0	0.337	Multimodal	35944950.7	1.000	43.887
47.0C	7600	839293	47.0	678.7	0.276	Multimodal	14212291.7	1.011	38.357
49.8C	8400	1346069	49.8	740.5	0.262	Multimodal	17431077.7	1.010	9.989
51.6C	9100	823566	51.6	870.0	0.251	Multimodal	25411417.8	1.014	11.713
54.8C	9700	1259181	54.8	1380.5	0.271	Multimodal	74863216.6	1.010	14.701
59.3C	11000	1580234	59.3	979.4	0.266	35.0	33528937.5	1.022	8.930
62.8C (Incomplete)	12000	829889	62.8	672.9	0.200	Multimodal	13934104.7	1.015	6.287
80.0C	24000	1608658	80.0	685.5	0.183	Multimodal	14547989.3	1.033	24.522

100% re-acetylated HMC chitosan 25mg BCIP

Item	Time (s)	Intensity (Cnt/s)	DLS Temp (C)	Radius (nm)	Amplitude	%PD	Mw-R (kDa)	Baseline	SOS
25.2C	0	1201216	25.Feb	1530.2	0.304	52.6	95251851.4	1.010	6.278
28.0C	100	610223	28.0	1095.7	0.254	Multimodal	43595329.6	1.015	43.787
31.8C	2800	591699	31.8	581.3	0.282	Multimodal	9891489.7	1.021	64.472
33.3C	3600	330933	33.3	475.7	0.252	Multimodal	6190027.2	1.002	9.719
34.7C	400	720662	34.7	683.7	0.299	Multimodal	14459291.6	1.025	60.795
36.9C	4600	620151	36.9	1049.4	0.219	Multimodal	39408116.0	1.017	32.889
38.8C	5100	801321	38.8	1039.2	0.319	Multimodal	38518765.8	1.022	115.893
41.2C	5900	1555485	41.2	1543.6	0.210	Multimodal	97206104.8	1.028	30.654
43.4C	6500	1013353	43.4	901.2	0.225	Multimodal	27600191.0	1.030	44.791
46.0C	7400	372538	46.0	618.6	0.273	Multimodal	11441495.1	1.018	61.864
50.0C	8300	542563	50.0	743.3	0.247	Multimodal	17582903.1	1.027	87.656
52.7C	9400	960250	52.7	1136.5	0.236	Multimodal	47492113.8	1.019	15.914
55.0C	9900	794302	55.0	1264.7	0.250	Multimodal	60981264.0	1.022	34.492
58.7C	11000	903003	58.7	948.0	0.246	Multimodal	31065012.9	1.022	75.236
62.2C (Incomplete)	12000	996101	62.2	903.1	0.278	Multimodal	27731335.6	1.022	21.744
79.7C (Incomplete)	18000	694981	79.7	1642.0	0.123	Multimodal	112334093.4	1.032	27.590

100% re-acetylated HMC chitosan 50mg BCIP

Item	Time (s)	Intensity (Cnt/s)	DLS Temp (C)	Radius (nm)	Amplitude	%PD	Mw-R (kDa)	Baseline	SOS
25.1C	0	1689160	251	18095	358	Multimodal	1409989545	1003	35371
25.9C	61	1330876	259	13608	335	Multimodal	723866429	1001	34858
26.6C	1200	1112974	266	12766	364	Multimodal	623377372	993	80678
27.6C	1600	1182160	276	13212	350	Multimodal	675533429	1001	17213
28.7C	200	1570212	287	15012	374	49.1	910728215	996	26527
29.9C	2500	1400586	299	13846	323	Multimodal	753800659	1008	94347
31.1C	2900	925623	311	13918	349	Multimodal	763047582	1009	115003
33.0C	3300	1309010	330	11898	444	Multimodal	528661390	1007	130053
37.0C	4300	1209037	370	13651	395	Multimodal	729186834	1009	198489
39.3C	5200	1474221	393	12051	374	Multimodal	544747559	1006	140900
41.7C	600	1265721	417	12497	364	Multimodal	593001636	1004	132532
43.7C	6600	1621261	437	11049	442	46.4	444538167	999	88829
45.9C	7300	1410801	459	12418	412	Multimodal	584262131	997	57634
48.1C	800	1170678	481	11405	337	Multimodal	478816777	1007	86157
51.1C	8700	961739	511	12507	462	Multimodal	594128784	1011	132626
54.8C	9900	1422155	548	13499	384	Multimodal	710346102	1014	160064
57.5C	11000	1560889	575	13367	361	Multimodal	694212032	1012	45218
61.2C	12000	1543749	612	12521	389	Multimodal	595680622	1017	65250
64.2C	13000	1733749	642	13184	372	Multimodal	672204554	1024	83696
70.0C	14000	1542603	700	11937	422	49.0	532682447	1014	24026
75.4C	16000	1785816	754	9770	408	Multimodal	333387088	1026	118637
77.6C	17000	1212393	776	13762	395	40.9	743148008	1037	16305
79.6C (Incomplete)	18000	2462378	796	13603	402	Multimodal	723156086	1025	175550

Characterization of optimized nanocapsules

75% re-acetylated shrimp nanocapsules with 7.5mgBCIP

Size measurement:

Item	Time (s)	Intensity (C	Normalized	DLS Temp (	Diffusion C	Radius (nm	%PD	SOS	% Acqs Unr
Meas 1	0	1055198	85640175	25	1,96E-09	1233,5	Multimoda	3,856	45
Meas 2	40	1181091	95857638	25	2,32E-09	1039,8	13,8	21,801	75
Meas 3	95	1230428	60297063	25	2,52E-09	957,2	27	14,06	50
Meas 4	1,40E+02	1116090	54693938	25	2,81E-09	858,7	26,8	3,207	40
Meas 5	1,80E+02	1161682	56928160	25	2,84E-09	849,2	15,9	17,851	35
Meas 6	2,20E+02	949712	46540605	25	2,95E-09	817,5	22,3	4,992	75
Meas 7	2,60E+02	1027533	50354224	25	2,97E-09	813,7	34,4	6,396	45
Meas 8	3,00E+02	926431	45399716	25	3,41E-09	708,6	42,3	6,52	45
Meas 9	3,40E+02	774036	37931603	25	3,20E-09	753,9	21,3	14,633	45
Meas 10	3,80E+02	775199	37988614	25	3,08E-09	785,1	20	7,996	55
Meas 11	4,20E+02	847232	41518587	25	3,27E-09	738,9	41,1	19,184	60
Meas 12	4,60E+02	861655	42225376	25	3,28E-09	737,1	23,1	12,922	55
Meas 13	5,00E+02	869812	42625124	25	3,30E-09	733	25,2	23,089	45
Meas 14	5,40E+02	1348348	66075742	25	3,31E-09	730,3	35,3	8,701	65
Meas 15	6,00E+02	1550347	36937035	25	3,15E-09	767,6	29,3	6,784	65
Meas 16	6,40E+02	1869538	44541758	25	3,21E-09	751,7	22,3	9,774	55
Meas 17	6,80E+02	1852295	44130933	25	3,19E-09	757,3	17,9	12,338	60
Meas 18	7,20E+02	1485891	35401373	25	3,50E-09	689,7	25	14,771	75
Meas 19	7,60E+02	1706802	40664572	25	3,37E-09	715,8	26,9	12,62	60
Meas 20	8,00E+02	1684842	40141366	25	3,10E-09	778,6	24,6	10,687	55
Meas 21	8,40E+02	1302243	31025951	25	3,61E-09	670	26,4	23,681	60
Meas 22	8,80E+02	1054350	25119895	25	3,48E-09	694,7	6,1	12,356	50
Meas 23	9,20E+02	1500734	35754997	25	3,32E-09	727,5	23,3	8,92	70
Meas 24	9,60E+02	1552347	36984669	25	3,50E-09	689,3	35	9,243	60
Meas 25	1,00E+03	1146497	27315289	25	3,62E-09	668,1	10,6	4,539	80
Meas 26	1,00E+03	1454483	34653066	25	3,53E-09	683,3	36	6,817	60
Meas 27	1,10E+03	1510752	35993672	25	3,50E-09	689,5	20,8	33,051	25
Meas 28	1,10E+03	1218685	29035175	25	3,43E-09	704,5	20,2	19,549	55
Meas 29	1,20E+03	1337867	31874703	25	3,60E-09	670,1	34,2	5,251	35
Meas 30	1,20E+03	1451205	34574964	25	3,76E-09	642,5	21,8	5,764	65
Meas 31	1,20E+03	1185360	28241210	25	4,28E-09	564,8	17,9	64,782	35
Meas 32	1,30E+03	902902	21511657	25	4,00E-09	603,8	29	5,536	55
Meas 33	1,30E+03	943118	22469798	25	3,82E-09	631,5	25,6	6,381	45
Meas 34	1,40E+03	1224462	29172821	25	4,23E-09	571	21,3	15,1	60
Meas 35	1,40E+03	1102327	26262942	25	3,75E-09	644,6	27	36,966	45
Meas 36	1,50E+03	1050541	25029151	25	4,02E-09	600,5	16,9	5,712	45
Meas 37	1,50E+03	739440	17617171	25	4,23E-09	571,1	25,8	11,743	80
Meas 38	1,50E+03	796498	18976566	25	3,86E-09	625,9	25,5	8,028	65
Meas 39	1,60E+03	956460	22787677	25	4,30E-09	561,6	44,8	31,771	35
Meas 40	1,60E+03	1019369	24286474	25	4,05E-09	596,1	24,7	4,555	60
Meas 41	1,70E+03	968251	23068583	25	4,18E-09	577,2	56,8	34,043	55
Meas 42	1,70E+03	842020	20061126	25	4,01E-09	602	20	19,787	60
Meas 43	1,70E+03	952432	22691695	25	3,98E-09	606,4	19,2	28,448	35
Meas 44	1,80E+03	963189	22947988	25	4,34E-09	556,5	19,5	46,211	50
Meas 45	1,80E+03	1001924	23870851	25	3,92E-09	616,9	44,4	44,098	55

Temperature dependent size measurement:

Item	Time (s)	Intensity (C	DLS Temp (	Radius (nm	Amplitude	%PD	Mw-R (kDa	Baseline	SOS
25.1C	0	1308507	25,1	1620,4	0,37	Multimoda	1,09E+08	0,993	13,355
25.7C	69	1512718	25,7	1169,7	0,381	39,5	50796425	1,004	7,458
26.4C	1,10E+02	1252873	26,4	1007,4	0,398	33,2	35812740	0,995	6,975
27.3C	1,50E+02	1053009	27,3	927,6	0,385	42,7	29523937	0,994	17,918
28.4C	1,90E+02	1225801	28,4	1008,2	0,408	25,9	35880173	0,993	7,998
29.5C	2,30E+02	954053	29,5	842,7	0,387	30,1	23584223	0,998	10,06
30.7C	2,70E+02	910644	30,7	869,6	0,416	28,1	25387792	0,997	5,543
31.9C	3,10E+02	889390	31,9	906,6	0,429	43,4	27982559	0,99	10,886
33.5C	3,50E+02	947225	33,5	863,7	0,419	Multimoda	24988142	0,994	12,62
36.3C	4,50E+02	1125634	36,3	877,4	0,423	45,3	25924259	0,989	11,4
37.6C	4,90E+02	973711	37,6	878,9	0,428	27,5	26025749	1	15,696
39.0C	5,30E+02	1022912	39	873,6	0,436	35,5	25663115	0,996	53,109
40.3C	5,70E+02	1015619	40,3	844,7	0,436	27,4	23715086	1,001	23,381
41.6C	6,20E+02	990558	41,6	822,8	0,422	23	22303302	0,998	12,75
43.0C	6,60E+02	906712	43	813,1	0,404	10,4	21691712	1,003	15,197
44.3C	7,00E+02	931698	44,3	838,7	0,434	23,6	23327076	0,999	22,893
45.7C	7,40E+02	1001637	45,7	894,5	0,44	35	27116272	0,994	14,251
47.0C	7,80E+02	973791	47	856,9	0,443	39,2	24526129	0,994	21,259
48.6C	8,20E+02	1279567	48,6	877,6	0,436	21,3	25933784	1,004	27,8
50.2C	8,70E+02	1582592	50,2	800,1	0,397	20,5	20893846	1,001	48,548
52.0C	9,10E+02	1880063	52	806,4	0,406	18,3	21275082	1,004	15,768
53.7C	9,80E+02	1637801	53,7	826,4	0,422	22,9	22531714	1,002	30,047
55.2C	1,00E+03	1780639	55,2	846	0,414	25,6	23803691	1,003	20,311
57.2C	1,10E+03	1732900	57,2	897,8	0,436	31,4	27356478	1,004	32,696
58.5C	1,10E+03	1570619	58,5	868,8	0,412	15,7	25333886	1,004	14,137
59.9C	1,20E+03	1454090	59,9	786,2	0,426	26,1	20049844	0,999	10,612
61.2C	1,20E+03	1376824	61,2	841,7	0,433	19,8	23518961	1,004	14,021
62.7C	1,20E+03	1822879	62,7	911,3	0,421	30,8	28323711	1,01	10,877
64.1C	1,30E+03	1456434	64,1	874,7	0,419	18,1	25738951	1,008	9,946
65.4C	1,30E+03	1579661	65,4	870,8	0,417	23,1	25468362	1,01	7,144
66.8C	1,40E+03	1784926	66,8	926,6	0,42	36,1	29453737	1,007	9,963
68.1C	1,40E+03	2007543	68,1	965,2	0,403	23,8	32400265	1,016	15,653
69.5C	1,50E+03	1855811	69,5	948,1	0,412	17,8	31075088	1,016	17,456
70.8C	1,50E+03	1961329	70,8	946,7	0,415	21,4	30970506	1,012	14,985
72.2C	1,50E+03	1994192	72,2	940,8	0,402	22,3	30515918	1,015	11,804
73.5C	1,60E+03	2051030	73,5	895,3	0,402	23,3	27174318	1,018	9,046
75.0C	1,60E+03	1968143	75	932,8	0,394	21,5	29914306	1,017	13,606
76.3C	1,70E+03	2089814	76,3	931,1	0,39	12,7	29790797	1,012	19,011
77.4C	1,70E+03	1961593	77,4	879	0,395	20,5	26035038	1,018	42,062
78.1C	1,70E+03	1934340	78,1	902,3	0,393	22,5	27675800	1,013	28,788
78.6C	1,80E+03	1816564	78,6	950,7	0,397	8,6	31275512	1,016	35,713
79.0C	1,80E+03	2096502	79	949	0,388	21,2	31146055	1,012	14,153
79.2C	1,90E+03	1980002	79,2	896,8	0,411	37,7	27282712	1,014	29,392